geosciences

MDPI

Article

Early Priabonian Larger Benthic Foraminifera in the Vicinity of Verona (N Italy)

Levent Sina Erkızan [1], György Less [1,*] and Cesare Andrea Papazzoni [2]

[1] Institute of Exploration Geosciences, University of Miskolc, H-3515 Miskolc, Hungary; levent.sina.erkizan@student.uni-miskolc.hu
[2] Dipartimento di Scienze Chimiche e Geologiche, Università di Modena e Reggio Emilia, I-41125 Modena, Italy; papazzoni@unimore.it
* Correspondence: gyorgy.less@uni-miskolc.hu; Tel.: +36-20-5005907

Abstract

The rich Eocene larger benthic foraminiferal (LBF) assemblages in the vicinity of Verona have long been well known. However, they are described in detail only from the Ypresian to Bartonian interval. Here, we present the results of our morphometrically based study of Priabonian LBF. The lowermost part of the succession, just above the uppermost occurrence of giant *Nummulites* (*N. biedai*), outcrops at Monte Cavro and contains *Heterostegina reticulata multifida* and *Nummulites hormoensis* as major constituents. These taxa clearly determine the earliest Priabonian Shallow Benthic Zone (SBZ) 18C. Slightly younger strata can be analyzed in the other three studied exposures on the northern side of Castel San Felice. These beds already represent the early Priabonian SBZ 19A Zone based on the first appearing *Spiroclypeus sirottii* and the presence of *Heterostegina reticulata mossanensis* and *Nummulites fabianii* (replacing *H. r. multifida* and *N. hormoensis*, respectively). The most abundant LBF in these beds are the very diverse and well-preserved orthophragmines represented the families Discocyclinidae (genera *Discocyclina* and *Nemkovella*) and Orbitoclypeidae (genera *Orbitoclypeus* and *Asterocyclina*). They determine the Orthophragmine Zone (OZ) 14. The distinction of six species of the genus *Discocyclina* (especially that of *D. euaensis* from *D. dispansa*) is discussed in detail. The exposures around Castel San Felice are considered as key localities for the SBZ 19A and OZ 14 Zones, containing their key LBF assemblages. Consistently, both orthophragmine and LBF range charts for the late Lutetian to Priabonian are updated.

Keywords: North Italy; Eocene; Priabonian; larger benthic foraminifera; morphometry; taxonomy; biostratigraphy

Academic Editor: Maria Helena Henriques

Received: 7 June 2025
Revised: 8 July 2025
Accepted: 8 August 2025
Published: 1 September 2025

Citation: Erkızan, L.S.; Less, G.; Papazzoni, C.A. Early Priabonian Larger Benthic Foraminifera in the Vicinity of Verona (N Italy). *Geosciences* **2025**, *15*, 334. https://doi.org/10.3390/geosciences15090334

1. Introduction

Larger benthic foraminifera (LBF) are probably the most widespread fossils in the tropical/subtropical shallow marine rocks of the Tethyan Paleogene (and especially Eocene) deposits [1], which is reflected also in the name "Nummulitique", widely used in the earlier French literature for the Eocene. LBF have been widely used for biostratigraphical purposes since the middle of the 19th century [2,3]. Due to the intensive work in IGCP projects 286 ("Early Paleogene Benthos") and 393 ("Neritic Events at the Middle–Upper Eocene boundary"), the Tethyan Paleocene and Eocene have been subdivided into twenty shallow benthic (SBZ) zones (SBZ 1–20 [4]), followed with six zones in the Oligo-Miocene (SBZ 21–26 [5]).

Simultaneously, refs. [6,7] worked out the stratigraphic subdivision of Tethyan late Paleocene and Eocene orthophragmines (the families Discocyclinidae and Orbitoclypeidae with similar morphostructures), which was incorporated into the shallow benthic zonation. A separate orthophragmine zonation with eighteen OZ prefixed zones was also developed [7]. Later, this zonation was significantly improved [8] and also geographically widened to the east and south. SBZ and OZ zones were first correlated by [7], with the most updated versions being found in [8,9]. In addition, ref. [9] includes the calibration of SBZ and OZ zones to the magnetostratigraphic chrons and plankton-based biozones.

Because of the discontinuous stratigraphic record of key taxa (characteristic for shallow marine organisms), these SBZ and OZ units are considered as Oppelzones (for a detailed explanation, see [10]), which are defined rather by their key assemblages recorded in particular key localities than by the (very often undetectable) zone boundaries. The vertical succession of zones can be proven sometimes by their superposition in the field. More often, however, it is based on a comparison of the evolutionary degrees of particular lineages occurring in neighboring zones. Fortunately, especially in the Eocene, numerous evolutionary lineages run parallel and co-occur in key localities.

Based on the above reasoning, detailed knowledge of characteristic LBF assemblages from key localities is essential, since they serve as references for the determination of LBF from other localities, which leads to the correct stratigraphic evaluation of the latter. Consequently, the key LBF assemblages (i) should be very rich and diverse, (ii) should contain well-preserved and isolated specimens, and (iii) the key localities should be easily accessible. In this paper, we present and describe, in detail, the early Priabonian key LBF assemblages in the vicinity of Verona (N Italy), which fulfill all these three conditions.

2. Geological Setting

Verona is located in northeastern Italy, on the southwestern margin of the Lessini Mountains, (Figure 1), which are part of the Southern Alps, originated by the collision of the Adria Plate with the southern European margin during the Cenozoic [11–13]. During the Paleogene, the Lessini area formed the so-called "Lessini Shelf" [14], a shallow marine platform limited on the western side by the Lombardy Basin, on the eastern side by the Belluno Basin, connected north to the emerged land, and extending south to the modern Berici Mts. The Lessini Shelf was, in turn, superimposed on the Early Jurassic Trento Platform [14,15], which began to drown in the Middle Jurassic and evolved into the Trento Plateau [16], a structural high with basinal sedimentation continuing until the early Eocene [14,17,18]. During this time interval, deep-water sediments belonging to the Rosso Ammonitico Veronese Fm. (upper Bajocian–upper Tithonian; [19]), Maiolica Fm. (upper Tithonian–lower Aptian; [20]), Scaglia Variegata Alpina Fm. (lower Aptian–Cenomanian; [20]), and Scaglia Rossa Fm. (Turonian–Ypresian; [14,17,20]) were deposited on the Trento Plateau. Then, the Cenozoic shallow-water carbonates started their deposition during the early Eocene on the higher parts of uplifted blocks (e.g., Torbole Limestone Fm. [17]), while in the surrounding deeper areas, slope and basinal sediments were deposited (e.g., Malcesine Limestone Fm. and Chiusole Fm [17]).

The Eocene strata cropping out in the vicinity of Verona are subdivided into three informally named formations (in quotation marks). These are the "Calcari argillosi e marne di colore biancastro" (whitish clayey limestone and marl), attributed to the lower Eocene (also "Calcari di Spilecco" [21] or "Calcari argillosi e marne" [22]), the "Calcari nummulitici" (nummulitic limestone), spanning the lower to middle Eocene, and the "Priabona marls", belonging to the upper Eocene [23].

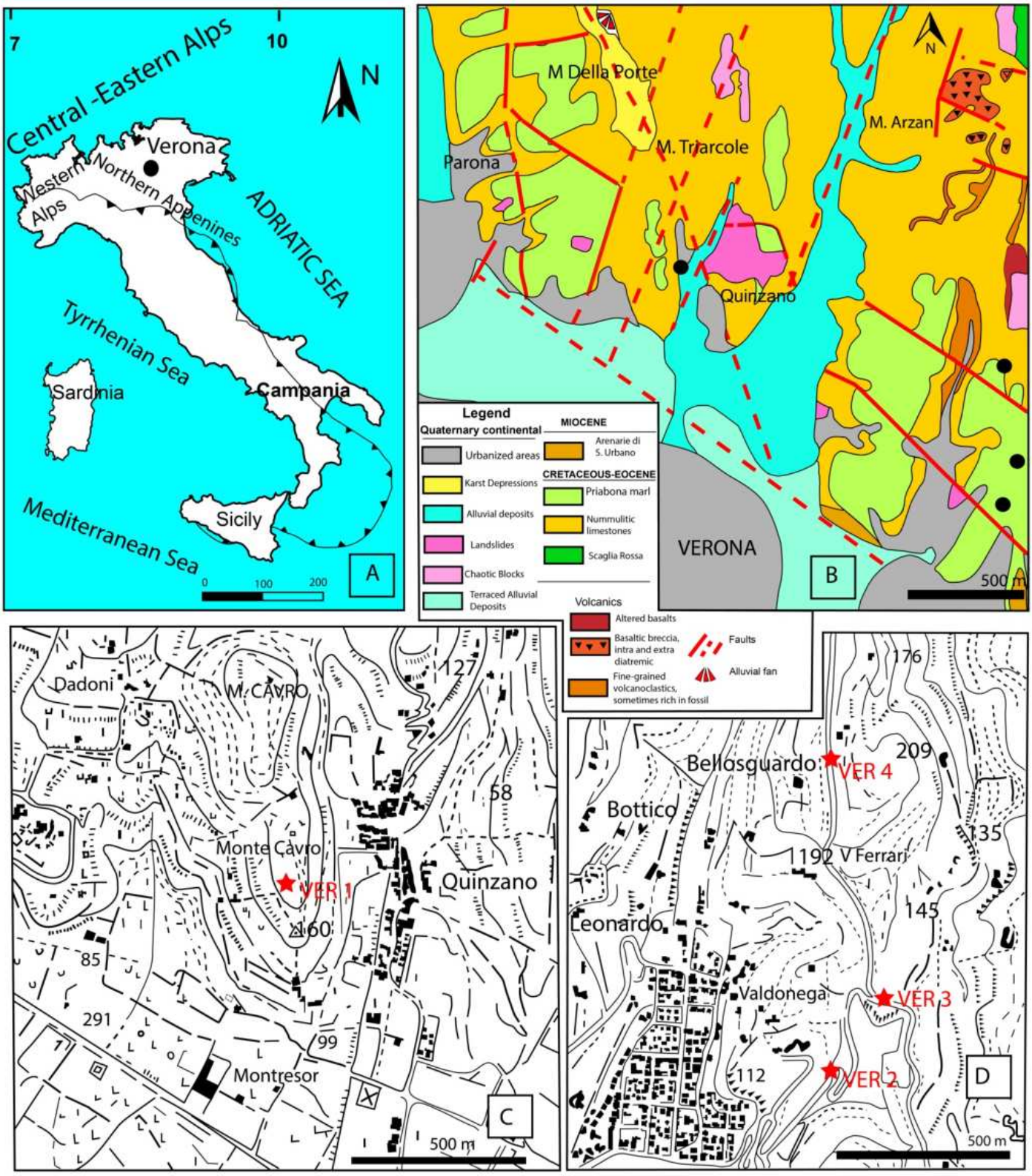

Figure 1. Location maps with sample locations, (**A**): map of Italy showing the location of Verona, (**B**): geology map of the vicinity of Verona [24], modified, and locations of the studied samples, (**C**): topographic map of the vicinity of Monte Cavro with the location of sample VER 1, and (**D**): topographic map of the vicinity of Verona, Castel San Felice, with the location of samples VER 2–4.

Among these formations, the older "Calcari argillosi e marne di colore biancastro" contain abundant planktonic foraminifera, sometimes together with LBF, mainly *Nummulites*, resedimented from shallower areas into the deeper basins [22].

Similarly, the lowermost part of the "Calcari nummulitici" may also contain resedimented LBF in the lower Eocene, which could be correlated with the Chiusole Fm. [17]. The remaining part of the "Calcari nummulitici", extensively cropping out just north of the city of Verona, is attributed to the Lutetian and Bartonian, with different (partly giant, with a diameter of B-forms exceeding 1.5 cm) *Nummulites* in its uppermost part [25].

The "Priabona marls" commonly crop out on top of the "Calcari nummulitici" in the hills north of Verona (see geological map [23]). They contain mainly orthophragmines and subordinately nummulitids, all indicating a Priabonian age [21–23]. Near Verona, the "Priabona marls" are locally covered by Middle Miocene calcarenites ("Arenarie e calcari di S. Urbano") [21], whereas the top of the Eocene and the Oligocene are most probably eroded and/or non-deposited [14,22,23,26].

3. Previous LBF Studies in the Vicinity of Verona

The Eocene larger foraminifera in the Verona area have been the subject of several studies, starting at least from the 19th century [27–29]. These papers, however, contain only faunal lists, and lack descriptions and illustrations of LBF. Later, in the early 20th century, ref. [30] widely treated the Veronese Eocene in the frame of the whole Veneto area and also gave only faunal lists. Ref. [26] focused strictly on the vicinity of Verona and reported, for the Eocene, the presence of "*Nummulites perforata*" (=*N.* ex gr. *perforatus*) and "*N. complanata*" (=*N.* ex gr. *millecaput*) from the "strati di S. Giovanni Ilarione" (Lutetian), the "*Nummulites* cfr. *Brongniarti*" (=*N. brongniarti*) and "*N. contorta*" (=*N. striatus*) from the "strati di Roncà" (Bartonian), and "*Orthophragmina ephippium*" (=*Discocyclina* spp.) from the "strati di Priabona" (Priabonian)

Concentrating on the systematics of orthophragmines, Paul Brönnimann also used material of the "Priabona marls" from the Castel San Felice outcrop. He presented excellent photos and drawings of *Aktinocyclina radians* [31] and *D.* aff. *varians* [32], re-evaluated by [6] as *Discocyclina radians labatlanensis* and *D. dispansa umbilicata*, respectively. According to our recent studies, however, these re-evaluations are questionable, since there is a clear inconsistency between the enlargements of drawings and photographs of the same individuals in Brönnimann's above publications. If we consider the magnifications given for the drawings, then the correct re-evaluations are *D. radians radians* and *D. dispansa dispansa*, respectively. This is confirmed by the fact that the dimensions in the text [31] confirm the magnifications given in the drawings.

Lukas Hottinger and Hans Schaub used the description and geological map in [26] to investigate the alveolines [33] and nummulitids [34,35] from Calcari nummulitici, which they subdivided into three parts. The lower part (Calcaire de la Vallé Gallina) is attributed to the middle–late Cuisian (late Ypresian) based on *Alveolina indicatrix*, *Nummulites* aff. *nitidus*, *N.* aff. *irregularis*, *N.* cf. *distans*, and *Assilina* aff. *laxispira*. The middle part (Calcaire d'Avesa) is attributed to the middle–upper Lutetian based on *Alveolina munieri*, *A.* aff. *munieri*, *A.* aff. *prorrecta*, *A.* cf. *elliptica nuttalli*, *Nummulites crassus*, *N.* aff. *crassus*, *N.* aff. *meneghinii*, *N. lorioli*, *N. alponensis*, *N.* cf. *millecaput*, *N. discorbinus*, *N.* aff. *biarritzensis*, *Assilina exponens*, and *A. gigantea*. Later, this association was marked as a key LBF assemblage for the SBZ 15 Zone by [4]. The upper part of Calcari nummulitici (Calcaire à Algues) is attributed to the Biarritzian (=Bartonian) based on *Alveolina fragilis*, *Nummulites* cf. *perforatus*, *N.* cf. *dufrenoyi*, *N. lyelli*, and *N. brongniarti* (this latter is only in [34]).

Ref. [36] studied the sedimentological aspects of Calcari nummulitici in detail and interpreted it as a nummulite bank in general. They mostly repeated the list of nummulitids

in [34], with the addition of some other forms. This fauna has, however, never been taxonomically described and illustrated.

An unpublished MSc thesis [24] (conducted under the supervision of the late Prof. Achille Sirotti) identified *Nummulites chavannesi*, *N. cunialensis*, *N. fabianii*, *N. incrassatus*, *N. pulchellus*, *N. stellatus*, *Operculina alpina*, *O. canalifera gomezi*, *Spiroclypeus granulosus*, *Grzybowskia reticulata*, *Pellatispira madaraszi*, *Discocyclina aspera*, *D. augustae*, *D. sella*, *Aktinocyclina radians*, *Orbitoclypeus nummuliticus*, *Asterocyclina stella*, *A. stellaris*, *A. stellata*, and *A. taramellii* from the "Priabona marls" of this area. On this basis, ref. [24] concluded that, here, the transition between the middle and upper Eocene (=Bartonian–Priabonian) is continuous, differently from the Priabona stratotype; however, he also noticed that the transition is often not visible because of the detritus and vegetation cover.

In the frame of the study of nummulite biostratigraphy at the middle/upper Eocene boundary, ref. [25] also investigated the Monte Cavro sequence representing the uppermost part of Calcari nummulitici. According to them, the lower part (samples MC 1–3 in [25]), still containing giant *Nummulites* (*N. biedai*), belongs to their *N. biedai* Zone. The other LBF in these samples are *N. chavannesi*, *N. hormoensis*, *N.* cf. *hormoensis*, *N. stellatus*, *N. striatus*, *N. variolarius/incrassatus*, *Operculina* aff. *alpina*, *Heterostegina reticulata*, *Discocyclina discus*, *D. pratti*, *Orbitoclypeus varians*, *O.* sp., *Asterocyclina stella*, *A.* sp., *Asterigerina* sp., *Calcarina* sp., *Fabiania* sp., *Gypsina linearis*, *G.* sp., *Haddonia heissigi*, *Silvestriella tetraedra*, and *Sphaerogypsina globula*. Giant *Nummulites* are already absent in the upper part (samples MC 4 and 5 in [25]), and the LBF fauna (belonging already to the *Nummulites variolarius/incrassatus* Zone) is much poorer. Besided the nominate taxon, it consists also of *N.* cf. *hormoensis*, *N. striatus*, *Orbitoclypeus* sp., *Asterigerina* sp., *Gypsina linearis*, *G.* sp., *Silvestriella tetraedra*, and *Sphaerogypsina globula*. Ref. [25] stated that the *N. biedai* Zone still represents the middle Eocene (Bartonian); the *N. variolarius/incrassatus* Zone, however, can be arranged both into the middle and upper Eocene.

It is clear from the above that the LBF from Calcari nummulitici have been studied more intensively than those from the Priabona marl. Therefore, in this article, we focus on the latter. This work has already begun with [37,38]. Nummulitids (*Heterostegina* and *Spiroclypeus*, respectively) with secondary chamberlets have been studied from Monte Cavro (sample MC 4, see above) and from the "Priabona marls" near Castel San Felice on the northern edge of Verona. The results are summarized and briefly presented in this article as well, since the sites are identical.

4. Materials and Methods

4.1. Localities

We examined four sites representing two levels of the Eocene sequence near Verona. The samples were collected in 1990 by the second and last author of this article under the guidance of the late Dr. Achille Sirotti, former professor at the University of Modena.

Sample Verona (VER) 1 (45°28′10.284″ N, 10°58′14.604″ E) comes from the stratigraphically lower-level outcropping in Monte Cavro (Figure 2), just about 4–5 km NNW of Verona. It is identical to sample Monte Cavro (MC) 4 in Figure 3. It represents the uppermost part of "Calcari nummulitici", already lacking giant *Nummulites* and belonging to the *N. variolarius/incrassatus* Zone in the above paper. Isolated LBF specimens can be collected from the weathered surface of the limestone. Small nummulitids dominate over orthophragmines in the LBF assemblage, and almost all specimens from both groups are megalospheric (A-forms).

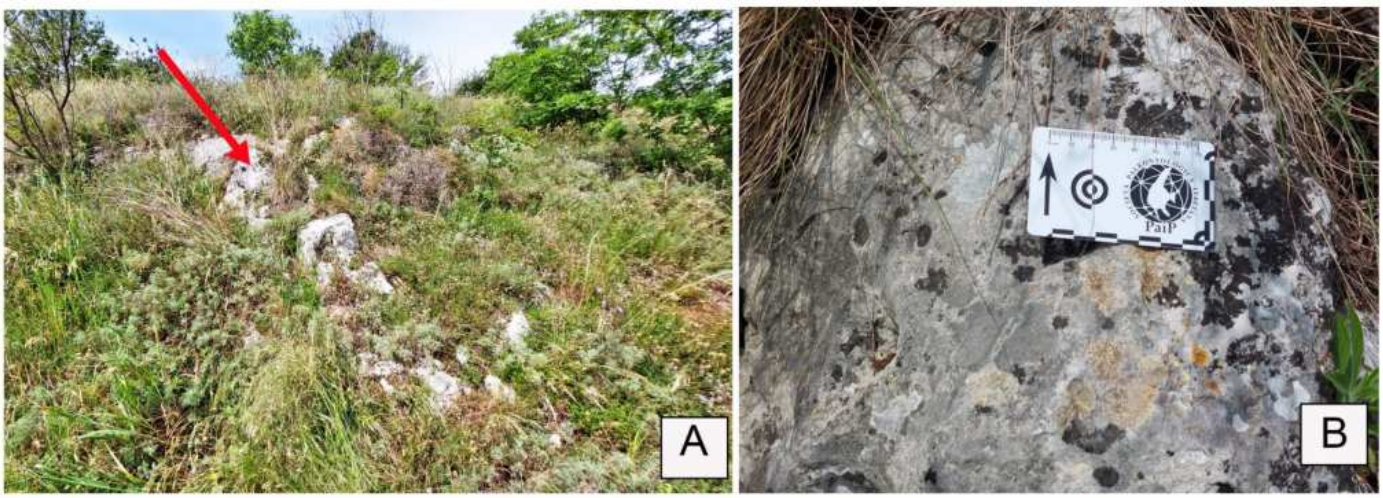

Figure 2. Photos of the Monte Cavro section. (**A**). General view showing the position of sampling site VER 1 and (**B**). close-up view. Photos: C.A. Papazzoni (2025).

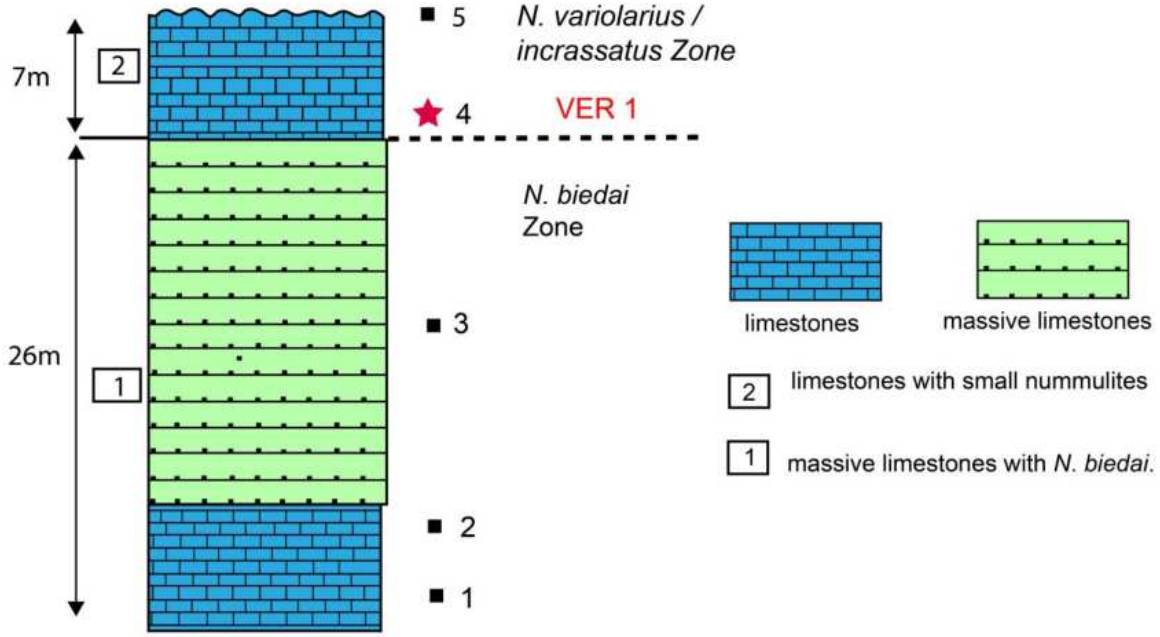

Figure 3. Simplified stratigraphic log of the Monte Cavro section [25].

The other three samples [Verona (VER) 2: hairpin bend—45°27′12.57″ N, 11°00′26.989″ E; VER 3: Villa Devoto—45°27′19.146″ N, 11°00′32.335″ E, and VER 4: Villa Le Are—45°27′38.856″ N, 11°00′26.64″ E] come from the overlying "Priabona marls" near Castel San Felice on the northern edge of Verona (Figure 4). The direct transition between the Calcari nummulitici and the "Priabona marls" is not visible near Verona. The relative stratigraphic positions of the three samples cannot be determined in the field. Wash residues contain abundant isolated LBF, among which orthophragmines strongly dominate over nummulitids. In these samples, too, microspheric (B) forms are very rare. This was revealed in the Verona material by snapping the specimens into two with pliers, due to their good or even excellent preservation.

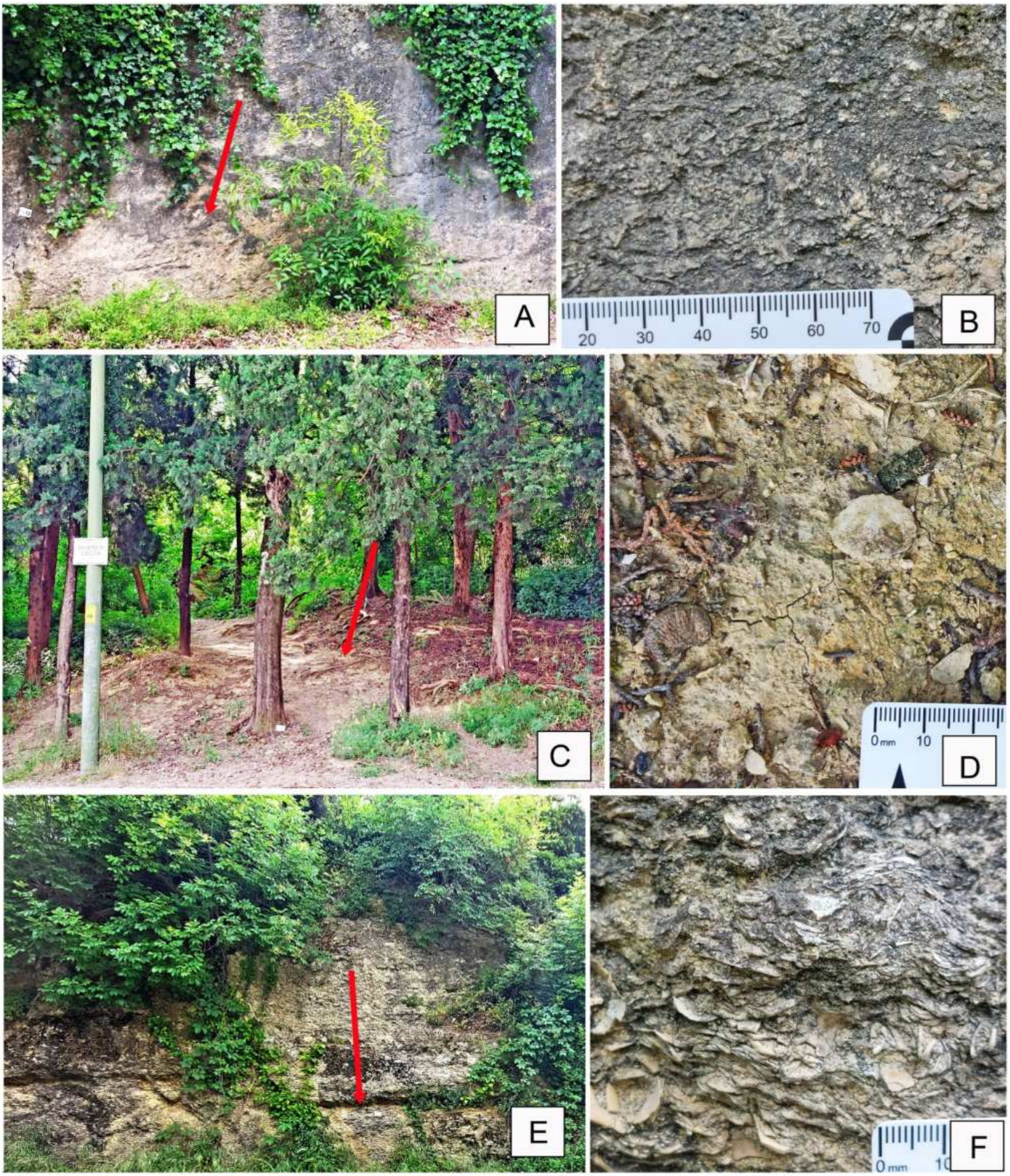

Figure 4. Outcrop photos ((**A**,**C**,**E**): general views; (**B**,**D**,**F**): close-up views) with sampling sites (red arrows) in the vicinity of Castel San Felice. (**A**,**B**). Hairpin bend, site VER 2. (**C**,**D**). Villa Devoto, site VER 3. (**E**,**F**). Villa Le Are, site VER 4. Photos: C.A. Papazzoni (2025).

4.2. Preparation and Depository

The identification of nummulitids and orthophragmines (the two most common LBF in the Tethyan Eocene, along with alveolinids) is based primarily on their internal features,

in addition to their external characteristics. The internal features are best studied in the equatorial section. This was revealed in the Verona material by breaking the specimens in half with pliers, due to their good or even excellent preservation.

The specimens were then stained with purple ink to make the morphology of the equatorial section more visible. The procedure is described in detail in [39]. The two main advantages of the method are that (i) it is very productive and (ii) it exposes the equatorial layer perfectly, along the weakest surface containing stolons; thus, they become visible. Meanwhile, since the equatorial layer is never completely flat, this can cause sharpness problems when photographing.

All equatorial sections were photographed and measured in the Geological Department of the University of Miskolc using the Discovery.V20 and Imager. A2m (Zeiss, Oberkochen, Germany) microscopes and the Axio Vision SE 64 Rel.4.8 software.

Figured specimens prefixed by E. are stored in the Eocene collection of the Supervisory Authority for Regulatory Affairs of Hungary (formerly Geological Institute of Hungary) in Budapest.

4.3. Taxon Determination

Recently, there has been general agreement among LBF experts working on diverse groups regarding the existence of long-lived evolutionary lineages. There are two different approaches to their treatment (see also [10]). Representatives of the Basel School [33,35,40,41] apply a typological approach. This is because they mainly work in the Eocene, where, in the case of all three major LBF groups (i.e., nummulitids, orthophragmines, and alveolinids), a considerable number of co-occurring evolutionary lineages run parallel. They use this method not only for the separation of lineages, but also for the characterization of the evolution within them. In this approach, a lineage is a succession of typical forms, with each including the holotype and the population from the type locality as well. Hence, these types (interpreted as distinct species) serve as central moments of the development of the given evolutionary lineage, and related populations from other sites are grouped around them.

In contrast, the morphometric Utrecht School (working mainly in the Upper Cretaceous and Oligo-Miocene, where only very few lineages of particular genera run parallel) does not characterize evolution with the help of "central moments", but subdivides it by artificial limits using a well-measurable, rapidly evolving quantitative parameter of the given lineage (as summarized in [42]). Simultaneously, the existence of numerous simultaneously running evolutionary lineages in the Eocene was questioned [42,43], which was considered as an artifact of the typological method using many discriminating ("yes/no") qualitative parameters instead of the quantitative ones used in the morphometric method.

In revising Tethyan orthophragmines, the above two methods were combined by the typological separation of lineages and their morphometrical subdivision [6,7]. Responding to the criticism by [42], in a case study of the late Ypresian site of Horsarrieu (SW France), ref. [44] showed the co-occurrence of numerous lineages both typologically and morphometrically. With this, ref. [44] certified the validity of the much quicker typological method and, therefore, gave priority to it. At the same time, the morphometric method appears to be much more objective in subdividing lineages, thus, it is highly recommended in this respect.

In practice, this means that (according to the protocol by [42]) the LBF in each sample are determined in three steps (experienced experts usually perform the first two steps at once). In the first step, the specimens are typologically grouped into populations whose members are clearly distinguishable from specimens of other populations in the same sample.

Since, in most cases, these populations are members of a lineage (or phylum), in the second step, the entire population is typologically assigned to an adequate lineage. In the case of orthophragmines and the genus *Heterostegina*, the lineages correspond to

species, while in the case of nummulitids (other than *Heterostegina*), they form a series of chronospecies.

Then, in the third step, the evolutionary degree of the given populations within the corresponding lineage is estimated morphometrically. Many lineages are used for biostratigraphic purposes after being artificially segmented into chronospecies (or chrono-subspecies in the case of orthophragmines and *Heterostegina*) separated by arbitrary biometric boundaries of a characteristic numerical evolutionary parameter.

In some populations, the mean of the defining parameter may be very close (closer than 1 s.e. of the mean) to the limit of two neighboring species/subspecies. In this case, we need an intermediate notation in the species/subspecies units. A two-species/subspecies exemplum intercentrale notation (abbreviated as ex. interc.) is used, in which the prevalent species/subspecies unit will be ranked first, followed by the closest specific/subspecific unit as the second part of the determination. If the population consists of only a single specimen, no species/subspecies is determined. In the case of only two or three specimens, the species/subspecies is determined as "cf.". Samples close to each other and containing practically the same assemblages with similar parameters are evaluated both separately and jointly. However, the species/subspecies determination is given for the joint sample.

5. Results

The LBF composition of the four samples is shown in Table 1. The VER 1 assemblage (Monte Cavro 4) from the uppermost part of the Calcari nummulitici is the least diverse. Nevertheless, the presence of *Nummulites hormoensis* (typical of SBZ 18) and *Heterostegina reticulata multifida* (typical of SBZ 18C only), also taking into account the absence of the genus *Spiroclypeus* (first reported in SBZ 19), is crucial in the definition of the SBZ 18C Subzone [4,8,37,45]. According to [4,37], the SBZ 18C is still placed in the late Bartonian, but [45] places it in the earliest Priabonian due to the revision of the Bartonian/Priabonian boundary [46,47]. Since orthophragmines are rare in sample VER 1, it cannot be precisely placed within the orthophragmine zonation in [6,7]. Based on the composition of the LBF, in which nummulitids dominate over orthophragmines, this sample represents a relatively protected, low-energy inner platform environment [25].

The LBF assemblages of the overlying "Priabona marls" (samples VER 2–4 from the Castel San Felice area) differ significantly from that of sample VER 1. The LBF fauna of the three samples is very similar (samples VER 3 and VER 4 are particularly similar), in which diverse assemblages orthophragmines strongly dominate over nummulitids, suggesting an outer platform environment. Sample VER 2 differs from the other two in the following three respects: (i) the presence of reticulate *Nummulites* (*N. fabianii*), (ii) the presence of *Discocyclina euaensis*, which is replaced by *D. dispansa* in samples VER 3 and 4, and (iii) the evolutionary degree of *Orbitoclypeus varians*, which is slightly less advanced (with *O. v. scalaris*) than in the other two samples (with *O. v. varians*). However, the latter does not necessarily mean that sample VER 2 is slightly older than the other two, since, at the same time, *Heterostegina reticulata mossanensis* appears to be slightly less developed in samples VER 3 and VER 4. Thus, their relative stratigraphic position cannot be clearly assessed.

Although nummulitids do not dominate samples VER 2–4, they play a key role in determining the SBZ 19A Subzone (as defined in [4,9,37,45]). These samples already contain *Spiroclypeus sirottii* (first reported in SBZ 19), *Heterostegina reticulata mossanensis* (SBZ 19A only), and *Nummulites fabianii* (SBZ 19 and 20). The latter two taxa replace *H. r. multifida* and *N. hormoensis* from sample VER 1. All other nummulitids are very rare (especially in sample VER 4) and occur in both older and younger strata, so their stratigraphic significance is limited. Considering the revision of the Bartonian/Priabonian boundary [46,47], according

to [8], the SBZ 19A Subzone corresponds to the early Priabonian (but not to the earliest, as was earlier suggested by [4]).

Table 1. Distribution of LBF in the studied early Priabonian samples from Verona. +: common, ×: sporadic.

	Family	**Discocyclinidae**									**Orbitoclypeidae**						**Nummulitidae**											
Locality	**Sample/Taxon**	***Disocyclina augustae augustae***	***D. dispansa dispansa***	***D. euaensis***	***D. pratti minor***	***D. radians* cf. *radians***	***D. trabayensis elazigensis***	***Nemkovella strophiolata tenella***	***N. daguini***	***Orbitoclypeus varians scalaris***	***O. varians varians***	***Asterocyclina alticostata* indet. ssp.**	***A. alticostata danubica***	***A. stellata* cf. *stellaris***	***A. stellata stellaris***	***Nummulites hormoensis***	***N. fabianii***	***N. chavannesi***	***N. incrassatus***	***N. budensis***	***N. pulchellus***	***Assilina alpina***	***Operculina* ex gr. *gomezi***	***Heterostegina reticulata multifida***	***H. reticulata mossanensis***	***Spiroclypeus sirottii***
Monte Cavro	VER 1											×		×		+			+	×				+		
Caster San Felice	VER 2	+		+			×	+		×			×		+		+	+	+	×		×			+	+
	VER 3	+	+				×	+			×		×		+			×	×			+	×		+	+
	VER 4	+	+		+	×	+	+	×		+		×		+			×			×	+	×		+	+

The rich and diverse orthophragmine assemblage is characteristic of the OZ 14 Zone [6,7]. Considering [8], *Discocyclina pratti minor* and *Nemkovella strophiolata tenella* are almost exclusively known from this zone. This zone is also marked by the lowest occurrence of *D. augustae augustae*, *D. trabayensis elazigensis*, *D. euaensis*, and *Asterocyclina alticostata danubica* and the highest of *D. dispansa dispansa* and *Orbitoclypeus varians scalaris*. *Nemkovella daguini*, *A. stellata stellaris*, and *O. v. varians* are known from both older and younger strata. The presence of *D. radians* cf. *radians* (represented by only two specimens) is stratigraphically irrelevant (further details in the systematical part). The stratigraphic range of the OZ 14 zone is relatively long, covering the latest Bartonian to early Priabonian interval from the base of the SBZ 18 Zone to the top of the SBZ 19A Subzone [8,45].

6. Systematical Part

- Order Foraminiferida Eichwald, 1830

The LBF listed in Table 1 belong to three different families, namely Discocyclinidae, Orbitoclypeidae, and Nummulitidae. Due to their morphological similarity and joint occurrence, the first two are often grouped informally under the name of orthophragmines. Their taxa, as well as those of nummulitids, are described below.

6.1. Orthophragmines

Late Paleocene and Eocene orbitoidal larger foraminifera with almost rectangular equatorial chamberlets constitute two systematically independent families, namely Discocylinidae Galloway, 1928 and Orbitoclypeidae Brönnimann, 1945, based on the significantly different microspheric juvenarium of their B-forms [32]. Their morphostructure is otherwise quite similar (for details see [6,8,32,42,48–52]). Therefore, and because these probable symbiont-bearing benthic forms can be found together in the peri-Mediterranean region

(commonly in the deeper part of the photic zone, i.e., basinward from shallow-water environments or transported into deep marine settings), orthophragmines, an informal collective name, is used to refer to both groups.

In the peri-Mediterranean region, Discocyclinidae are represented by the following two genera: *Discocyclina* Gümbel, 1870 and *Nemkovella* Less, 1987. *Discocyclina* can be distinguished from *Nemkovella* by the presence of annular stolons in the equatorial chamberlets. Orbitoclypeidae also have two genera in this region, *Orbitoclypeus* Silvestri, 1907 and *Asterocyclina* Gümbel, 1870. *Asterocyclina* is differentiated from *Orbitoclypeus* by having an equatorial layer axially subdivided within the ribs. A synoptic summary for distinguishing the four peri-Mediterranean genera is shown in Figure 5. Therefore, ribbing is taxonomically useful only on the specific level (further details in [6,50]). Refs. [8,52] also distinguished the genus *Hexagonocyclina* within Orbitoclypeidae based on the primitive periembryonal morphology of A-forms.

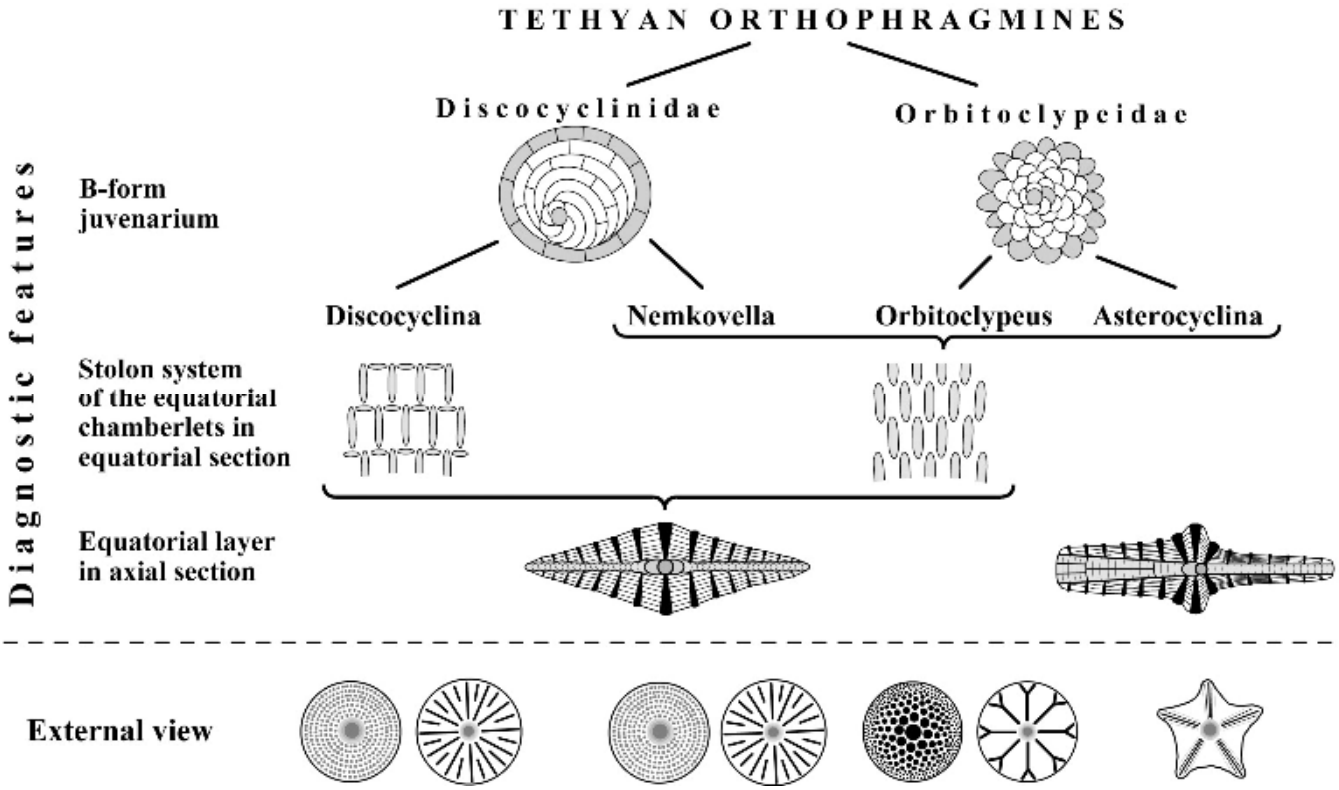

Figure 5. Features separating Tethyan orthophragmine families and genera [53].

However, we believe that this feature is not significant enough to distinguish it as a separate genus; therefore, we place these forms in *Orbitoclypeus*. Ref. [54] separated the new genus *Virgasterocyclina* from *Asterocyclina* based on the presence of radially thickened lateral walls, i.e., rods, along the ribs. However, this feature appears independently in the peri-Mediterranean Priabonian and also in the American–Caribbean middle–upper Eocene, in phylogenetically clearly different Asterocyclinae. Therefore, we prefer to keep these forms within *Asterocyclina*.

All four Tethyan genera consist of several long-living, simultaneously running evolutionary lineages considered to be species. These species very often coexist in particular samples, in which they are typologically distinguished by the combination of some clearly qualitative features, such as the external shape (i.e., the presence/absence of ribs and bulges) and other characteristics (Figure 6) that are (excepting the type of rosette) recognizable in the equatorial section of the A-forms. Therefore, the significance of microspheric

forms (constituting only about 1–10% of most of the populations) is subordinate in the specific determination. Some primarily quantitative features (that are, in fact, evaluated qualitatively and, therefore, recognizable at once by an expert) are also used in species determination. These are the size of the A-form embryo and the shape and width of equatorial chamberlets. Most of the species constitute long-living evolutionary lineages with definite internal development that allows their morphometric subdivision into artificial subspecies (for theoretical background, see [42]).

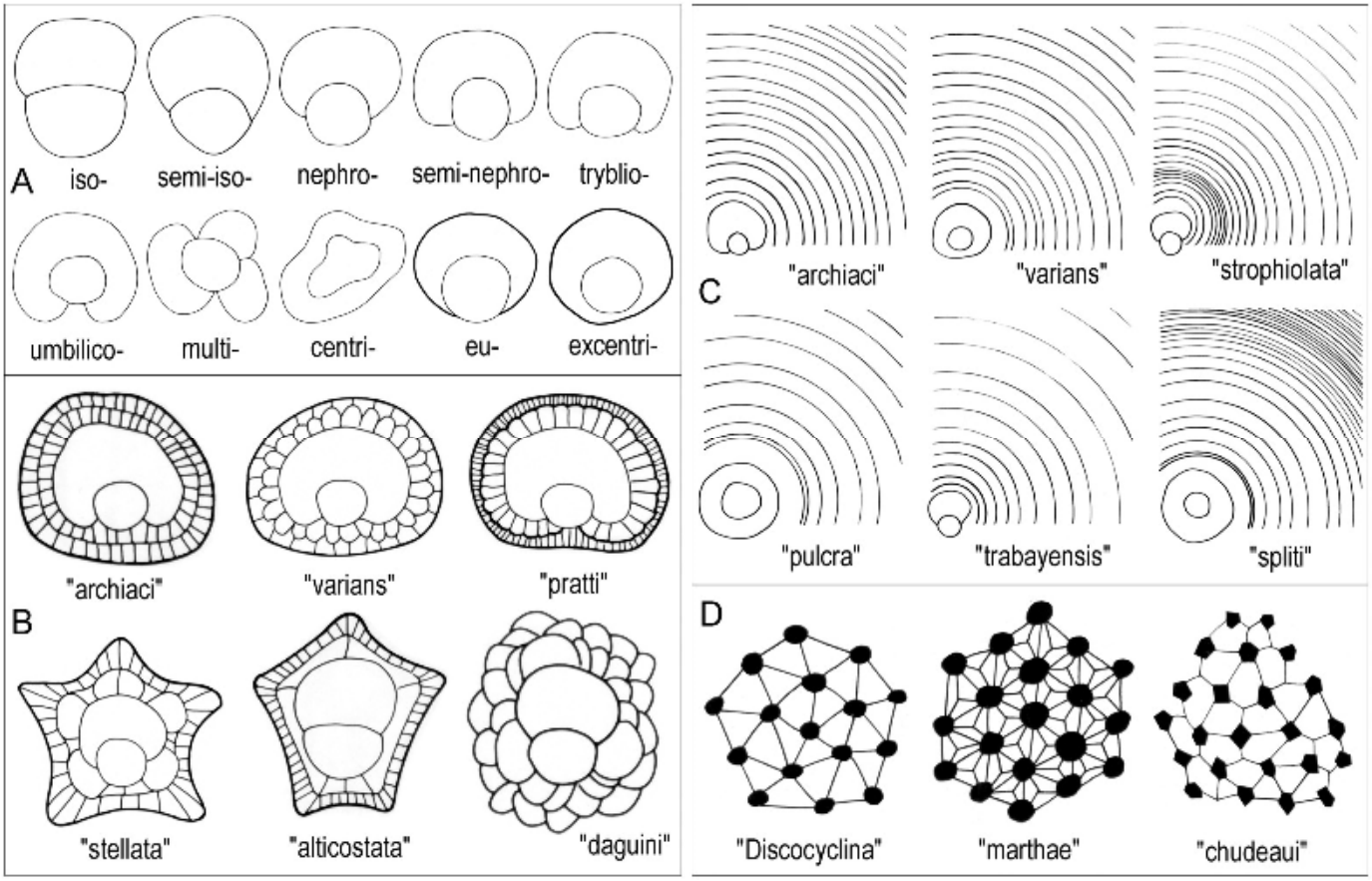

Figure 6. Qualitative features of Tethyan orthophragmines [6]. (**A**): Different embryo types (suffix "-lepidine" is to be added to each type); (**B**): different types of the adauxiliary chamberlets; (**C**): different growth patterns of the equatorial annuli; and (**D**). different types of the rosette (the network of piles and lateral chamberlets on the test's surface).

These subspecies are defined by biometric limits of the populational means of the outer cross diameter of the deuteroconch (the second chamber of the A-form embryo) in the equatorial section (marked by "d", see Figure 7) [6]. This quantitative feature has been chosen from among several other evolutionary parameters because it is the most easily and objectively measurable and reveals the fastest and clearest progress [7].

Other parameters shown in Figure 7 are used to describe taxa in detail, since they can confirm determinations in dubious cases. As the orthophragmine assemblage of Castel San Felice is exceptionally diverse and may serve as a key assemblage for the OZ 14 Zone, in this paper, we perform a full morphometric analysis to characterize the taxa as completely as possible. It consists of eight measurements and counts in the equatorial section of megalospheric (A) forms, as listed below and shown in Figure 7. Morphometric data are summarized in Tables 2–4.

- p and d: Outer diameter of the protoconch and deuteroconch perpendicular to their common axis (in μm);

- I and J: Outer circumference of the protoconch embraced (I) and not embraced (J) by the deuteroconch;
- N: Number of the adauxiliary chamberlets (in Figure 7, N =15);
- H: Characteristic height of undeformed adauxiliary chamberlets (in μm);
- n: Characteristic number of annuli within 0.5 mm distance measured from the edge of the deuteroconch (in Figure 7, n ≈ 6.7);
- w: Characteristic width of the equatorial chamberlets around the peripheral part of the equatorial layer (in μm).

Six of these parameters (p, d, N, H, n, and w) are used directly, while five other ones are calculated as follows:

- A: Degree of embracement of the protoconch by the deuteroconch (in %) calculated as $A = 100 \times I/(I + J)$;
- W: Estimated width of the adauxiliary chamberlets (in μm) calculated as $W = [(d + H) \times \pi - p]/(N + 1)$;
- F: Estimated shape of the adauxiliary chamberlets (in %) calculated as $F = 100 \times H/(H + W)$;
- h: Estimated height of the equatorial chamberlets close to the embryo (in μm) calculated as $h = (500 - H)/(n - 1)$;
- G: Estimated shape of the equatorial chamberlets close to the embryo (in %) calculated as $G = 100 \times h/(h + w)$.

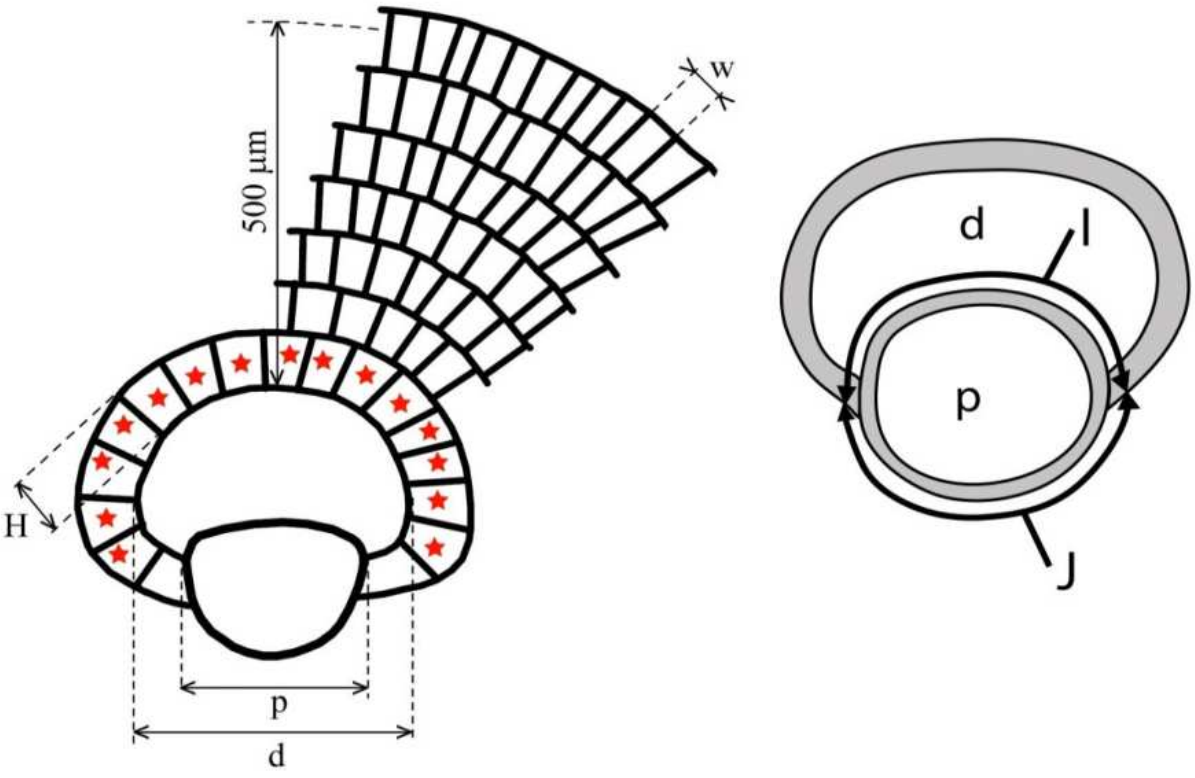

Figure 7. Measurement system for orthophragmines.

6.1.1. Family Discocyclinidae Galloway, 1928

Two genera, namely *Discocyclina* and *Nemkovella*, are recorded from Verona. The diagnostic difference between them is the presence (*Discocyclina*) and absence (*Nemkovella*) of proximal annular stolon.

Table 2. Statistical data of the embryonal part of orthophragmine populations from Verona.

Parameters		Outer Cross-Diameter of the Protoconch			Outer Cross-Diameter of the Deuterococh			Deuteroconchal Embracement			Subspecies
		p (μm)			d (μm)			A			
Species	**Sample**	**No**	**Range**	**Mean ± s.e.**	**No**	**Range**	**Mean ± s.e.**	**No**	**Range**	**Mean ± s.e.**	
Discocyclina augustae	**VER 2–4**	**75**	**110–195**	**137.4 ± 1.9**	**83**	**170–355**	**260.5 ± 4.0**	**75**	**45–80**	**60.2 ± 0.8**	*augustae*
	VER 2	21	110–155	131.2 ± 2.9	22	180–355	259.8 ± 7.9	22	51–80	62.4 ± 1.6	
	VER 3	16	120–195	146.9 ± 5.0	18	205–300	270.0 ± 6.0	16	49–68	58.8 ± 1.4	
	VER 4	38	110–180	136.8 ± 2.5	43	170–335	256.9 ± 6.0	37	45–71	59.5 ± 1.1	
D. dispansa	**VER 3 + 4**	**30**	**150–365**	**245.8 ± 8.2**	**32**	**360–655**	**503.8 ± 12.7**	**30**	**60–100**	**75.4 ± 1.7**	*dispansa*
	VER 3	7	150–260	212.9 ± 14.8	7	360–585	479.3 ± 34.6	7	66–86	76.5 ± 2.7	
	VER 4	23	195–365	255.9 ± 8.7	25	400–655	510.6 ± 12.7	23	60–100	75.1 ± 2.0	
D. euaensis	**VER 2**	**24**	**140–355**	**199.0 ± 10.2**	**27**	**385–715**	**515.6 ± 14.9**	**21**	**66–100**	**79.2 ± 1.7**	—
D.pratti	**VER 4**	**6**	**225–340**	**282.5 ± 17.7**	**11**	**500–1100**	**778.6 ± 49.4**	**7**	**62–100**	**76.7 ± 5.8**	*minor*
D. radians	**VER 4**	**1**		**155.0**	**2**	**325–375**	**350.0**	**1**		**56.0**	cf. *radians*
D. trabayensis	**VER 2–4**	**26**	**60–120**	**77.3 ± 2.7**	**25**	**110–190**	**137.0 ± 4.0**	**20**	**44–73**	**53.2 ± 1.5**	*elazigensis*
	VER 2	2	85–120	102.5	2	155–160	157.5	2	45–54	49.2	
	VER 3	2	65–120	92.5	2	130–180	155.0	2	56–57	56.4	
	VER 4	22	60–85	73.6 ± 1.3	21	110–190	133.4 ± 3.9	16	44–73	54.2 ± 1.7	
Nemkovella strophiolata	**VER 2–4**	**44**	**100–175**	**134.6 ± 2.5**	**48**	**175–335**	**235.0 ± 4.3**	**39**	**38–67**	**48.8 ± 0.9**	*tenella*
	VER 2	9	100–145	125.0 ± 5.4	13	185–335	238.5 ± 9.6	7	42–67	52.5 ± 3.6	
	VER 3	7	115–175	144.3 ± 8.0	7	175–285	243.6 ± 14.7	5	38–50	46.2 ± 1.9	
	VER 4	28	110–160	135.3 ± 2.5	28	195–280	231.2 ± 4.5	27	43–61	48.4 ± 0.8	
N. daguini	**VER 4**	**1**		**60.0**	**1**		**80.0**	**1**		**40.0**	—
Orbitoclypeus varians	**VER 2**	**10**	**180–280**	**221.0 ± 8.8**	**10**	**335–445**	**375.0 ± 10.2**	**9**	**63–100**	**85.8 ± 4.0**	*scalaris*
	VER 3 + 4	**27**	**180–315**	**235.1 ± 7.8**	**28**	**355–580**	**428.0 ± 10.7**	**24**	**60–100**	**82.9 ± 2.1**	*varians*
	VER 3	2	225–265	245.0	2	355–490	422.5	2	62–84	73.3	
	VER 4	25	180–315	234.3 ± 8.3	26	360–580	428.5 ± 10.9	22	60–100	83.8 ± 2.0	

Table 2. *Cont.*

Parameters		Outer Cross-Diameter of the Protoconch			Outer Cross-Diameter of the Deuterococh			Deuteroconchal Embracement			Subspecies
		p (μm)			d (μm)			A			
Species	Sample	No	Range	Mean ± s.e.	No	Range	Mean ± s.e.	No	Range	Mean ± s.e.	
Asterocyclina alticostata	**VER 1**	**1**		**420.0**	**1**		**610.0**	**1**		**40.1**	—
	VER 2–4	**7**	**260–410**	**342.1 ± 22.3**	**7**	**380–570**	**472.9 ± 23.0**	**7**	**37–55**	**43.0 ± 2.0**	*danubica*
	VER 2	2	280–340	310.0	2	415–435	425.0	2	240–40	40.2	
	VER 3	2	395–410	402.5	2	490–505	497.5	2	2|42–44	43.0	
	VER 4	3	260–410	323.3	3	380–570	488.3	3	37–55	45.0	
A. stellata	**VER 1**	**2**	**125–145**	**135.0**	**2**	**195–205**	**200.0**	**2**	**47–47**	**47.2**	cf. *stellaris*
	VER 2–4	**80**	**100–200**	**136.3 ± 2.1**	**83**	**155–300**	**211.0 ± 3.0**	**71**	**31–64**	**46.7 ± 0.7**	*stellaris*
	VER 2	26	110–165	136.2 ± 2.8	27	160–270	206.3 ± 4.8	23	31–52	45.1 ± 1.0	
	VER 3	21	100–165	130.7 ± 3.5	22	175–225	198.6 ± 3.1	18	31–54	44.8 ± 1.3	
	VER 4	33	100–200	140.0 ± 3.7	34	155–300	222.8 ± 5.4	30	38–64	49.1 ± 1.1	

Table 3. Statistical data of the adauxiliary chamberlets of orthophragmine populations from Verona.

Parameters		Number			Height			Width			Shape			Subspecies
		N			H (μm)			W (μm)			F			
Species	Sample	No	Range	Mean ± s.e.	No	Range	Mean ± s.e.	No	Range	Mean ± s.e.	No	Range	Mean ± s.e.	
Discocyclina augustae	**VER 2–4**	**58**	**14–32**	**22.0 ± 0.47**	**74**	**44–81**	**58.9 ± 1.0**	**58**	**30–49**	**38.3 ± 0.5**	**58**	**51–71**	**60.6 ± 0.6**	*augustae*
	VER 2	16	14–32	22.3 ± 1.19	20	44–69	55.6 ± 1.8	16	32–49	37.9 ± 1.2	16	51–68	59.9 ± 1.1	
	VER 3	10	17–28	22.6 ± 0.95	15	50–81	67.8 ± 2.0	10	33–44	39.5 ± 1.1	10	54–71	63.1 ± 1.5	
	VER 4	32	16–30	21.6 ± 0.51	39	45–68	57.1 ± 1.1	32	30–47	38.1 ± 0.7	32	54–66	60.2 ± 0.7	
D. dispansa	**VER 3 + 4**	**25**	**30–54**	**40.4 ± 1.29**	**32**	**50–102**	**83.1 ± 2.1**	**25**	**28–50**	**39.0 ± 1.2**	**25**	**61–74**	**68.2 ± 0.7**	*dispansa*
	VER 3	5	35–42	38.2 ± 1.43	7	50–102	86.6 ± 6.9	5	33–50	40.4 ± 2.6	5	67–73	69.2 ± 1.0	
	VER 4	20	30–54	41.0 ± 1.55	25	61–94	82.2 ± 1.8	20	28–48	38.7 ± 1.3	20	61–74	67.9 ± 0.8	
D. euaensis	**VER 2**	**21**	**28–43**	**35.6 ± 0.86**	**27**	**93–137**	**110.7 ± 1.7**	**21**	**36–60**	**48.5 ± 1.3**	**21**	**66–73**	**69.5 ± 0.4**	—

Table 3. *Cont.*

Parameters		Number			Height			Width			Shape			Subspecies
		N			H (μm)			W (μm)			F			
Species	**Sample**	**No**	**Range**	**Mean ± s.e.**	**No**	**Range**	**Mean ± s.e.**	**No**	**Range**	**Mean ± s.e.**	**No**	**Range**	**Mean ± s.e.**	
D.pratti	**VER 4**	**6**	**34–50**	**42.2 ± 2.06**	**11**	**82–140**	**104.6 ± 4.8**	**6**	**44–75**	**56.3 ± 4.5**	**6**	**52–70**	**63.4 ± 2.5**	*minor*
D. radians	**VER 4**	**2**	**26–28**	**27.0**	**2**	**82–95**	**88.7**	**2**	**40–53**	**46.7**	**2**	**61–70**	**65.5**	cf. *radians*
D. trabayensis	**VER 2–4**	**16**	**8–11**	**9.6 ± 0.25**	**20**	**25–41**	**33.0 ± 0.8**	**16**	**36–51**	**43.0 ± 1.0**	**16**	**36–50**	**43.2 ± 0.9**	*elazigensis*
	VER 2	1		11.0	1		41.0	1	36–51	44.2	1		48.1	
	VER 3				1		30.0							
	VER 4	15	8–11	9.5 ± 0.25	18	25–37	32.6 ± 0.7	15		42.9 ± 1.0	15	36–50	42.9 ± 0.9	
Nemkovella strophiolata	**VER 2–4**	**39**	**11–20**	**15.2 ± 0.38**	**48**	**37–58**	**43.6 ± 0.5**	**39**	**36–54**	**45.9 ± 0.7**	**39**	**42–56**	**48.6 ± 0.5**	*tenella*
	VER 2	9	12–20	14.9 ± 0.79	13	37–58	44.0 ± 1.3	9	36–52	46.2 ± 1.6	9	45–52	48.2 ± 0.9	
	VER 3	5	12–18	14.6 ± 1.04	7	40–48	44.5 ± 1.1	5	45–51	48.2 ± 1.2	5	44–52	47.6 ± 1.1	
	VER 4	25	11–19	15.4 ± 0.47	28	37–52	43.1 ± 0.6	25	37–54	45.0 ± 1.0	25	42–56	49.1 ± 0.7	
N. daguini	**VER 4**	**1**		**2.0**	**1**		**25.0**	**1**		**90.0**	**1**		**21.7**	—
Orbitoclypeus varians	**VER 2**	**10**	**23–37**	**29.2 ± 1.19**	**10**	**54–100**	**78.8 ± 4.6**	**10**	**33–53**	**40.5 ± 2.0**	**10**	**59–71**	**65.8 ± 1.0**	*scalaris*
	VER 3 + 4	**27**	**24–38**	**30.3 ± 0.70**	**28**	**55–99**	**82.5 ± 2.1**	**27**	**35–56**	**44.3 ± 1.2**	**27**	**56–71**	**65.1 ± 0.7**	*varians*
	VER 3	2	24–37	30.5	2	55–93	73.9 ±	2	41–43	41.9	2	56–69	62.8	
	VER 4	25	25–38	30.3 ± 0.67	26	67–99	83.1 ± 1.9	25	35–56	44.5 ± 1.3	25	60–71	65.2 ± 0.6	
Asterocyclina alticostata	**VER1**	**1**		**4.0**	**1**		**68.0**	**1**		**342.0**	**1**		**16.6**	—
	VER 2–4	**7**	**3–5**	**4.1 ± 0.24**	**7**	**67–99**	**83.4 ± 4.2**	**7**	**229–395**	**278.4 ± 20.9**	**7**	**17–29**	**23.5 ± 1.5**	*danubica*
	VER 2	2	4–4	4.0	2	75–87	81.2	2	252–260	256.1	2	23–25	24.0	
	VER 3	2	5–5	5.0	2	97–99	98.1	2	241–248	244.8	2	29–29	28.6	
	VER 4	3	3–4	3.7	3	67–84	75.1	3	229–395	315.7	3	17–23	19.6	
A. stellata	**VER 1**	**2**	**3–4**	**3.5**	**2**	**49–55**	**52.2**	**2**	**125–173**	**148.7**	**2**	**24–28**	**26.3**	cf. *stellaris*
	VER 2–4	**76**	**3–6**	**3.5 ± 0.07**	**78**	**40–89**	**57.0 ± 1.0**	**76**	**87–255**	**156.4 ± 3.0**	**73**	**21–38**	**26.7 ± 0.4**	*stellaris*
	VER 2	24	3–5	3.5 ± 0.12	26	40–69	52.2 ± 1.5	24	109–201	149.2 ± 4.7	23	21–32	25.7 ± 0.5	
	VER 3	18	3–6	3.4 ± 0.20	19	43–67	56.0 ± 1.5	18	87–188	152.0 ± 6.2	17	21–38	27.0 ± 1.0	
	VER 4	34	3–5	3.6 ± 0.09	33	40–89	61.3 ± 1.6	34	123–255	163.9 ± 4.3	33	21–32	27.1 ± 0.5	

Table 4. Statistical data of the equatorial chamberlets of orthophragmine populations from Verona.

Parameters		No of Annuli in the First 0.5 mm from the Deuteroconch			Height			Width			Shape			Subspecies
		n			h (μm)			w (μm)			G			
Species	**Sample**	**No**	**Range**	**Mean ± s.e.**	**No**	**Range**	**Mean ± s.e.**	**No**	**Range**	**Mean ± s.e.**	**No**	**Range**	**Mean ± s.e.**	
Discocyclina augustae	**VER 2–4**	**71**	**10.2–17.5**	**13.2 ± 0.2**	**70**	**28–49**	**36.6 ± 0.6**	**71**	**21–32**	**25.7 ± 0.3**	**70**	**49–66**	**58.7 ± 0.5**	*augustae*
	VER 2	20	10.2–17.5	13.6 ± 0.4	20	28–49	36.2 ± 1.2	20	22–32	25.9 ± 0.6	20	49–65	58.1 ± 1.0	
	VER 3	15	11.0–16.0	12.5 ± 0.4	14	30–44	38.0 ± 1.2	15	21–30	25.8 ± 0.7	14	51–66	59.6 ± 1.1	
	VER 4	36	10.8–15.6	13.3 ± 0.2	36	30–44	36.3 ± 0.6	36	22–29	25.5 ± 0.3	36	51–64	58.6 ± 0.5	
D. dispansa	**VER 3 + 4**	**30**	**7.7–12.1**	**9.8 ± 0.2**	**30**	**38–61**	**48.0 ± 1.1**	**30**	**23–33**	**27.0 ± 0.4**	**30**	**54–70**	**63.8 ± 0.6**	—
	VER 3	6	7.7–12.1	10.0 ± 0.8	6	38–61	47.9 ± 3.9	6	24–31	26.7 ± 1.0	6	61–69	63.8 ± 1.4	*dispansa*
	VER 4	24	8.0–11.5	9.8 ± 0.2	24	40–60	48.1 ± 1.1	24	23–33	27.1 ± 0.5	24	54–70	63.9 ± 0.7	
D.euaensis	**VER 2**	**27**	**5.9–8.8**	**7.0 ± 0.1**	**27**	**50–79**	**65.8 ± 1.5**	**27**	**22–33**	**29.6 ± 0.5**	**27**	**62–74**	**68.8 ± 0.6**	
D.pratti	**VER 4**	**10**	**4.6–6.1**	**5.1 ± 0.1**	**10**	**79–110**	**96.8 ± 3.0**	**10**	**28–42**	**36.3 ± 1.3**	**10**	**66–79**	**72.6 ± 1.2**	*minor*
D.radians	**VER 4**	**2**	**9.5–9.7**	**9.6**	**2**	**47–49**	**47.8**	**2**	**25–25**	**24.8**	**2**	**65–67**	**65.9**	cf. *radians*
D. trabayensis	**VER 2–4**	**20**	**11.0–21.0**	**16.7 ± 0.4**	**19**	**24–33**	**29.5 ± 0.6**	**20**	**24–32**	**27.9 ± 0.5**	**19**	**48–57**	**51.3 ± 0.5**	
	VER 2	2	11.0–15.0	13.0	1		32.8	2	27–31	29.0	1		51.4	*elazigensis*
	VER 3	1	17.2	17.2	1		28.9	1		29.9	1		49.2	
	VER 4	17	15.0–21.0	17.1 ± 0.4	17	24–33	29.3 ± 0.6	17	24–32	27.6 ± 0.6	17	48–57	51.5 ± 0.5	
Nemkovella strophiolata	**VER 2–4**	**44**	**12.8–19.0**	**15.7 ± 0.2**	**44**	**25–39**	**31.4 ± 0.5**	**44**	**23–37**	**30.4 ± 0.5**	**44**	**42–58**	**50.8 ± 0.5**	
	VER 2	13	13.3–17.5	15.3 ± 0.3	13	28–37	32.2 ± 0.8	13	27–35	31.2 ± 0.8	13	44–55	50.8 ± 0.9	*tenella*
	VER 3	5	12.8–17.0	15.1 ± 0.8	5	29–39	33.0 ± 2.0	5	25–33	30.0 ± 1.2	5	49–54	52.3 ± 1.0	
	VER 4	26	14.0–19.0	16.0 ± 0.2	26	25–35	30.6 ± 0.5	26	23–37	30.1 ± 0.7	26	42–58	50.6 ± 0.7	
N. daguini	**VER 4**	**1**		**23.0**	**1**		**21.6**	**1**		**26.0**	**1**		**45.4**	—
Orbitoclypeus varians	**VER 2**	**10**	**8.8–13.0**	**10.4 ± 0.4**	**10**	**37–55**	**45.7 ± 1.7**	**10**	**31–39**	**34.9 ± 0.6**	**10**	**49–64**	**56.5 ± 1.2**	*scalaris*
	VER 3 + 4	**28**	**7.2–12.1**	**10.2 ± 0.2**	**28**	**39–65**	**46.2 ± 1.1**	**28**	**32–43**	**36.8 ± 0.6**	**28**	**50–61**	**55.5 ± 0.6**	
	VER 3	2	10.5–11.0	10.8	2	41–47	43.8	2	34–40	37.1	2	50–58	54.1	*varians*
	VER 4	26	7.2–12.1	10.1 ± 0.2	26	39–65	46.3 ± 1.2	26	32–43	36.8 ± 0.6	26	51–61	55.6 ± 0.6	

Table 4. *Cont.*

Parameters		No of Annuli in the First 0.5 mm from the Deuteroconch			Height			Width			Shape			Subspecies
		n			h (μm)			w (μm)			G			
Species	**Sample**	**No**	**Range**	**Mean ± s.e.**	**No**	**Range**	**Mean ± s.e.**	**No**	**Range**	**Mean ± s.e.**	**No**	**Range**	**Mean ± s.e.**	
Asterocyclina alticostata	**VER1**	**1**		**7.2 ±**	**1**		**69.7**	**1**		**41.6**	**1**		**62.6**	—
	VER 2–4	**7**	**8.5–11.8**	**10.2 ± 0.4**	**7**	**39–54**	**45.9 ± 1.8**	**7**	**30–45**	**37.8 ± 1.7**	**7**	**51–61**	**54.8 ± 1.5**	*danubica*
	VER 2	2	9.5–11.0	10.3	2	41–50	45.6	2	40–40	40.0	2	51–56	53.2	
	VER 3	2	8.5–9.5	9.0	2	47–54	50.4	2	30–36	32.9	2	60–61	60.5	
	VER 4	3	10.0–11.8	10.9	3	39–48	43.0	3	35–45	39.6	3	51–54	52.1	
A. stellata	**VER1**	**2**	**18.0–18.0**	**18.0**	**2**	**26–27**	**26.3**	**2**	**25–27**	**26.0**	**2**	**49–51**	**50.3**	cf. *stellaris*
	VER 2–4	**57**	**14.5–20.7**	**17.3 ± 0.2**	**56**	**23–33**	**27.4 ± 0.3**	**58**	**22–32**	**27.8 ± 0.4**	**56**	**45–56**	**49.8 ± 0.4**	*stellaris*
	VER 2	20	14.5–19.5	17.4 ± 0.3	20	25–33	27.5 ± 0.5	21	22–32	28.1 ± 0.7	20	45–56	49.8 ± 0.7	
	VER 3	13	15.0–20.0	17.2 ± 0.4	12	23–32	27.8 ± 0.8	13	25–31	28.5 ± 0.4	12	45–56	49.3 ± 0.9	
	VER 4	24	15.8–20.7	17.3 ± 0.3	24	23–30	27.1 ± 0.4	24	24–32	27.2 ± 0.5	24	45–55	50.0 ± 0.6	

Genus *Discocyclina* Gümbel, 1870

Representatives of six species of this genus were found in the three samples from Verona, Castel San Felice. For comparison, they are shown together at the same magnification in Figures 8 and 9.

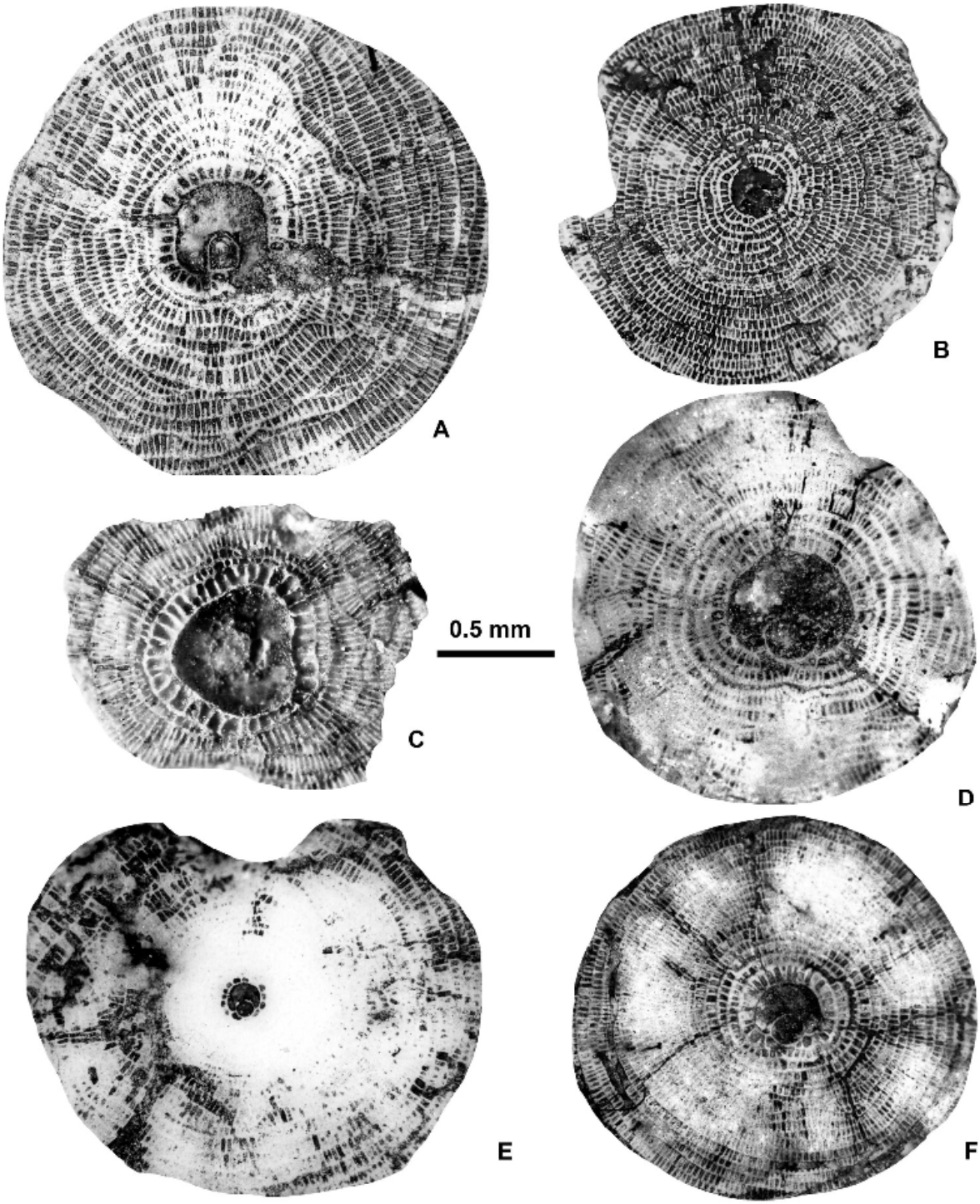

Figure 8. Equatorial sections of A-forms of different *Discocyclina* in Castel San Felice. (**A**): *D. euaensis* Whipple, E.2025.44, (**B**): *D. augustae augustae* van der Weijden, E.2025.10, (**C**): *D. pratti minor* Meffert, E.2025.52, (**D**): *D. dispansa dispansa* (Sowerby), E.2025.28, (**E**): *D. trabayensis elazigensis* Özcan & Less, E.2025.57, and (**F**): *D. radians* cf. *radians* (d'Archiac), E.2025.56. (**A**,**B**,**E**): VER 2; (**C**,**F**): VER 4; and (**D**): VER 3.

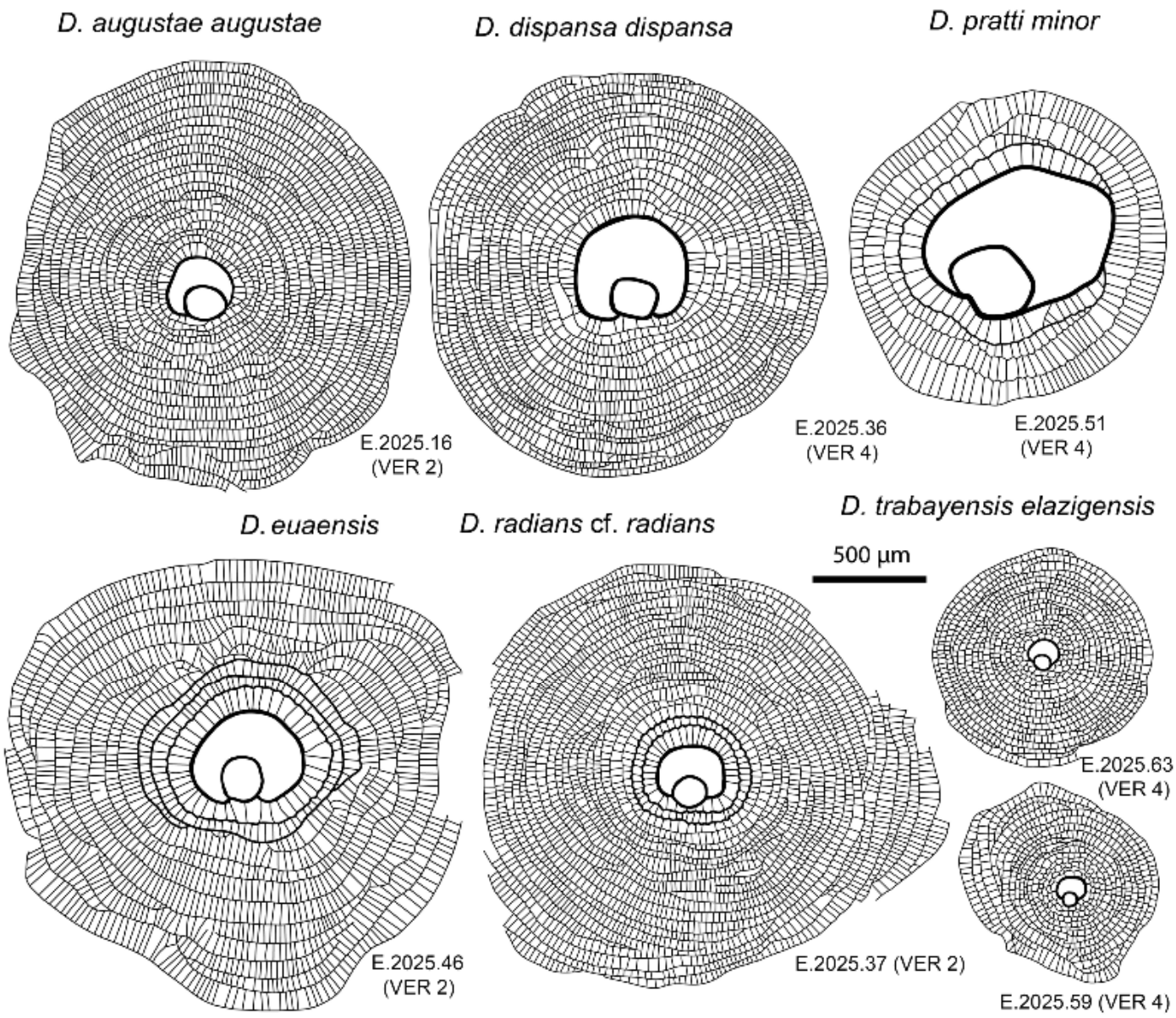

Figure 9. Drawings of equatorial sections of different A-forms of *Discocyclina* in Castel San Felice.

1. *Discocyclina augustae* van der Weijden, 1940

This very common unribbed species is usually small and flat. It has a very small to small, semi-iso- to nephrolepidine embryo, narrow and low "archiaci"-type adauxiliary chamberlets, and also narrow and relatively low equatorial chamberlets, mostly with a "strophiolata" type growth pattern.

Discocyclina augustae forms an evolutionary lineage with four chrono-subspecies, including *D. a. sourbetensis* (d_{mean} < 145 µm; SBZ 8–13; OZ 4–?9), *D. a. atlantica* (d_{mean} = 145–180 µm; SBZ 13–17; OZ 9–12), *D. a. olianae* (d_{mean} = 180–225 µm; SBZ 17–19a; OZ 12–14), and *D. a. augustae* (d_{mean} > 225 µm; SBZ 18c–20; OZ 14–16) [7,8].

This species is the most common in all three samples (VER 2–4) from Castel San Felice. Their quantitative parameters are very similar (Tables 2–4), therefore, they can be jointly evaluated and determined as *Discocyclina augustae augustae*.

- *Discocyclina augustae augustae* van der Weijden, 1940

  Figures 8B, 9, 10A–L and 11.
  Discocyclina augustae n. sp.—[55]: 23–26, Plate 1: 4, 5, 7, 8, Plate 2: 1, 2, 11.

Discocyclina augustae augustae van der Weijden.—[6]: 155–156, Plate 10: 5–6, 8–12, Plate 11: 1–4. (with synonymy).—[56]: Plate 1: 3, 4.—[8]: Figure 52.13.

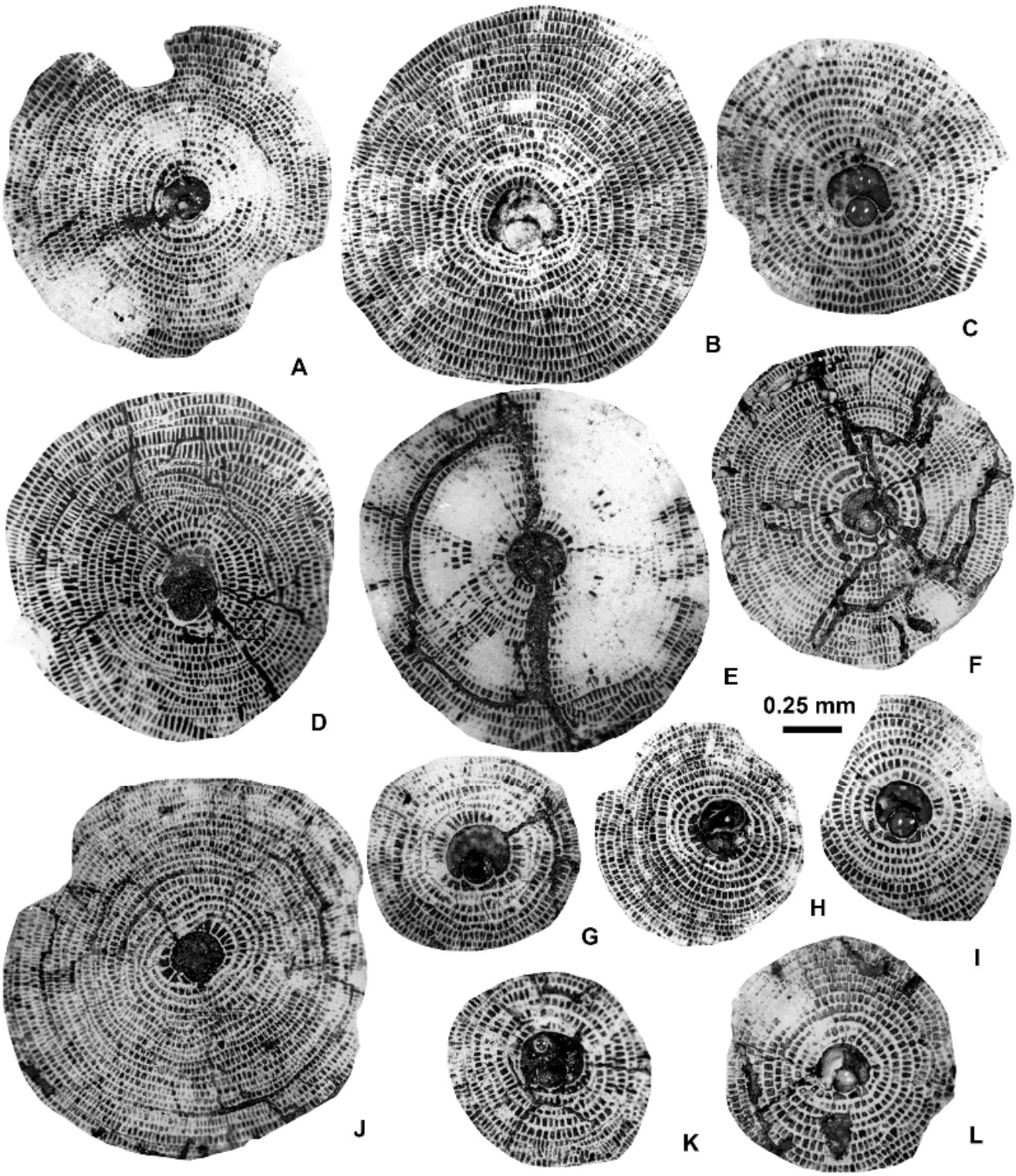

Figure 10. Equatorial sections of *Discocyclina augustae augustae* van der Weijden A-forms. (**A**): E.2025.14, (**B**): E.2025.16, (**C**): E.2025.15, (**D**): E.2025.23, (**E**): E.2025.22, (**F**): E.2025.17, (**G**): E.2025.13, (**H**): E.2025.21, (**I**): E.2025.20, (**J**): E.2025.9, (**K**): E.2025.24, and (**L**): E.2025.18. (**A**–**C**): VER 3; (**D**–**F**), (**H**,**I**,**K**,**L**): VER 4; and (**G**,**J**): VER 2.

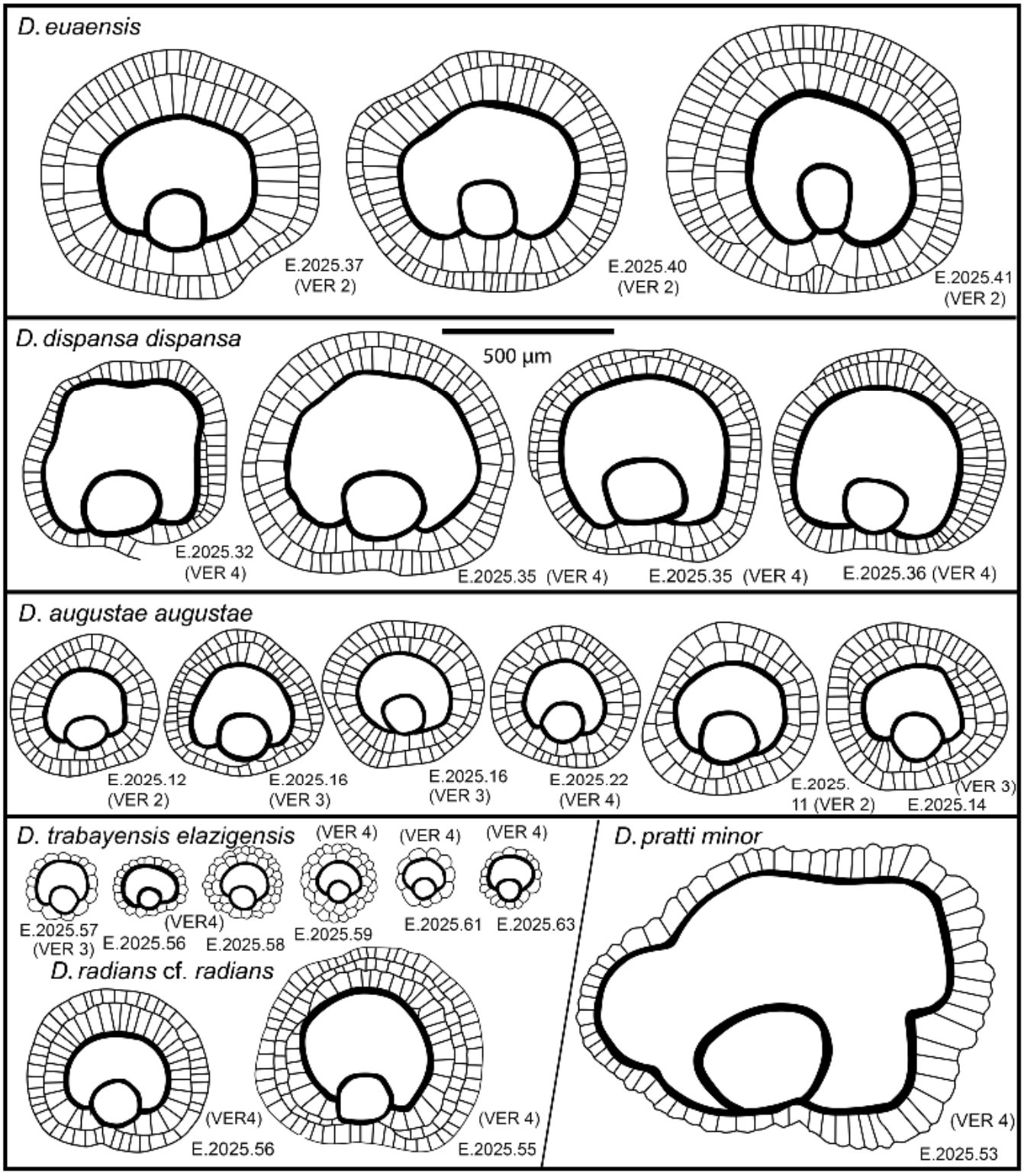

Figure 11. Comparative line drawings of the embryonal part of six species of *Discocyclina.*

Discocyclina augustae augustae and *D. dispansa dispansa* bear very similar qualitative features. *D. a. augustae* differs from *D. d. dispansa* (i) in the smaller embryo (parameters p and d, Table 2), (ii) in the less embraced protoconch by the deuteroconch (parameter A), and by the generally lower equatorial chamberlets (parameters n and h). Bivariate plots in Figure 12 also confirm the typological separation of the taxa, although a few specimens appear to be quantitatively transitional between the two taxa. The other taxon, which can be confused with *D. a. augustae*, is *D. trabayensis elazigensis*. The latter, however, has

a significantly smaller embryo and far fewer adauxiliary chamberlets (of "varians" type) than *D. a. augustae* (with "archiaci" type adauxiliary chamberlets), as shown in Figure 13. Finally, although the size and type of the embryo are very similar for both *D. a. augustae* and *Nemkovella strophiolata tenella*, the equatorial chamberlets of the latter lack proximal annular stolon, therefore, they belong to different genera.

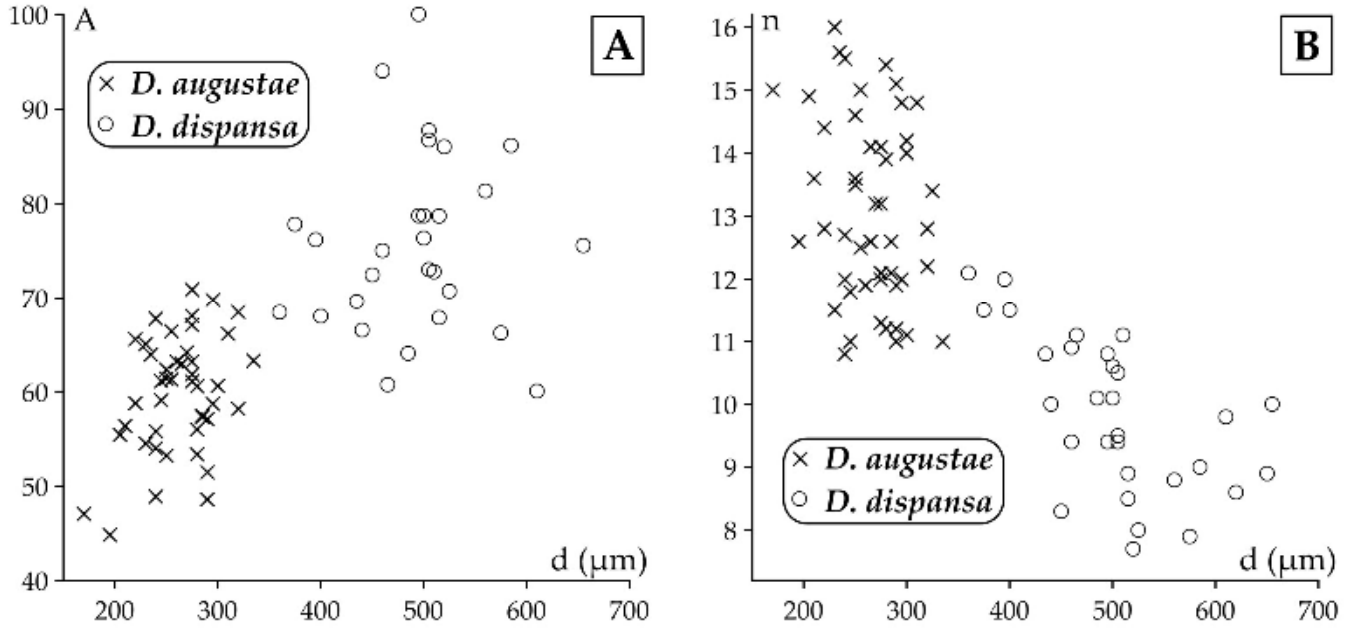

Figure 12. Distribution of *Discocyclina augustae augustae* and *D. dispansa dispansa* specimens in samples VER 3 and VER 4 (**A**) on the d–A (deuteroconch diameter vs. deuteroconchal embracement) and (**B**) on the d–n (deuteroconch diameter vs. annuli number in the first 0.5 mm from the deuteroconch's rim) bivariate plots.

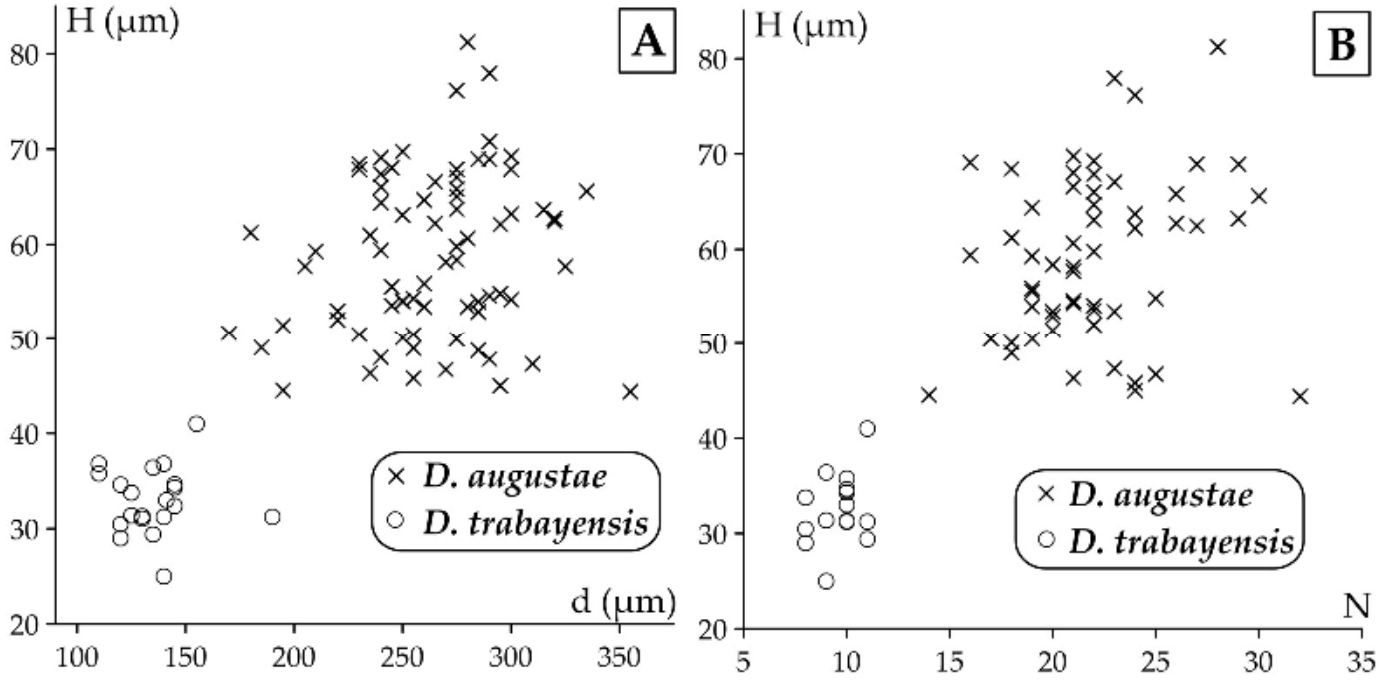

Figure 13. Distribution of *Discocyclina augustae augustae* and *D. trabayensis elazigensis* specimens in samples VER 2–4 (**A**) on the d–H (deuteroconch diameter vs. height of adauxiliary chamberlets) and (**B**) on the N–H (number of adauxiliary chamberlets vs. height of adauxiliary chamberlets) bivariate plots.

2. *Discocyclina dispansa* (Sowerby, 1840)

This widespread, flat or saddle-shaped unribbed species has a small- to medium-sized semi-nephro- to trybliolepidine embryo, moderately wide and high "archiaci"-type adauxiliary chamberlets, and also moderately wide and high equatorial chamberlets, mostly with a "strophiolata" or "varians" type growth pattern.

Discocyclina dispansa forms an evolutionary lineage with six chrono-subspecies, as follows: *D. d. broennimanni* (d_{mean} < 160 µm; SBZ 7–9; OZ 3–4); *D. d. taurica* (d_{mean} = 160–230 µm; SBZ 10–12; OZ 5–8b); *D. d. hungarica* (d_{mean} = 230–290 µm; SBZ 12–?17; OZ 8b–?12); *D. d. sella* (d_{mean} = 290–400 µm; SBZ ?13–18; OZ ?9–14); *D. d. dispansa* (d_{mean} = 400–520 µm; SBZ 17–19a; OZ 13–14); and *D. d. umbilicata* (d_{mean} > 520 µm; SBZ 19–20; OZ 14–16) [7,8].

This species is a common one in samples VER 3 and 4 from Castel San Felice, however, in sample VER 2, it is replaced by *Discocyclina euaensis*. The quantitative parameters in samples VER 3 and 4 are very similar (Tables 2–4), therefore, they can be jointly evaluated and determined as *Discocyclina dispansa dispansa*.

- *Discocyclina dispansa dispansa* (Sowerby, 1840)

Figures 8D, 9, 11 and 14A–I.

Lycophris dispansus n. sp.—[57]: 327, Plate 24: 16, 16a–b.

Discocyclina dispansa (Sowerby).—[58]: 254, 257–259, 262, Plate 3: 1–5, Plate 8: 1, 2, Plate 11: 1–12, Figures 5–7 and 11.

Discocyclina dispansa dispansa (Sowerby)—[6]: 163–164, Plate 13: 9, 12. Plate 14: 3, 6. (with synonymy).—[53]: Plate 2: 18, Figure 13.—[59]: Figure 28d–f.—[60]: 144, 146, 147, Figures 9B and 10.—[61]: 36, 38, 39, Figures 9, 12, 15 and 17.—[62]: Figure 12f.—[8]: Figures 23.3,4, 30.2,3, 57.5–8 and 60.

The distinction of *Discocyclina dispansa dispansa* from *D. augustae augustae* is discussed above (see also Figure 12), whereas that from *D. euaensis* can be found below at the latter taxa. *D. d. dispansa* can be safely separated from *D. pratti minor* based on the different type of adauxiliary chamberlets ("archiaci" vs. "pratti" for the latter). Also, the embryo of *D. p. minor* is usually larger, the protoconch is embraced more by the deuteroconch, and the equatorial chamberlets are significantly higher than in the case of *D. d. dispansa* (see below).

3. *Discocyclina euaensis* Whipple, 1932

Figures 8A, 9, 11 and 15A–G.

Discocyclina euaensis n. sp.—[63]: 84, pl. 22: 3–7, Figure 6.

Discocyclina assamica Samanta (partim).—[58]: 242, 245, 248–249, pl. 1: 1, 3–5 (non 2), pl. 9: 1–8 (non 9–12), Figures 5–7.

Discocyclina euaensis Whipple.—[6]: 175–176, pl. 19: 4–6. (with synonymy).—[53]: 500–501, pl. 3: 20, 21, 23, Figure 15.—[64]: 24, Figure 17.—[8]: 44, Figures 61.1–6 and 62.—[65]: 465, pl. 4: G–H.

Discocyclina pratti pratti (Michelin)—[59]: Figure 27q–t.

Discocyclina dispansa ex. interc. *umbilicata* (Deprat) et *dispansa* (Sowerby).—[66]: Figure 33f–g.

This unribbed species usually has a medium-sized flat test. The medium-sized embryonic apparatus is semi-nephro- to trybliolepidine. The adauxiliary chamberlets are wide, moderately high, and of the "pratti" type. The equatorial chamberlets are typically narrow and high with a "pulcra" type growth pattern. *Discocyclina euaensis* occurs in the SBZ 17–20 and OZ 13–16 Zones, respectively. It is not yet subdivided into chrono-subspecies; however, it seems that populations with a d_{mean} below 400–450 µm are characteristic for the Bartonian, while those with a d_{mean} above this value mainly occur in the Priabonian. In Verona, this taxon occurs only in sample VER 2, where it substitutes *D. dispansa dispansa* occurring in the other samples (VER 3 and 4) from Castel San Felice.

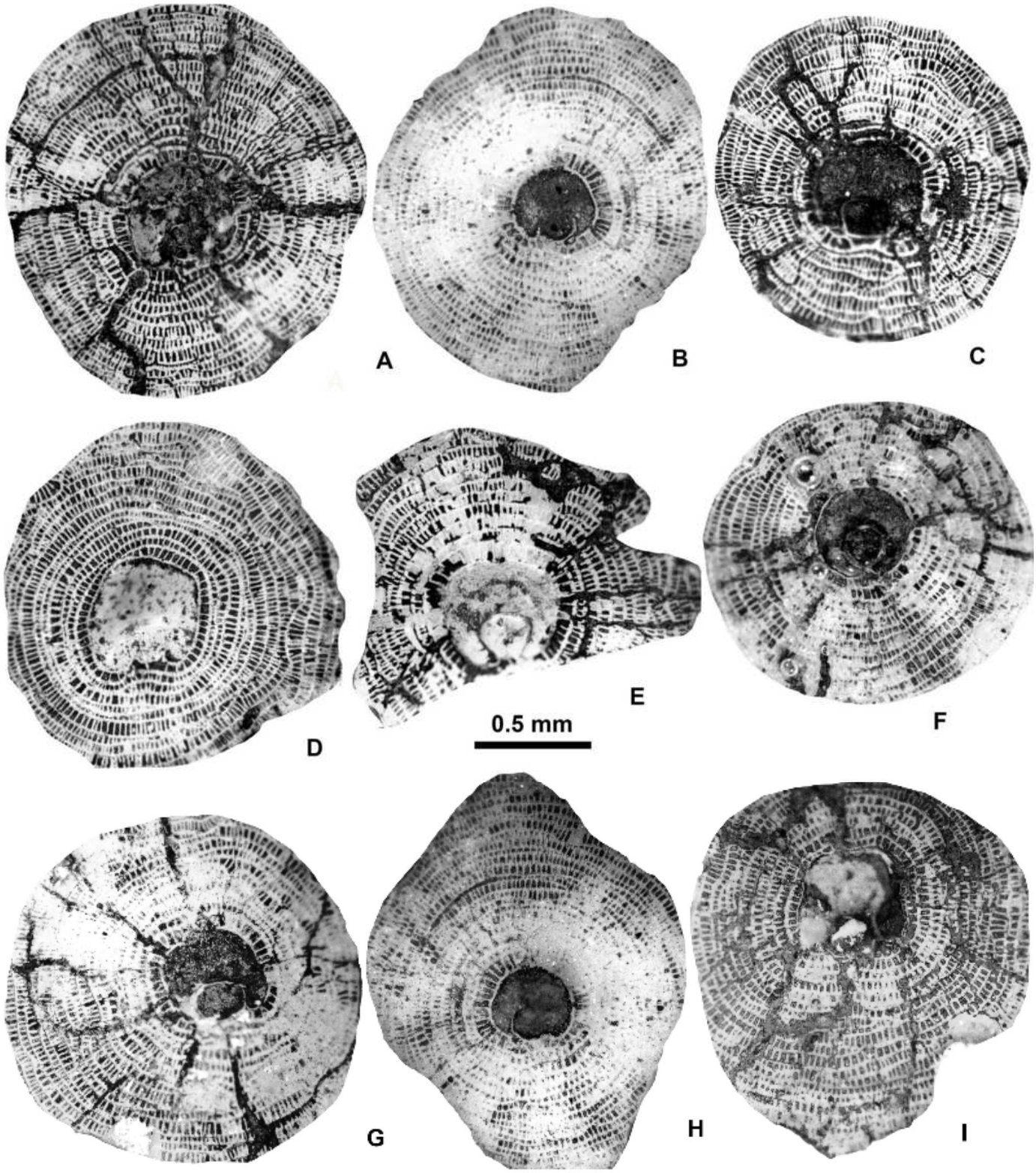

Figure 14. Equatorial sections of *Discocyclina dispansa dispansa* (Sowerby) A-forms. (**A**): E.2025.36, (**B**): E.2025.26, (**C**): E.2025.35, (**D**): E.2025.30, (**E**): E.2025.27, (**F**): E.2025.31, (**G**): E.2025.33, (**H**): E.2025.25, and (**I**): E.2025.32. (**A**,**C**,**D**,**F**,**G**,**I**): VER 4 and (**B**,**E**,**H**): VER 3.

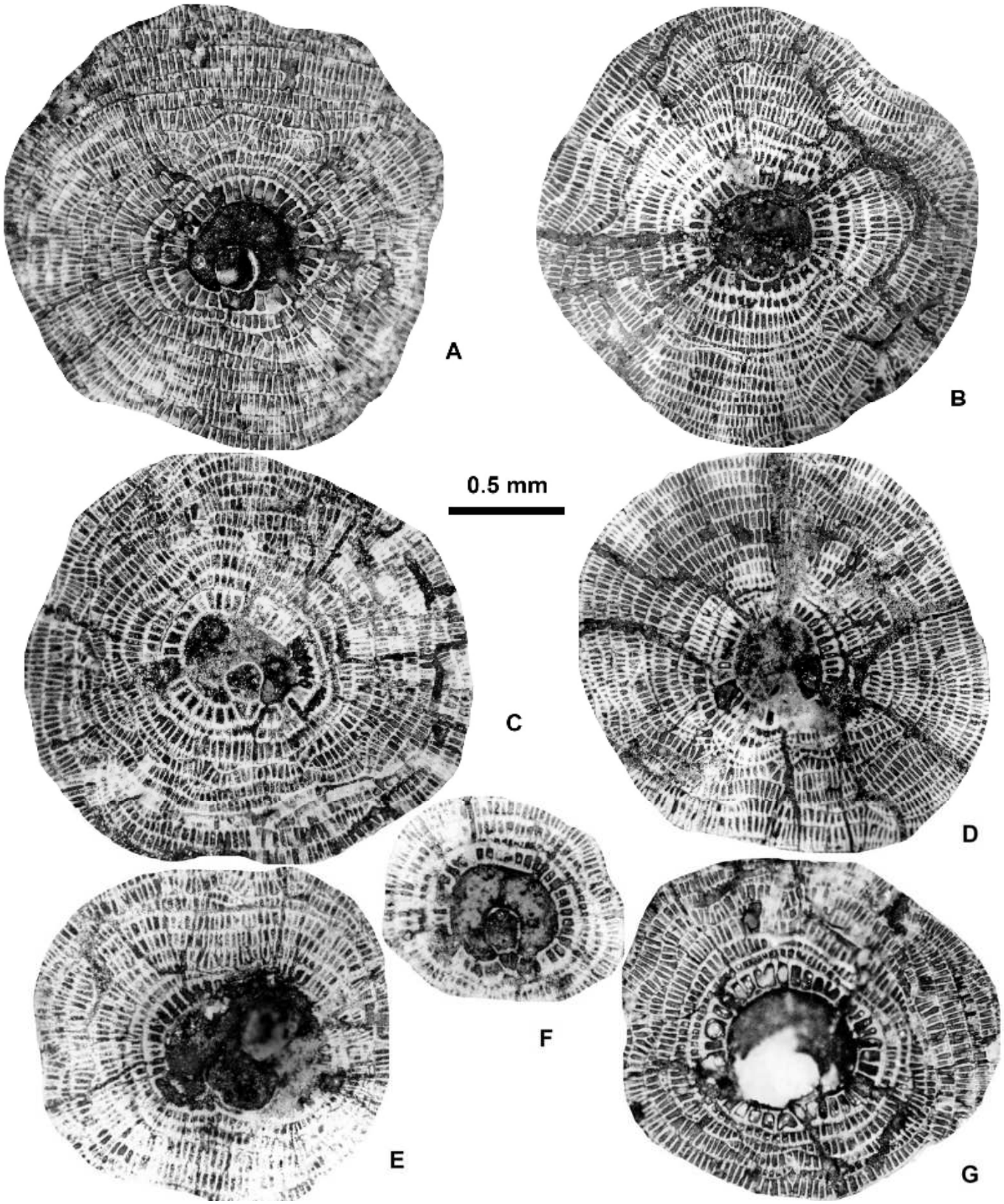

Figure 15. Equatorial sections of *Discocyclina euaensis* Whipple A-forms from sample VER 2. (**A**): E.2025.46, (**B**): E.2025.37, (**C**): E.2025.45, (**D**): E.2025.38, (**E**): E.2025.42, (**F**): E.2025.41, and (**G**): E.2025.39.

Since the *Discocyclina euaensis* population from sample VER 2 is the richest known so far from the peri-Mediterranean region, we had the opportunity to check the possible existence of the species in other localities published in our earlier publications. As a result,

we found that the populations (i) in [59] determined as *D. pratti* from samples Teke 4 and 6 and (ii) in [66] identified with *D. dispansa* from sample Kırklareli C 19 (see synonymy list) correspond, in fact, to *D. euaensis*.

Discocyclina euaensis and *D. dispansa dispansa* have a similar size and embryo type, however, they are different in (i) their type of adauxiliary chamberlets, which is of the "pratti" type for *D. euaensis* instead of the "archiaci" type for *D. d. dispansa*, and (ii) the height of both the adauxiliary and equatorial chamberlets, which are significantly larger in the case of *D. euaensis* (Figure 16). Although they are similar to *D. pratti minor* in their "pratti"-type adauxiliary chamberlets, some size parameters (d, n, and h), however, are usually smaller in the case of *D. euaensis* (see below). Finally, it is almost impossible to distinguish it from the advanced members of the *D. radians* lineage (e.g., *D. r. labatlanensis*) based solely on the characteristics of the A-form equatorial sections, however the latter is a ribbed form, unlike the unribbed *D. euaensis*.

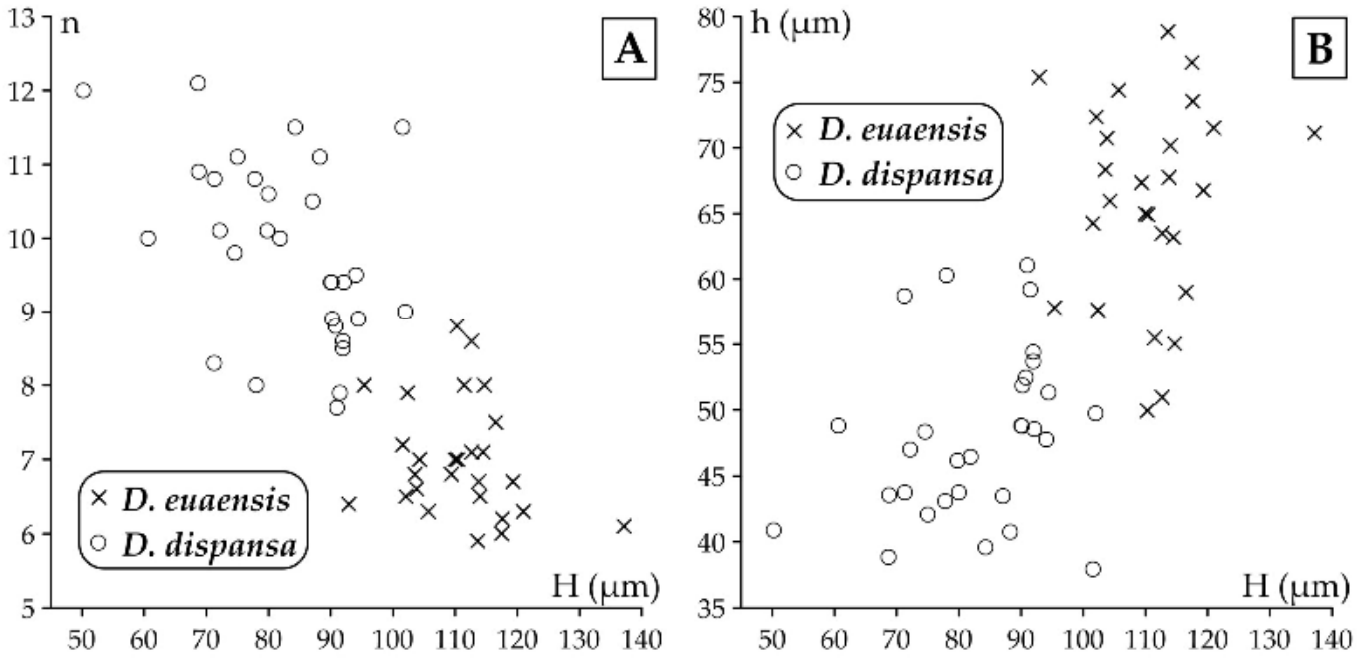

Figure 16. Distribution of specimens of *Discocyclina euaensis* (in sample VER 2) and of *D. dispansa dispansa* (in samples VER 3 and VER 4) (**A**) on the H–n (height of adauxiliary chamberlets vs. annuli number in the first 0.5 mm from the deuteroconch's rim) and (**B**) on the H–h (height of adauxiliary chamberlets vs. height of equatorial chamberlets) bivariate plots.

4. *Discocyclina pratti* (Michelin, 1846)

This rather widespread, relatively large, flat, rarely saddle-shaped, unribbed species has a medium-sized to large tryblio- to excentrilepidine embryo, numerous moderately wide and high "pratti"-type adauxiliary chamberlets, and narrow but high equatorial chamberlets with a "pulcra" type growth pattern.

Discocyclina pratti forms an evolutionary lineage with three chrono-subspecies, such as *D. p. montfortensis* (d_{mean} < 510 μm; SBZ 13–16; OZ 8b–12); *D. p. pratti* (d_{mean} = 510–700 μm; SBZ ?15–18; OZ 12–14); and *D. p. minor* (d_{mean} > 700 μm; SBZ 18c–19b; OZ 14–15) [7,8].

In Verona, *Discocyclina pratti* is rather rare, and we found it only in sample VER 4 from Castel San Felice, where, based on Tables 2–4, it is represented by *D. p. minor*.

- *Discocyclina pratti* minor Meffert, 1931

  Figures 8C, 9, 11 and 17A–F.

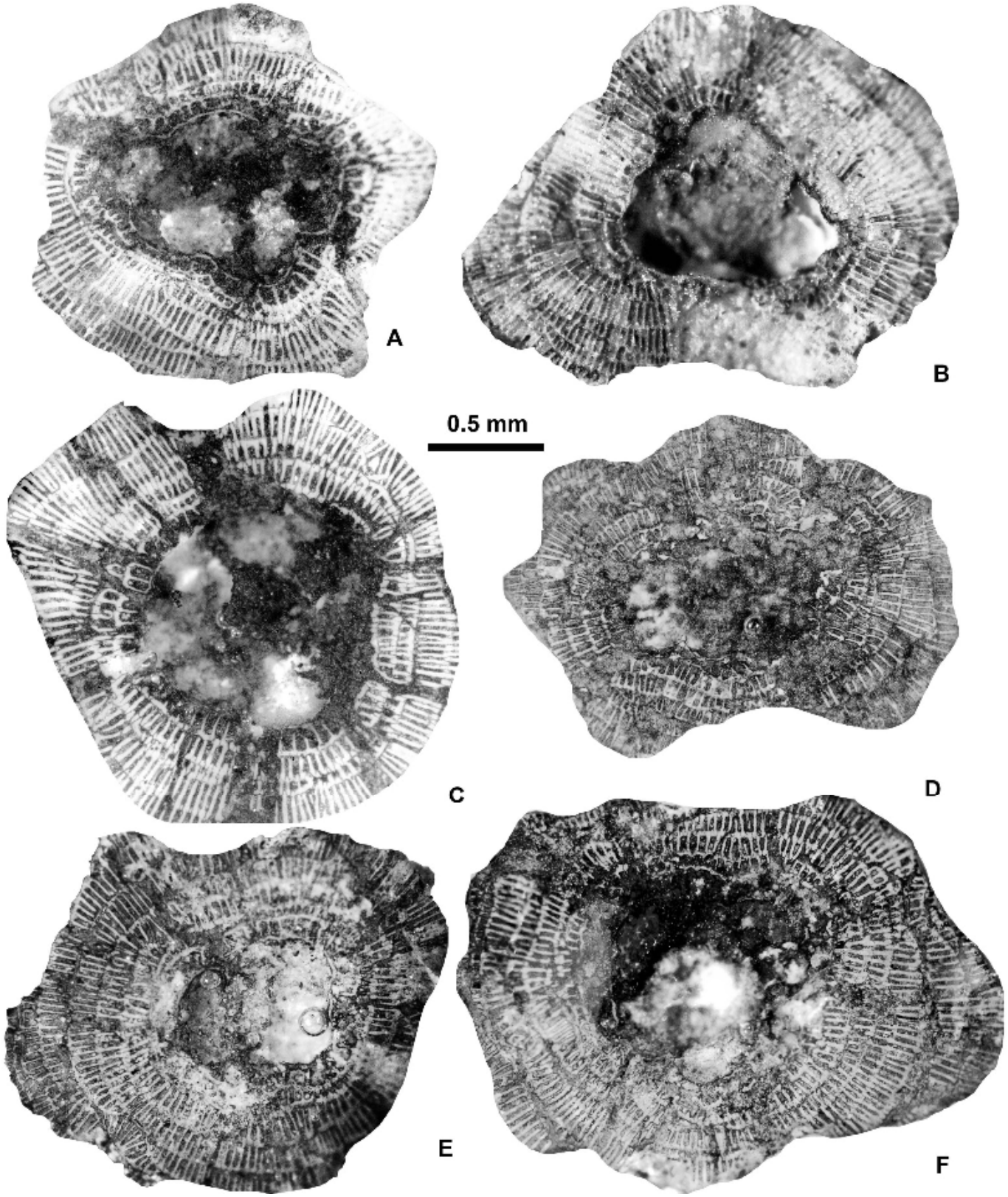

Figure 17. *Discocyclina pratti minor* Meffert A-forms from sample VER 4. (**A**): E.2025.53, (**B**): E.2025.48, (**C**): E.2025.54, (**D**): E.2025.47, (**E**): E.2025.50, and (**F**): E.2025.49.

Discocyclina umbo var. *minor* n. var.—[67]: 28–31, 54–55, Plate 6: 1–5, Plate 7: 2, Figures 4–6.
Discocyclina pratti minor Meffert—[6]: 179–180, Plate 20: 12, Plate 21: 1–3. (with synonymy)—[66]: Figure 33s.—[60]: 151, Figure 15.—[68]: Figures 24c–e and 25a–d.—[8]: Figure 81.

The distinction of *Discocyclina pratti minor* from *D. dispansa dispansa* and *D. euaensis* is discussed in the remarks on these taxa (see also Figures 18 and 19).

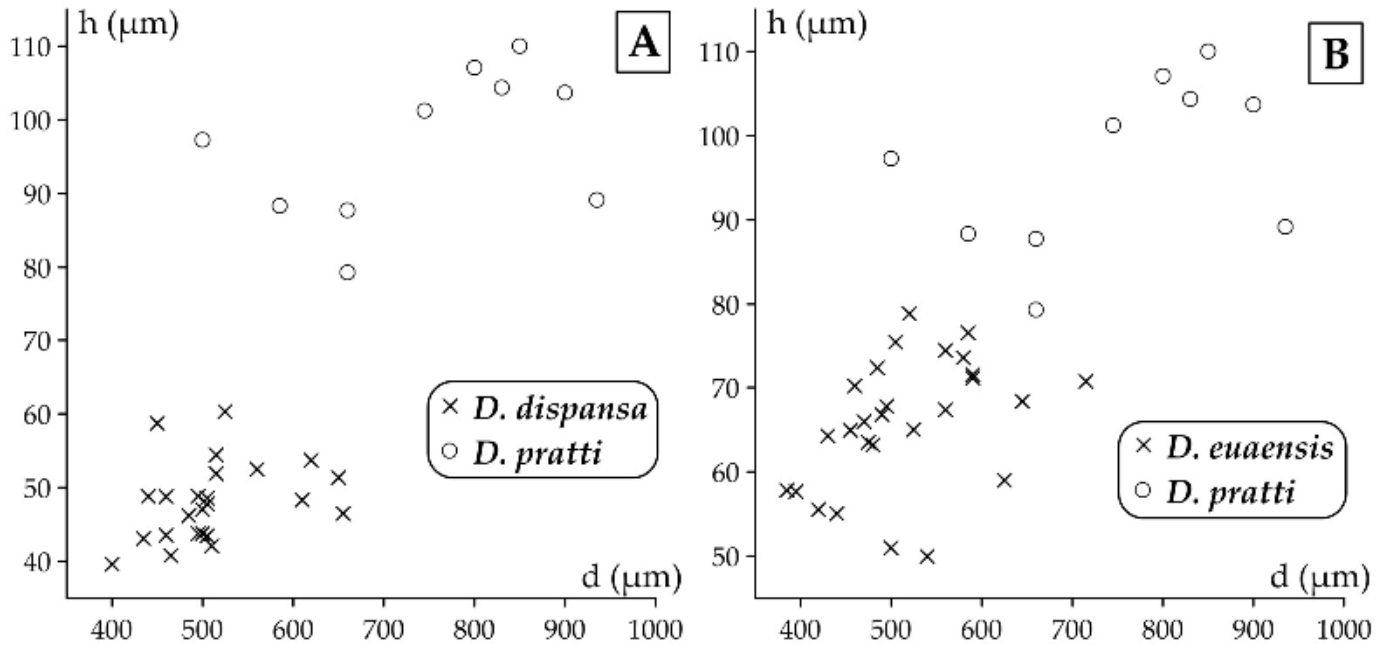

Figure 18. Distribution of specimens on the d–h (deuteroconch diameter vs. height of equatorial chamberlets) bivariate plots for (**A**) *Discocyclina pratti minor* and *D. dispansa dispansa* in sample VER 4 and for (**B**) *D. pratti minor* in sample VER 4 and *D. euaensis* in sample VER 2.

5. *Discocyclina radians* (d'Archiac, 1850)

Figures 8F, 9, 11 and 19A,B.

Orbitolites radians n. sp.—[2]: 405–406, Plate 8: 15, 15a–b.

Discocyclina radians (d'Archiac).—[6]: 166–169, Plate 15: 1–15, Plate 16: 1–7. (with three subspecies and synonymies)—[8]: 52, 54. (with four subspecies).

This ribbed species bears a small- to medium-sized semi-nephro- to trybliolepidine-type embryo, wide and moderately high "pratti"-type adauxiliary chamberlets, and narrow and high equatorial chamberlets with a "pulcra"-type growth pattern.

Discocyclina radians forms an evolutionary lineage with four chrono-subspecies, as follows: *D. r.* n. ssp. Caupenne (in Less, 1998 with d_{mean} < 240 μm; SBZ 12–13; OZ 8b); *D. r. noussensis* (d_{mean} = 240–300 μm; SBZ 13; OZ 9); *D. r. radians* (d_{mean} = 300–375 μm; SBZ 13–19a; OZ ?9–14); and *D. r. labatlanensis* (d_{mean} > 375 μm; SBZ ?16–20; OZ ?12–16) [7,8].

We found only two specimens of this species in sample VER 4 from Castel San Felice. Based on the data in Tables 2–4, it can be determined as *Discocyclina radians* cf. *radians*. This is roughly in agreement with the data of [31] (more details in Chapter 3).

6. *Discocyclina trabayensis* Neumann, 1955

This small and flat unribbed species has a very small iso- to nephrolepidine embryo, very low, relatively wide, characteristic "varians"-type adauxiliary chamberlets (lobulate in outline), and narrow equatorial chamberlets with a "trabayensis"-type growth pattern.

Discocyclina trabayensis forms an evolutionary lineage with three chrono-subspecies, including *D. t. trabayensis* (d_{mean} < 125 μm; SBZ 10–17; OZ 5–13); *D. t. elazigensis* (d_{mean} = 125–170 μm; SBZ 18–19; OZ 14–15); and *D. t. vicenzensis* (d_{mean} > 170 μm; SBZ 20; OZ 16) [7,8].

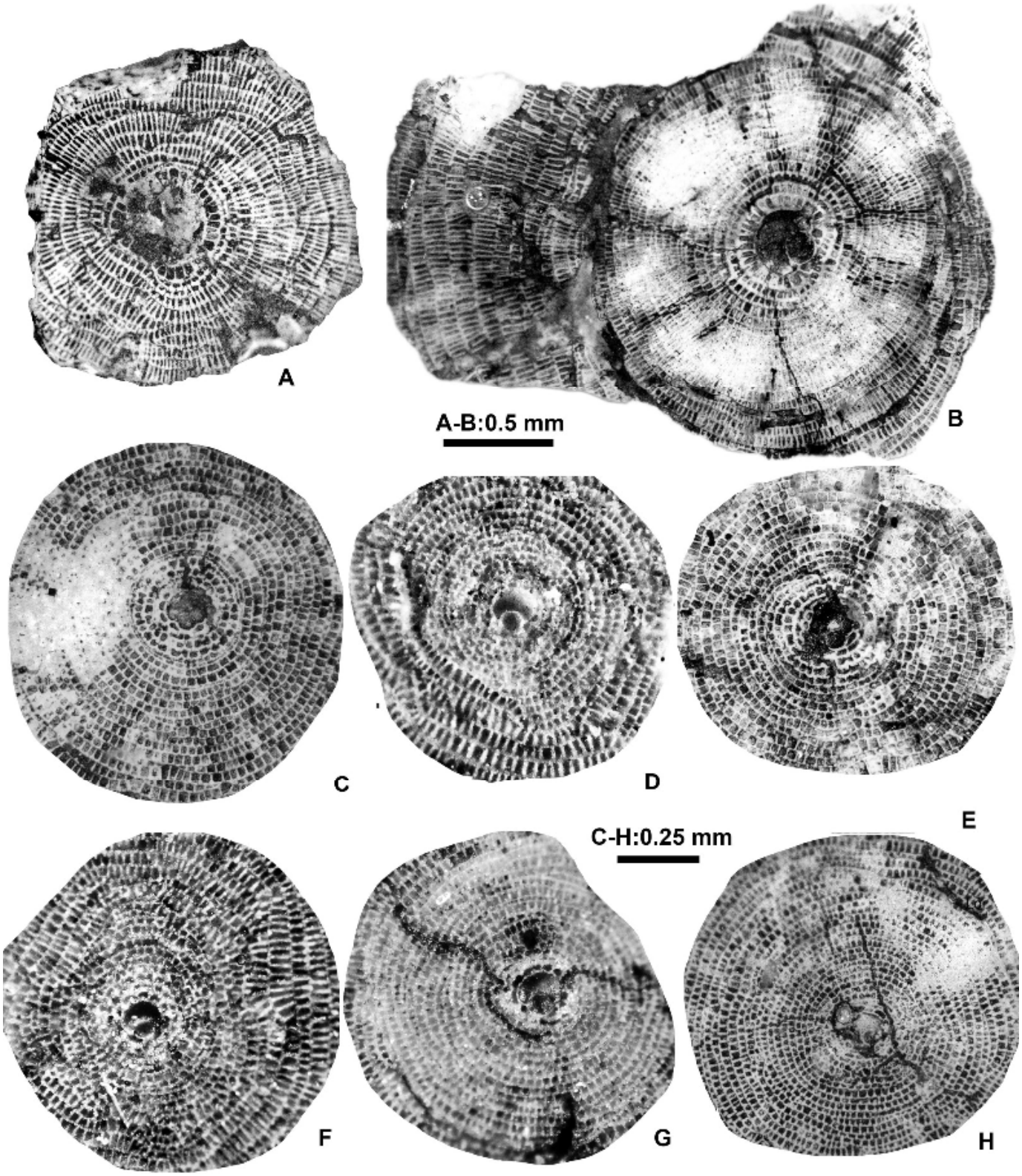

Figure 19. Equatorial sections of *Discocyclina radians* cf. *radians* (d'Archiac) (**A**,**B**) and *D. trabayensis elazigensis* Özcan & Less (**C**–**H**), (**A**): E.2025.55, (**B**): E.2025.56, (**C**): E.2025.60, (**D**): E.2025.63, (**E**): E.2025.62, (**F**): E.2025.61, (**G**): E.2025.59, and (**H**): E.2025.64. All A-forms from sample VER 4.

In Castel San Felice, *Discocyclina trabayensis* is common in sample VER 4, but rather rare in the other two (VER 2 and 3). Based on their quantitative parameters (Tables 2–4), the three populations can be jointly evaluated and determined as *D. t. elazigensis.*

- *Discocyclina trabayensis elazigensis* Özcan et Less, 2006

  Figures 8E, 9, 11 and 19C–I.

  Discocyclina trabayensis elazigensis n. ssp.—[53]: 495, Plate 2: 7–9, Figure 12. (with synonymy).

  Discocyclina trabayensis elazigensis Özcan et Less.—[66]: Figure 33l–o.—[8]: Figures 111.4–8 and 112.

  Discocyclina trabayensis elazigensis may be confused with *D. augustae augustae*, but due to its very small embryo and characteristic "varians"-type adauxiliary chamberlets, this taxon is easily identified (see also Figure 13).

Genus Nemkovella Less, 1987

Representatives of two species of this genus were found in Castel San Felice.

7. *Nemkovella strophiolata* (Gümbel, 1870)

This is a small, moderately flat, unribbed species with a small semi-iso to nephrolepidine embryo, low but relatively wide, very diagnostic, arcuate, "varians"-type adauxiliary chamberlets, and moderately narrow and low, slightly hexagonal equatorial chamberlets with a "strophiolata"-type growth pattern.

Nemkovella strophiolata forms an evolutionary lineage with the following four chronosubspecies: *N. s. fermonti* (d_{mean} < 150 µm; SBZ 10–13; OZ 6–9); *N. s. strophiolata* (d_{mean} = 150–185 µm; SBZ 12–16; OZ 8b–12); *N. s.* n. ssp. Padragkút (in Less, 1998 with d_{mean} = 185–230 µm; SBZ 15–18; OZ 11–14); and *N. s. tenella* (d_{mean} > 230 µm; SBZ 18–19a; OZ 14) [7,8].

This species occurs in samples VER 2–4 from Castel San Felice and is particularly common in sample VER 4. The quantitative parameters of the three populations are very similar (Tables 2–4) and can, therefore, be evaluated and determined together as *Nemkovella strophiolata tenella*.

- *Nemkovella strophiolata tenella* (Gümbel, 1870)

  Figure 20A–K and Figure 21.

  Orbitoides (*Discocyclina*) *tenella* n. sp.—[69]: 698, pl. 3: 1, 2, 30–31.

  Nemkovella strophiolata tenella (Gümbel)—[6]: 190–191, pl. 25: 11–12. (with synonymy).—[53]: pl. 3: 9–11, Figure 13.—[8]: Figure 124.9,10.

This easily recognizable taxon can sometimes be confused with *Discocyclina augustae augustae*, which, however, has proximal annular stolons that are absent in *Nemkovella*. Therefore, the equatorial chamberlets of the latter are slightly hexagonal, unlike those of *Discocyclina*, which are rectangular. Although they belong to different families (which is clear from their microspheric juvenarium, see Figure 5), the megalospheric specimens of *N. strophiolata tenella* and the advanced *Orbitoclypeus varians* (*O. v. scalaris* and *O. v. varians*) are identical in the absence of proximal annular stolon of equatorial chamberlets and may, therefore, be confused. Figure 22 shows that their quantitative parameters differ significantly. In addition, the slightly undulated annuli characteristic of *O. varians* are never observed in *N. strophiolata*.

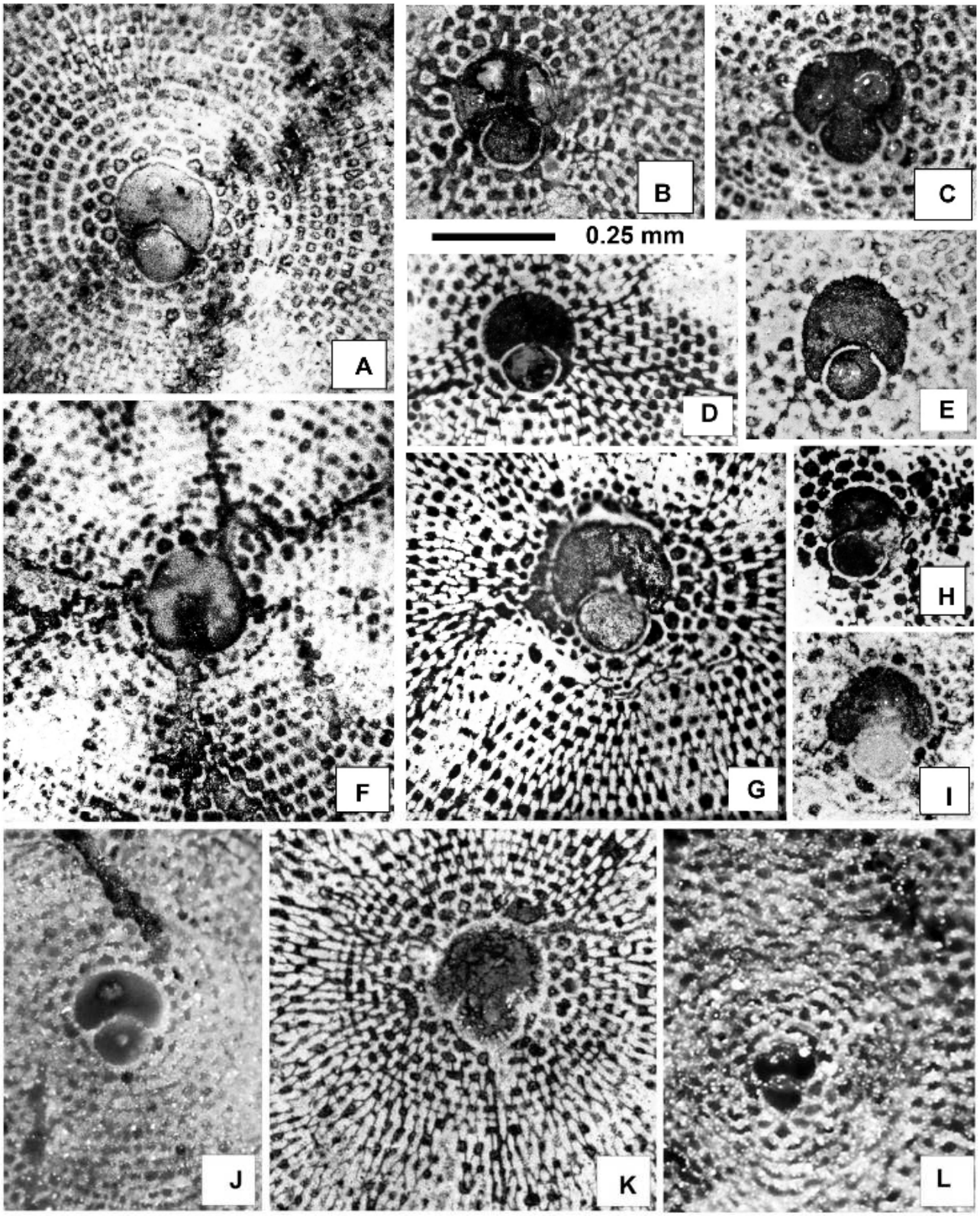

Figure 20. Equatorial sections of *Nemkovella strophiolata tenella* (Gümbel) (**A**–**K**) and *N. daguini* (Neumann) (**L**). (**A**): E.2025.163, (**B**): E.2025.84, (**C**): E.2025.74, (**D**): E.2025.77, (**E**): E.2025.71, (**F**): E.2025.162, (**G**): E.2025.81, (**H**): E.2025.82, (**I**): E.2025.164, (**J**): E.2025.76, (**K**): E.2025.80, and (**L**): E.2025.85. (**A**,**F**,**I**): VER 2 and (**B**–**E**,**G**–**L**): VER 4. All A-forms.

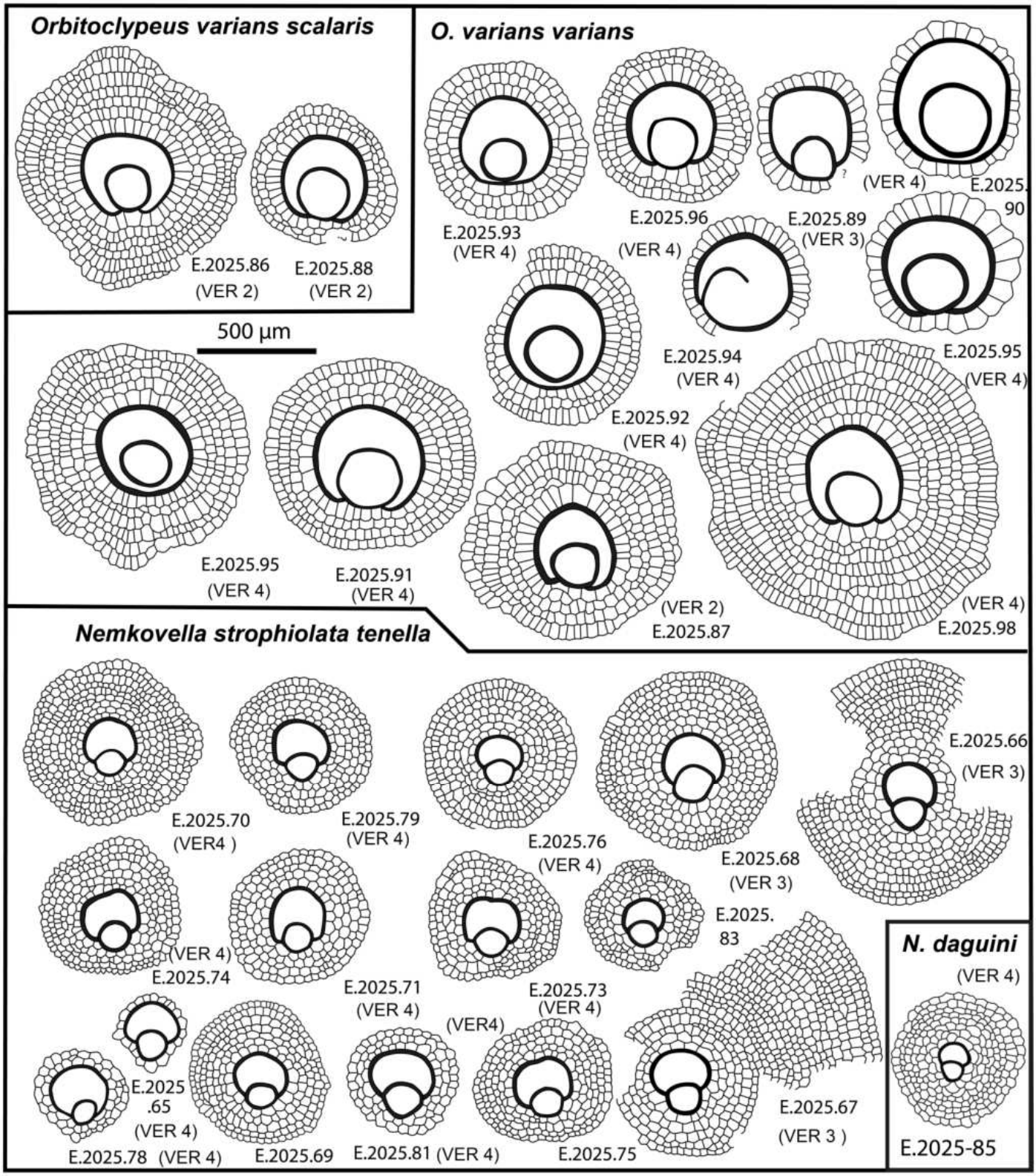

Figure 21. Line drawings of *Orbitoclypeus varians scalaris* (Schlumberger), *O. v. varians* (Kaufmann), *Nemkovella strophiolata tenella* (Gümbel), and *N. daguini* (Neumann).

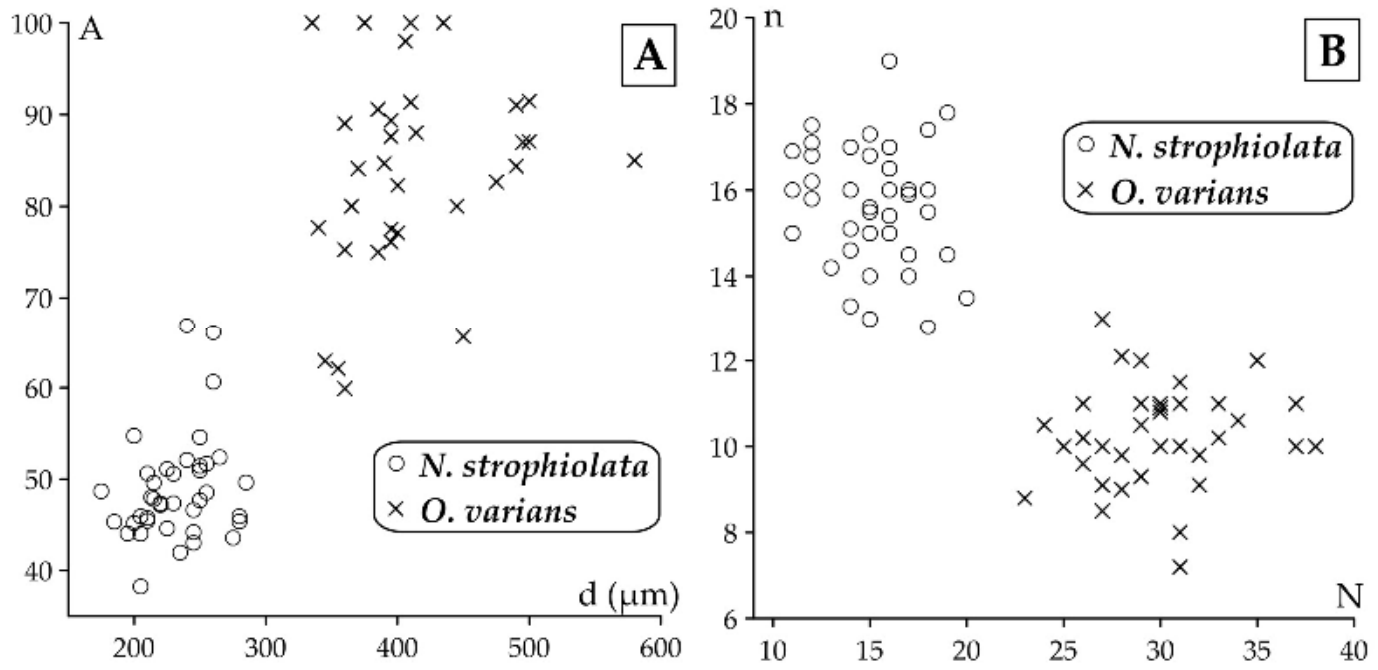

Figure 22. Distribution of *Nemkovella strophiolata tenella* and *Orbitoclypeus varians* specimens in samples VER 2–4 (**A**) on the d–A (deuteroconch diameter vs. deuteroconchal embracement) and (**B**) on the N–n (number of adauxiliary chamberlets vs. annuli number in the first 0.5 mm from the deuteroconch's rim) bivariate plots.

8. *Nemkovella daguini* (Neumann, 1958)

Figures 20L and 21.

Discocyclina daguini n. sp.—[70]: 89, Plate 17: 7–10.

Orbitoclypeus daguini (Neumann)—[6]: 222–224, Plate 36: 1–6, Figure 31a,b

Nemkovella daguini (Neumann)—[53]: 503–504, Plate 2: 1–4, Plate 3: 14, Plate 5: 6, Figure 6.—[71]: 19–23, Figures 5A–C, 6A–H, 7A–K, 8, 9A–H, 10A–I and 11A–E. (with synonymy)—[8]: 68, 71, Figures 25.7–8, 36.6–8, 117.1–6 and 118.—[64]: 24, Figure 16K.

Nemkovella daguini is a very small and strongly inflated taxon without ribs. The very small embryo varies from the almost iso- to nephrolepidine type. The pre-annular stage includes auxiliary, adauxiliary, and orbitoidal chamberlets. The two principal auxiliary chambers are larger than the nearby orbitoidal chamberlets, tangentially elongated, and similar in size and shape to the 1–3 (usually 2) adauxiliary chamberlets. The latter are arcuate in shape, radially low, tangentially wide, and are isolated from each other, leading to the formation of 'orbitoidal' chamberlets.

The chamberlets following the auxiliary chamberlets on the protoconchal side form very short spirals. The arrangement of the equatorial chamberlets around the deuteroconch is typically orbitoidal ("daguini" type of [6]). Annular growth is reached in the successive growth stages. The annular chamberlets are low and hexagonal. Most specimens have wavy annuli, with their number varying between four and six. This wavy pattern is attenuated with successive growth, and the latest annuli have a circular outline. *Nemkovella daguini*, ranging from SBZ 11 to SBZ 20 and OZ 8a to OZ 16, respectively, is not yet subdivided into chrono-subspecies.

We found only one specimen of this extremely small, otherwise nonconfusable taxon in sample VER 4. Based on its nepionic arrangement, formerly (see synonymy list), it was assigned to the genus *Orbitoclypeus*. However, ref. [53] (Plate 3: 14) found a B-form characteristic of discocyclinids, so it had to be reclassified into the genus *Nemkovella*.

6.1.2. Family Orbitoclypeidae Brönnimann, 1945

Two genera, namely *Orbitoclypeus* and *Asterocyclina*, are recorded from Verona. The equatorial layer of the first is not subdivided into sublayers, whereas in the case of the last taxon, it is.

Genus *Orbitoclypeus* Silvestri, 1907

This genus is represented in Castel San Felice by one single species.

9. *Orbitoclypeus varians* (Kaufmann, 1867)

This widespread, unribbed species is medium-sized, slightly inflated, with a "marthae"-type rosette. The excentri- to eulepidine embryo is small- to medium-sized. Adauxiliary chamberlets are of the "varians" type with an average size and shape. The equatorial chamberlets are moderately wide and high, arranged into undulated annuli with a "varians"-type growth pattern.

Orbitoclypeus varians forms an evolutionary lineage with six chrono-subspecies, as follows: *O. v. portnayae* (d_{mean} < 165 µm; SBZ 10–11; OZ 5–8a); *O. v. ankaraensis* (d_{mean} = 165–205 µm; SBZ 12–13, OZ 8b); *O. v. angoumensis* (d_{mean} = 205–255 µm; SBZ 13–14; OZ 9–10); *O. v. roberti* (d_{mean} = 255–320 µm; SBZ 15–17; SBZ 11–13); *O. v. scalaris* (d_{mean} = 320–400 µm; SBZ 16–19; OZ 12–15); and *O. v. varians* (d_{mean} > 400 µm; SBZ 17–20; OZ 13–16) [7,8].

Orbitoclypeus varians is the only representative of this genus in our samples and, based on its qualitative features, cannot be confused with any other taxa. It occurs in all three samples of Castel San Felice, but is most common in VER 4 and very rare in VER 3. Based on the data in Tables 2–4, the populations of these two samples can be joined and determined as *O. v. varians*. However, the population of sample VER 2 appears to be slightly less developed and can be identified as *O. v. scalaris*.

Orbitoclypeus varians scalaris (Schlumberger, 1903)

Figures 21 and 23A,B.

Orthophragmina scalaris n. sp.—[72]: 277–278, Plate 8: 4, Plate 9: 12–13.

Orbitoclypeus varians scalaris (Schlumberger)—[6]: 211–212, Plate 30: 6–12. (with synonymy)—[53]: Plate 3: 15, Plate 5: 7, 8.—[59]: Figures 28w–x and 29a–e.—[66]: Figure 34l,m,o. —[73]: Figure 14D.—[64]: Figure 18A,B. —[68]: Figure 26a.—[8]: Figures 28.3, 4, 37.10, 153.4–6 and 156.

Orbitoclypeus varians varians (Kaufmann, 1867)

Figures 21 and 23C–F.

Orbitoides varians n. sp.—[74]: 158–160, Plate 10: 1–10.

Orbitoclypeus varians varians (Kaufmann).—[6]: 212–214, Plate 31: 1–12, Plate 32: 1–4. (with synonymy).—[75]: 9, Plate 4: 1, Plate 5: 1–2.—[56]: Plate 1: 5, 6.—[53]: Figure 15.—[66]: Figure 34p.—[73]: Figure 14E–G.—[64]: Figure 18C.—[62]: Figure 15e–g.—[68]: Figure 26b–g.—[8]: Figure 153.7–9.

Genus *Asterocyclina* Gümbel, 1870

We found this genus in both Monte Cavro and Castel San Felice. It is represented by two species (*Asterocyclina alticostata* and *A. stellata*) which can be easily distinguished not only by their different types of adauxiliary chamberlets ("alticostata" vs. "stellata"), but also by their quantitative parameters (Tables 2–4 and Figure 24).

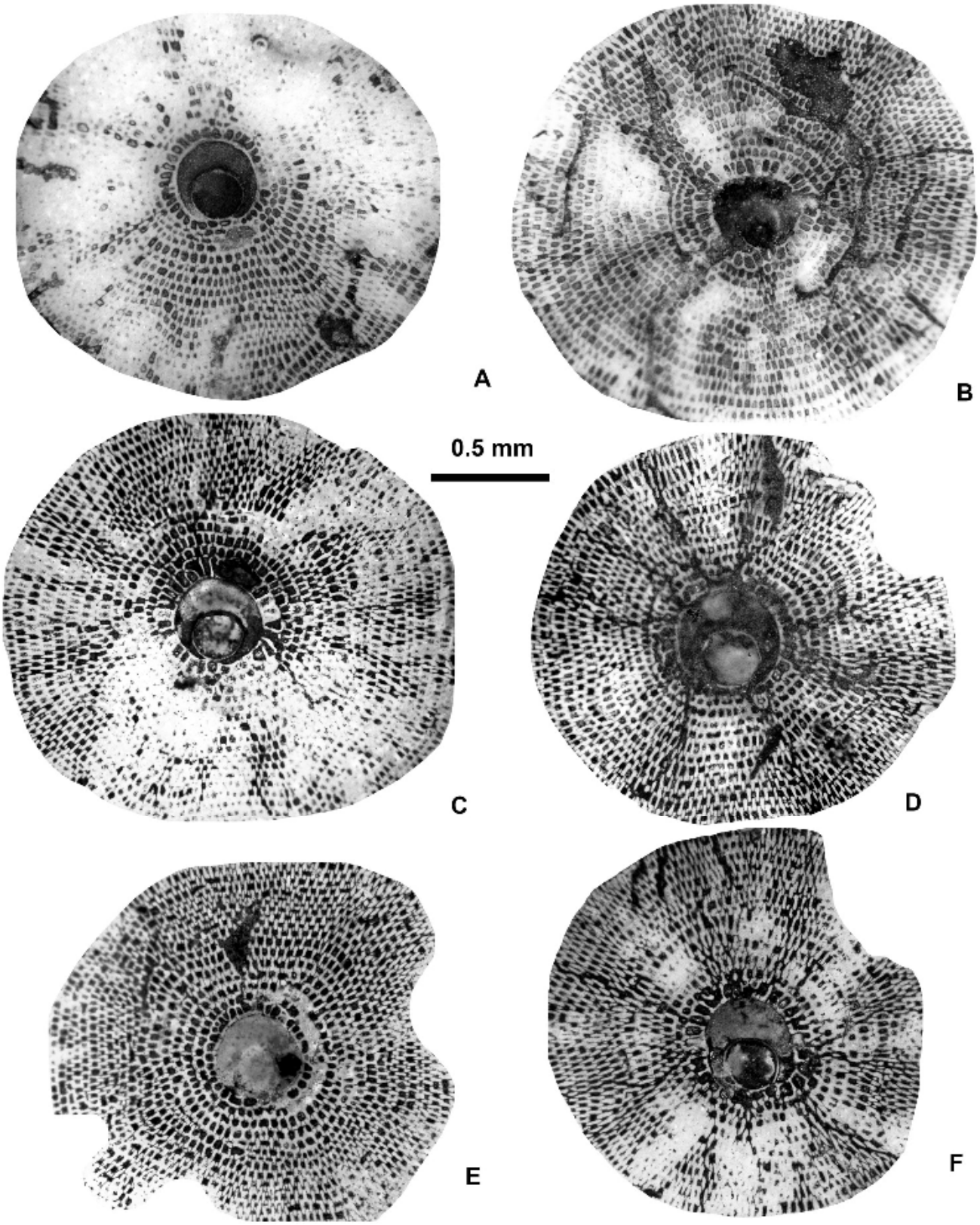

Figure 23. Equatorial sections of *Orbitoclypeus varians scalaris* (Schlumberger) (**A**,**B**) and *O. v. varians* (Kaufmann) (**C**–**F**). (**A**): E.2025.88, (**B**): E.2025.86, (**C**): E.2025.100, (**D**): E.2025.97, (**E**): E.2025.93, and (**F**): E.2025.98. (**A**,**B**): VER 2 and (**C**–**F**): VER 4. All A-forms.

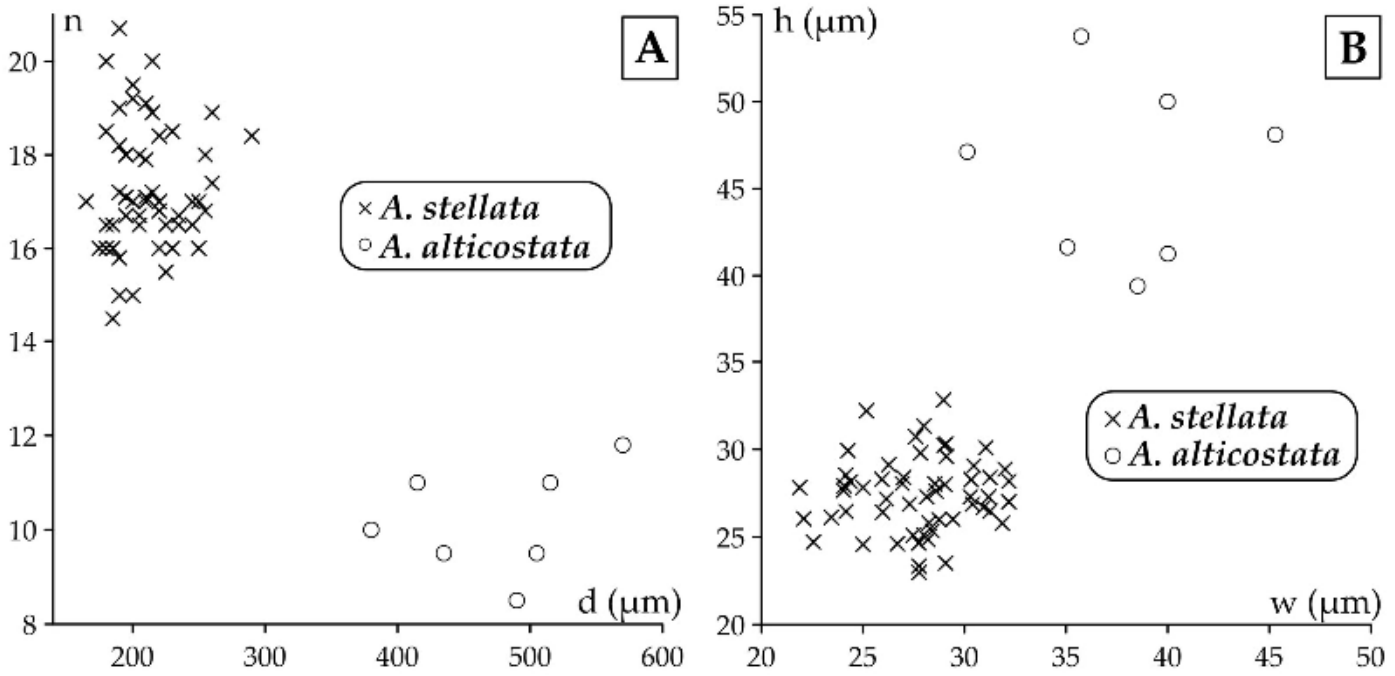

Figure 24. Distribution of *Asterocyclina alticostata danubica* and *A. stellata stellaris* specimens in samples VER 2–4 (**A**) on the d–n (deuteroconch diameter vs. annuli number in the first 0.5 mm from the deuteroconch's rim) and (**B**) on the w–h (width vs. height of the equatorial chamberlets) bivariate plots.

10. *Asterocyclina alticostata* (Nuttall, 1926)

This widespread species is star-shaped, usually with five to seven rays and a "chudeaui"-type rosette. It has a medium-sized to relatively large isolepidine embryo, very few, very wide, and moderately low "alticostata"-type adauxiliary chamberlets, and also wide and moderately high equatorial chamberlets arranged into asteroidal annuli with a "strophiolata"- or "varians"-type growth pattern.

Asterocyclina alticostata includes four subspecies, as follows: *A. a. gallica* (d_{mean} < 275 μm; SBZ 10–13; OZ 6–9); *A. a. cuvillieri* (d_{mean} = 275–350 μm; SBZ 14–15; OZ 10–11); *A. a. alticostata* (d_{mean} = 350–450 μm; SBZ 16–19a; OZ 12–14); and *A. a. danubica* (d_{mean} > 450 μm; SBZ 18–20; OZ 14–16) [7,8].

Asterocyclina alticostata occurs in all our samples from Verona, however, it is extremely rare in all of them. Therefore, in sample VER 1 from Monte Cavro (where only one single specimen was found), it cannot be determined on the subspecies level, although the numerical parameters (Tables 2–4) are closest to *A. a. danubica*. The quantitative parameters of the three populations from Castel San Felice are similar, thus, they can be jointly evaluated and determined as *A. a. danubica.*

Asterocyclina alticostata danubica Less, 1987

Figures 25B–D and 26.

Asterocyclina alticostata danubica n. ssp.—[6]: 243–244, Plate 45: 4–11. (with synonymy).

Asterocyclina alticostata danubica Less—[53]: Plate 3: 27, 28.—[59]: Figure 31e–g.—[66]: Figure 35t.—[64]: 26, Figure 19A,B.—[68]: Figure 28b–d.—[8]: Figures 27.5, 159.9,10 and 160.—[54]: Figure 2K.—[65]: 467, Figure 4N–P.

11. *Asterocyclina stellata* (d'Archiac, 1846)

This widespread species is a star-shaped form, usually with five rays and a "marthae"-type rosette. It has a small semi-iso- to nephrolepidine embryo, few wide and low "stellata"-

type adauxiliary chamberlets, and also narrow and low equatorial chamberlets arranged into asteroidal annuli with a "strophiolata"-type growth pattern.

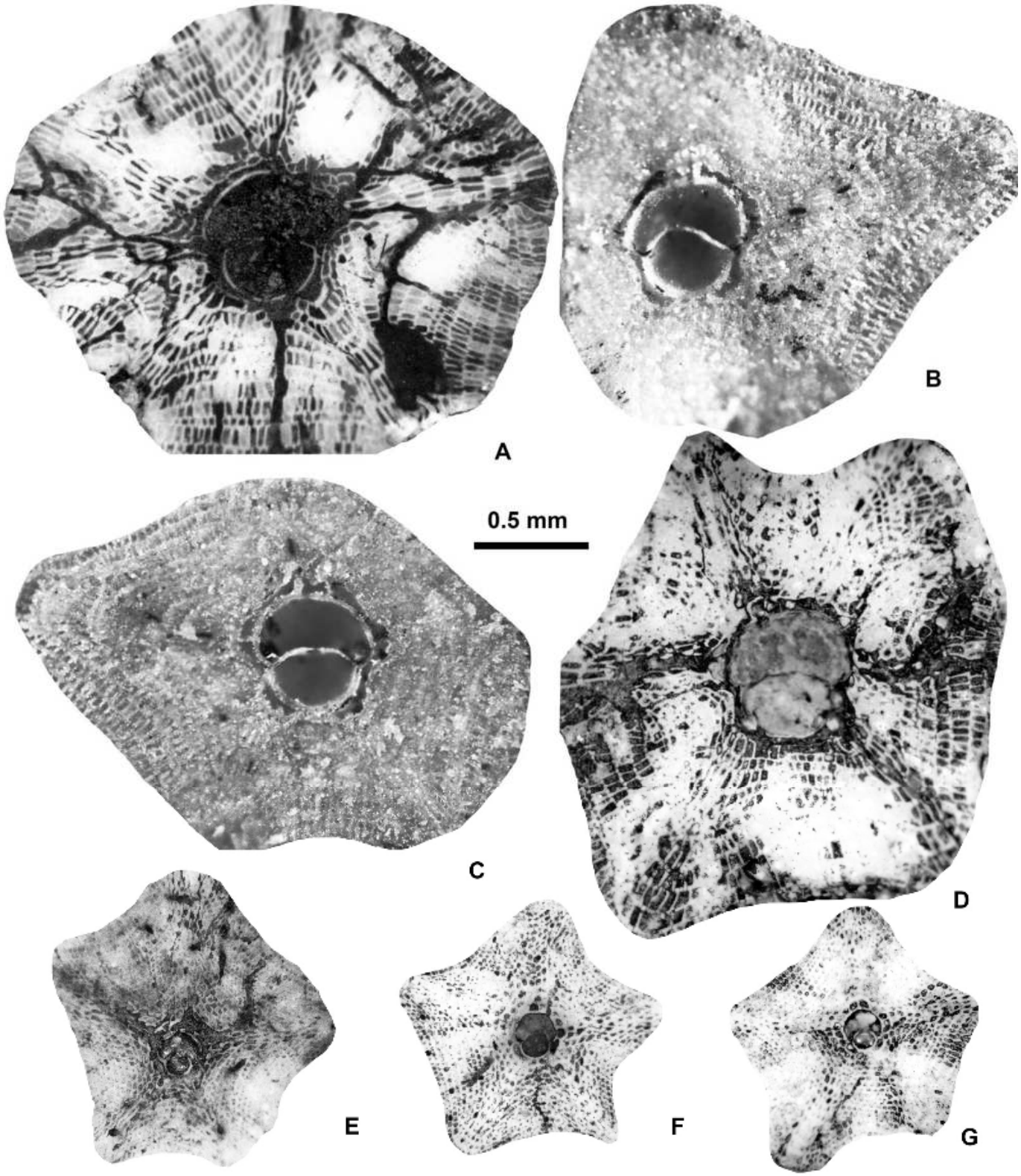

Figure 25. Equatorial sections of *Asterocyclina alticostata* indet. ssp. (**A**), *A. alticostata danubica* Less (**B**–**D**), *A. stellata* cf. *stellaris* (Brünner in Rütimeyer) (**E**), and *A. stellata stellaris* (Brünner in Rütimeyer) (**F**–**G**). (**A**): E.2025.101, (**B**): E.2025.104, (**C**): E.2025.103, (**D**): E.2025.106, (**E**): E.2025.107, and (**F**): E.2025.118, (**G**): E.2025.117. (**A**,**E**): VER 1 (Monte Cavro 4); (**B**,**C**): VER 3; (**D**): VER 4; and (**F**,**G**): VER 2. All A-forms.

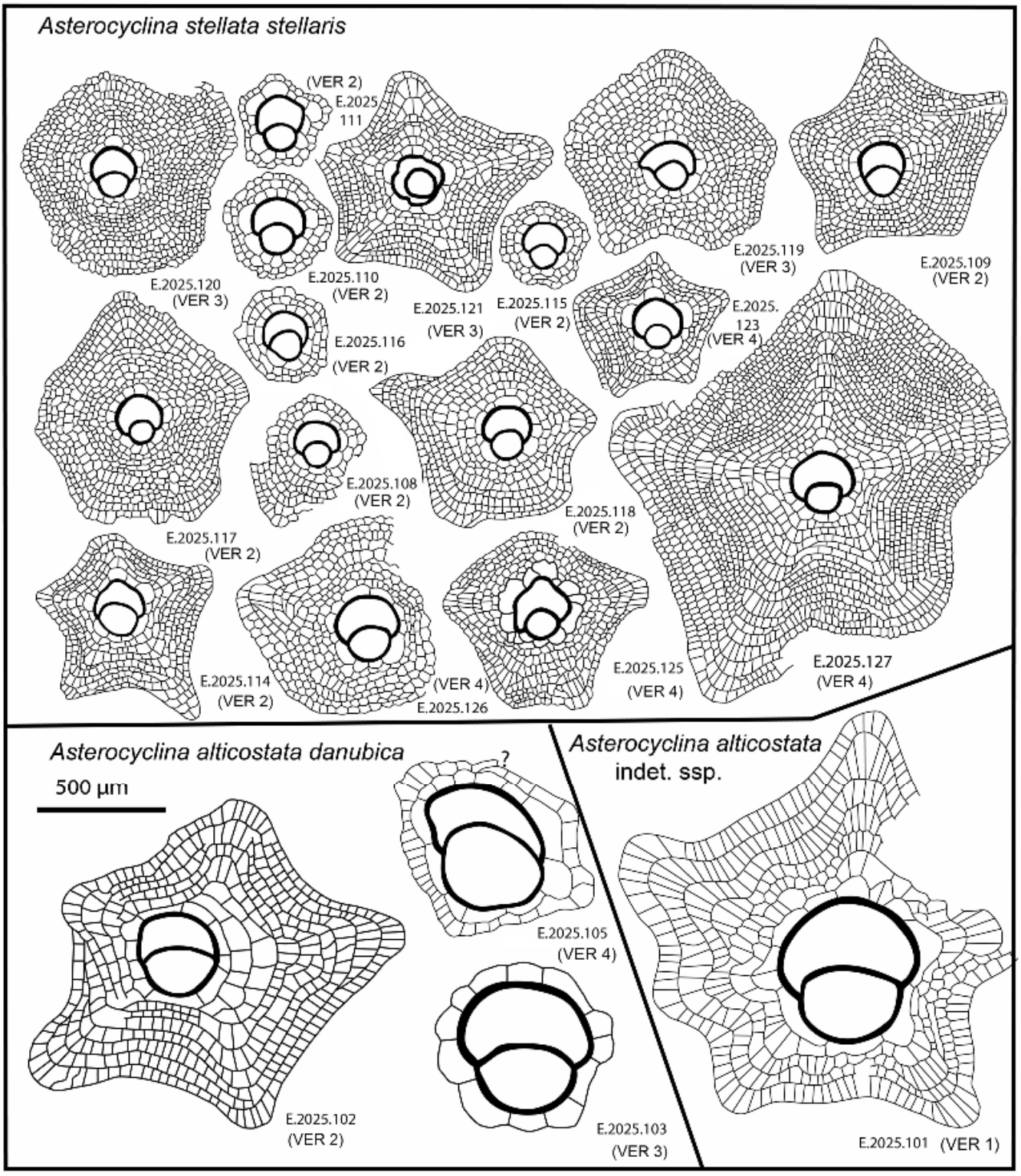

Figure 26. Line drawings of *Asterocyclina* in the vicinity of Verona.

Asterocyclina stellata is arbitrarily subdivided into four chrono-subspecies, including *A. s. adourensis* (d_{mean} < 150 µm; SBZ 10–16; OZ 6–12); *A. s. stellata* (d_{mean} = 150–190 µm; SBZ 14–17; OZ 10–13); *A. s. stellaris* (d_{mean} = 190–240 µm; OZ 13–15); and *A. s. buekkensis* (d_{mean} > 240 µm; SBZ 20; OZ 16) [7,8].

Asterocyclina stellata is abundant in all samples from Castel San Felice (VER 2–4) and also rarely occurs in Monte Cavro (VER 1). The latter, containing only two specimens, can be determined as *A. s.* cf. *stellaris*, whereas the three populations from Castel San

Felice (VER 2–4) bear similar quantitative parameters (Tables 2–4). Thus, they can be jointly evaluated and determined as *A. s. stellaris*.

- *Asterocyclina stellata stellaris* (Brünner in Rütimeyer, 1850)

  Figures 25F–G, 26 and 27A–H.

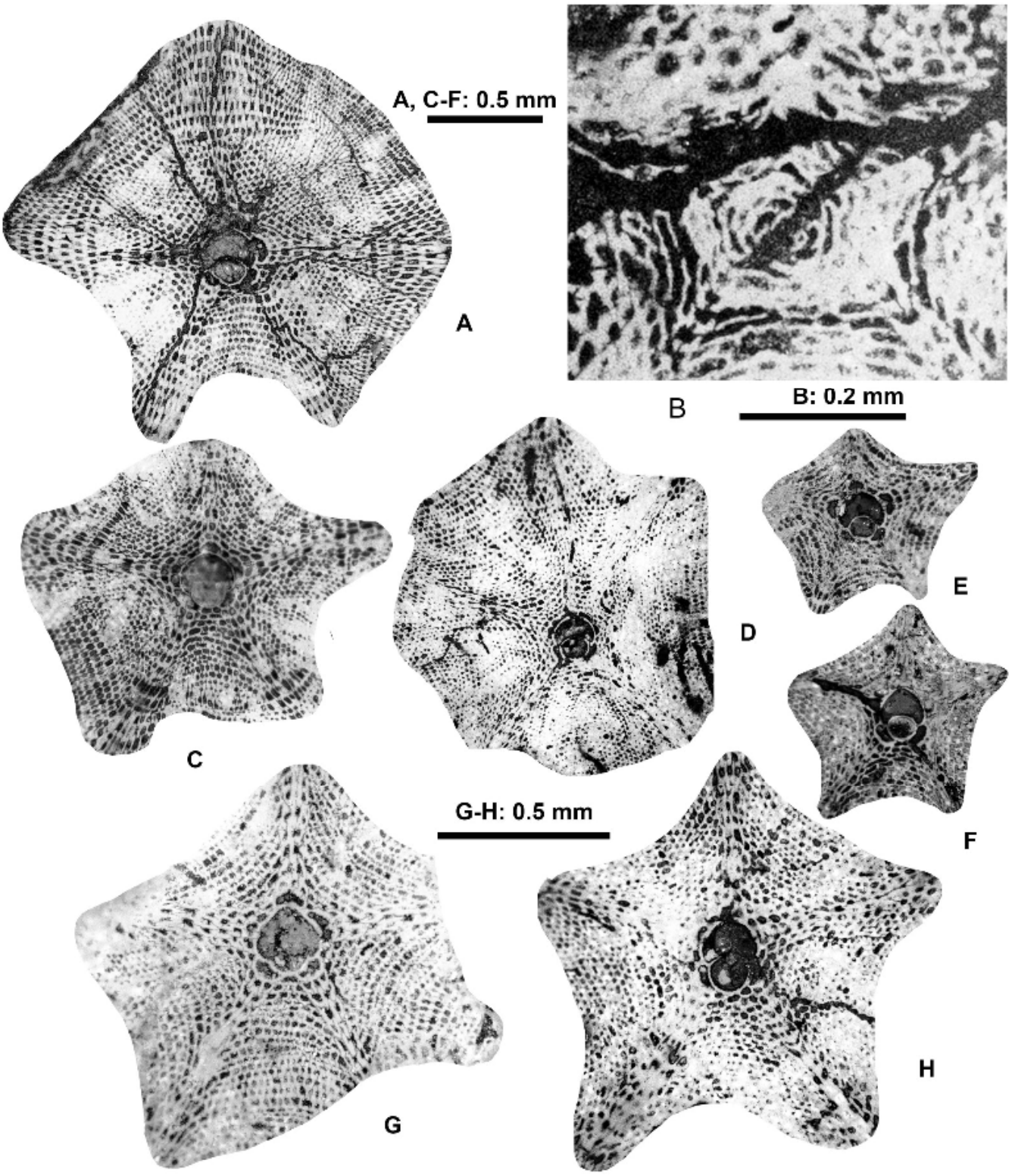

Figure 27. Equatorial sections of *Asterocyclina stellata stellaris* (Brünner in Rütimeyer). (**A**): E.2025.113, (**B**): E.2025.107, (**C**): E.2025.128, (**D**): E.2025.126, (**E**): E.2025.123, (**F**): E.2025.124, (**G**): E.2025.121, and (**H**): E.2025.122. (**A**): VER 2, (**B**–**F**,**H**): VER 4;(**G**)**:** VER 3. (**B**): B form, all the others are A-forms.

Orbitolites stellaris Brünner 1848.—[76]: 118, Plate 5: 74.

Asterocyclina stellata stellaris (Brünner in Rütimeyer)—[6]: 236–237, Plate 39: 11–12, Plate 40: 1–11, Plate 41: 1–6. (with synonymy).—[75]: 1–4, Plate 6: 1–7, Figure 4.—[53]: Plate 4: 8–12.—[59]: Figure 29q–s.—[66]: Figure 35a–f.—[73]: Figure 15A–D.—[64]: 26, Figure 18G–K.—[68]: Figure 28e,g.—[8]: Figures 27.6, 172.7–8 and 173.—[65]: 467, Plate 4: K. L.

6.2. Family Nummulitidae de Blainville, 1827

For the generic classification of the family, we apply the principles and subdivision of [40], with the addition by [77], to the distinction of *Assilina* and *Operculina*. Five genera are recorded in our material, three of them (*Nummulites*, *Assilina*, and *Operculina*) with no secondary chamberlets and the other two (*Heterostegina* and *Spiroclypeus*) with subdivided chambers. Our material from Verona is incorporated into the recent revision of the Eocene representatives of these last two genera [37,38], therefore, here, we give only brief information about them. In our material, we found only the megalospheric A-forms, so we will not deal with the B-forms in this paper.

6.2.1. Genus *Nummulites* Lamarck, 1801

The determination of *Nummulites* is based on both the surface characteristics and the features of the equatorial section. Based on their surface characteristics, the representatives of the genus *Nummulites* in the studied samples can be classified into two categories, as follows: *N. hormoensis* and *N. fabianii* (the successive members of the *N. fabianii* lineage) belong to the reticulate, while *N. incrassatus*, *N. chavannesi*, *N. pulchellus*, and *N. budensis* belong to the radiate forms. Granulate forms are missing from our material. Following [78], a measurement and parameter system was introduced by [56] to characterize the equatorial section of A-forms that is slightly modified here. It consists of four measurements (in μm) and two counts in the equatorial section of megalospheric (A) forms, as listed below and shown in Figure 28.

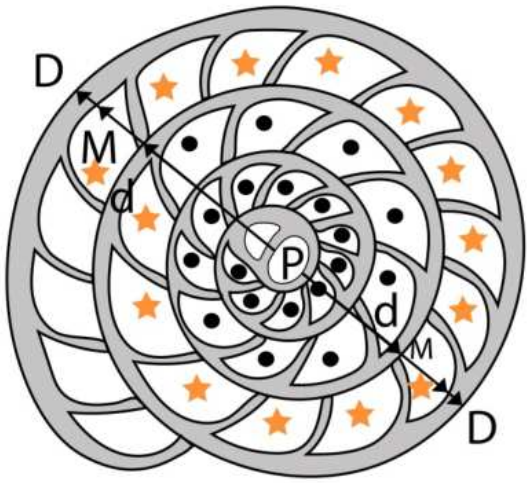

Figure 28. Measurement system for nummulitids without secondary chambers.

- P: Inner cross-diameter of the proloculus;
- d: Outer diameter of the two first whorls along the axis of the embryo;
- E: Total number of chambers in the first two whorls (excluding the first two chambers). In Figure 28, these chambers are marked by • (E = 19);
- M: Inner diameter of the first three whorls along the axis of the embryo;
- D: Outer diameter of the first three whorls along the axis of the embryo;
- N: Exact number of chambers in the third whorl. In Figure 28, these chambers are marked by * (N = 13.6).

Three of these parameters (P, d, and E) are used directly; four other parameters are calculated as follows. Morphometric data are summarized in Table 5.

- L: $L = d \times \pi/N$—estimated average length of chambers in the third whorl (in µm);
- K: $K = 100 \times (D - d)/(D - P)$—index of spiral opening (in %) expressed by the ratio of the height of the third whorl vs. the height of the first three whorls (without the proloculus);
- F: $F = 100 \times [(D - d)/2]/[(D - d)/2 + L]$—estimated isometry index ("shape") of chambers in the third whorl (in %);
- m: $m = 100 \times (D - M)/(D - d)$—relative width of the spiral cord in the third whorl (in %).

Although it is generally accepted that (like orthophragmines) *Nummulites* are also arranged in long-lived evolutionary lineages, not only is their separation from each other typology-based, but so is their internal subdivision, and their constituent elements are considered separate species [35]. Attempts have been made to subdivide the lineages of *Nummulites* on a morphometric basis only in the case of reticulate forms (*N. fabianii* lineage: [59,66,68,79–82] and *N. ptukhiani* lineage: [83]). The *N. fabianii* lineage (occurring in both Monte Cavro and Castel San Felice) is arbitrarily subdivided into species by using the criteria shown in Table 5. Figure 29 shows the disposition of the two populations observed in our material (Monte Cavro: sample VER 1 and Castel San Felice: sample VER 2) in the P–L bivariate plot of Bartonian and Priabonian populations of the *N. fabianii* lineage.

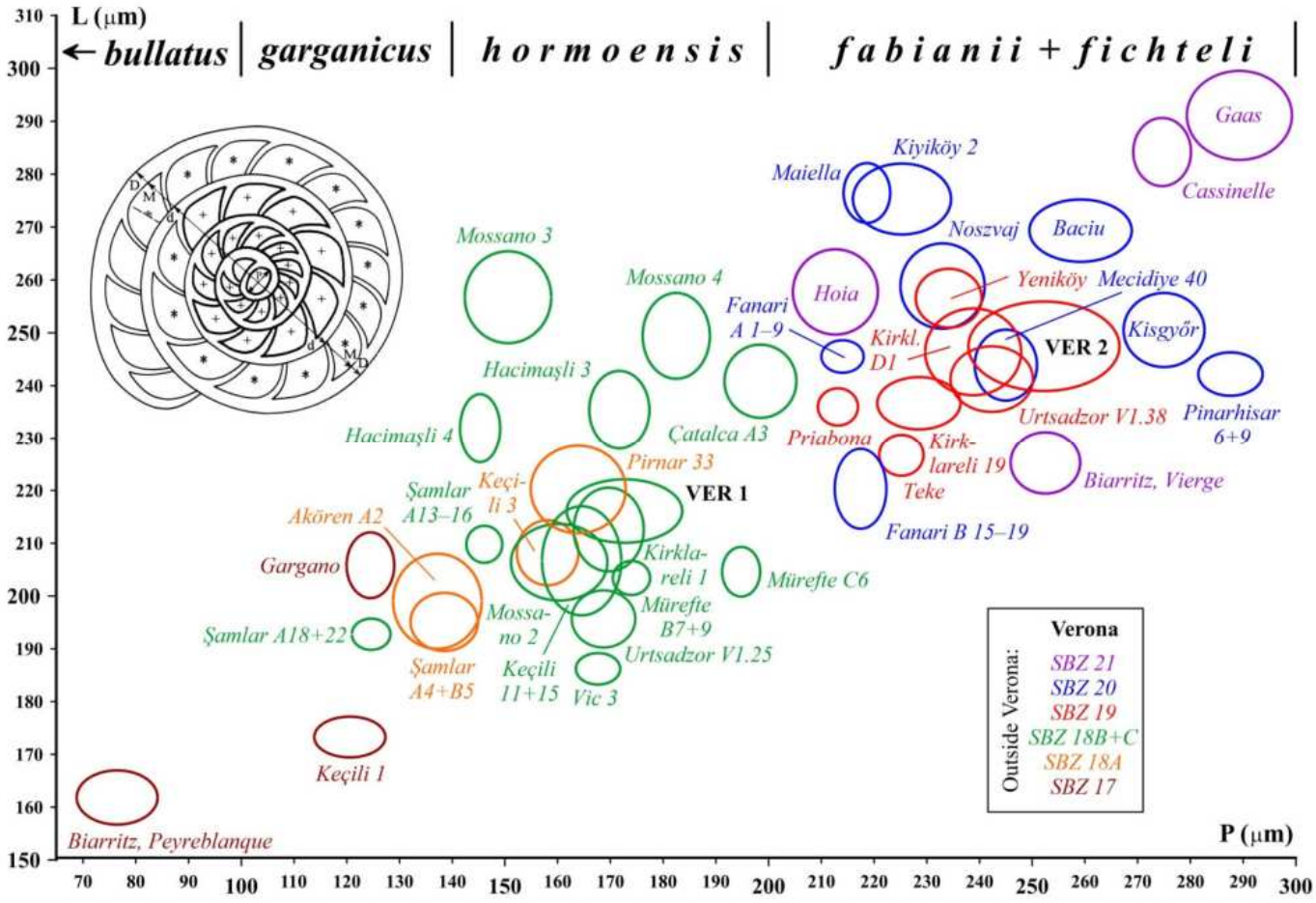

Figure 29. Distribution of populations of the *Nummulites fabianii* lineage (with their proposed specific subdivision [59]) from Verona and other localities from the peri-Mediterranean region (mean values at the 68% confidence level corresponding to 1 s.e.) on the P–L (inner cross diameter of the proloculus vs. average length of chambers in the third whorl) bivariate plot. For the summary list of localities see [45], for Fanari (Greece) see [65], for Urtsadzor (Armenia) see [68].

Table 5. Statistical data of *Nummulites* populations from Verona.

Parameters		Inner Cross-Diameter of the Proloculus			Outer Diameter of the First Two Whorls			Number of Post-Embryonic Chambers in the First Two Whorls			Index of Spiral Opening		
											3. Whorl vs. First 3 Whorls		
		P (μm)			d (μm)			E			K = 100 × (D − d)/(D − P)		
Taxon	**Sample**	**No**	**range**	**mean ± s.e.**	**No**	**range**	**mean ± s.e.**	**No**	**range**	**mean ± s.e.**	**No**	**range**	**mean ± s.e.**
N. hormoensis	**VER 1**	**15**	**100–235**	**172.7 ± 10.6**	**15**	**960–1360**	**1191 ± 30**	**15**	**21–26**	**22.87 ± 0.35**	**14**	**29.7–39.3**	**33.64 ± 0.70**
N. fabianii	**VER 2**	**9**	**180–340**	**252.2 ± 14.3**	**8**	**1190–1745**	**1446 ± 61**	**8**	**18–26**	**22.75 ± 0.82**	**7**	**26.8–41.0**	**33.09 ± 1.74**
N. chavannesi	**VER 2–4**	**19**	**150–450**	**264.2 ± 16.0**	**19**	**1060–2140**	**1507 ± 60**	**19**	**24–30**	**26.89 ± 0.45**	**19**	**33.7–55.6**	**43.20 ± 1.06**
	VER 2	15	160–350	259.0 ± 13.0	15	1060–1735	1466 ± 51	15	24–30	26.93 ± 0.47	15	37.1–55.6	44.50 ± 0.98
	VER 3	2	210–450	330.0	2	1425–2140	1783	2	24–30	27.00	2	33.7–34.7	34.20
	VER 4	2	150–325	237.5	2	1140–1925	1533	2	25–28	26.50	2	41.5–43.4	42.46
N. budensis	**VER 1**	**1**		**70.0**	**1**		**780**	**1**		**23.00**	**1**		**51.70**
	VER 2	**1**		**60.0**	**1**		**650**	**1**		**24.00**	**1**		**45.37**
N. pulchellus	**VER 4**	**2**	**125–140**	**132.5**	**2**	**890–930**	**910**	**2**	**33–34**	**33.50**	**2**	**39.5–41.0**	**40.29**
N. incrassatus	**VER 1**	**5**	**160–200**	**185.0 ± 6.6**	**5**	**1090–1910**	**1466 ± 122**	**5**	**21–25**	**23.60 ± 0.78**	**5**	**30.4–38.5**	**34.39 ± 1.21**
	VER 2 + 3	**6**	**100–225**	**145.0 ± 16.1**	**6**	**990–1495**	**1168 ± 84**	**5**	**18–25**	**21.00 ± 1.17**	**6**	**32.3–42.7**	**38.82 ± 1.47**
	VER 2	5	100–225	145.0 ± 19.3	5	990–1495	1119 ± 84	5	18–25	21.00 ± 1.17	5	35.9–42.7	40.13 ± 1.02
	VER 3	1		145.0	1		1415				1		32.27

Table 5. *Cont.*

Parameters		Third whorl								
		average length of chambers			average shape of chambers			relative width of the spiral cord		
		L = d × π/N (μm)			F = 100 × (D − d)/(D −d + 2d × π/N)			m = 100 × (D − M)/(D − d)		
Taxon	**Sample**	**No**	**range**	**mean ± s.e.**	**No**	**range**	**mean ± s.e.**	**No**	**range**	**mean ± s.e.**
N. hormoensis	**VER 1**	**14**	**183–259**	**216.1 ± 5.8**	**14**	**48.6–60.1**	**54.34 ± 0.87**	**14**	**42.9–53.0**	**46.86 ± 0.87**
N. fabianii	**VER 2**	**7**	**220–287**	**247.5 ± 8.5**	**7**	**47.2–61.8**	**53.90 ± 1.92**	**7**	**28.5–42.2**	**38.00 ± 1.71**
N. chavannesi	**VER 2–4**	**19**	**170–292**	**222.4 ± 7.6**	**19**	**59.5–78.6**	**67.73 ± 1.01**	**19**	**8.9–23.2**	**12.78 ± 0.85**
	VER 2	15	170–278	218.3 ± 7.9	15	60.5–78.6	68.78 ± 0.98	15	8.9–23.2	12.02 ± 0.96
	VER 3	2	218–292	255.3	2	59.5–59.6	59.58	2	14.0–14.7	14.34
	VER 4	2	188–252	220.2	2	66.8–69.3	68.05	2	15.8–18.1	16.93
N. budensis	**VER1**	**1**		**116.7**	**1**		**76.51**	**1**		**27.63**
	VER 2	**1**		**113.5**	**1**		**68.35**	**1**		**18.37**
N. pulchellus	**VER 4**	**2**	**106–112**	**109.1**	**2**	**70.2–71.0**	**70.62**	**2**	**18.2–19.0**	**18.59**
N. incrassatus	**VER 1**	**5**	**200–316**	**236.6 ± 18.2**	**5**	**53.3–63.2**	**58.35 ± 1.79**	**5**	**25.7–54.9**	**33.03 ± 4.98**
	VER 2 + 3	**6**	**191–232**	**210.3 ± 6.4**	**6**	**52.6–65.5**	**60.30 ± 1.60**	**6**	**28.2–37.1**	**32.99 ± 1.30**
	VER 2	5	191–232	211.6 ± 7.6	5	52.6–65.5	60.41 ± 1.92	5	28.2–37.1	33.63 ± 1.39
	VER 3	1		203.9	1		59.73	1		29.75

12. *Nummulites hormoensis* Nuttall & Brighton, 1931

Figure 30A–F.

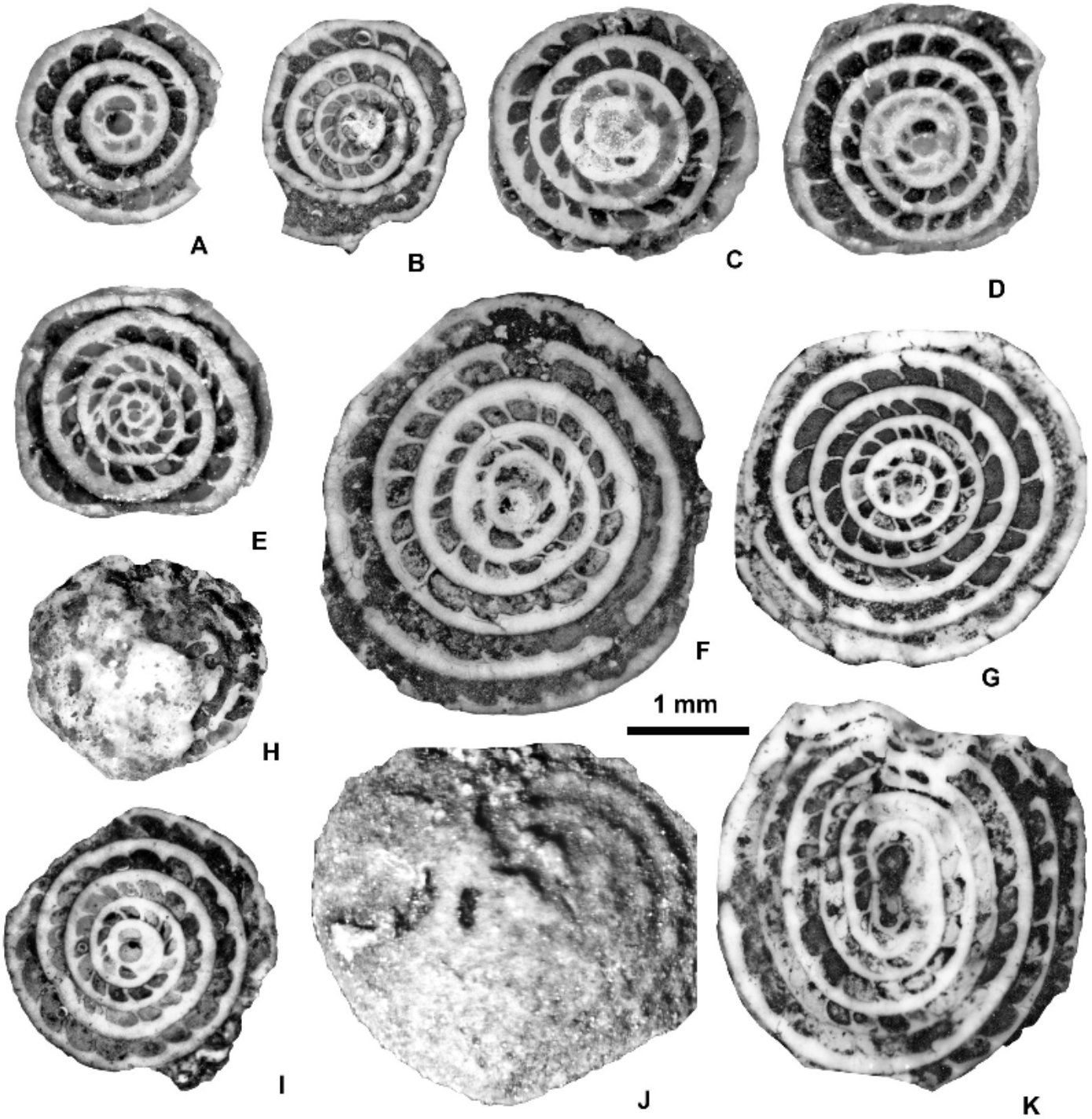

Figure 30. Equatorial sections and external views of reticulate *Nummulites*: *N. hormoensis* Nuttall & Brighton (**A**–**F**) and *N. fabianii* (Prever in Fabiani) (**G**–**K**). (**A**): E.2025.132, (**B**): E.06.36, (**C**): E.2025.131, (**D**): E.2025.130, (**F**): E.06.50, (**C**): E.06.53, (**H**): E.06.34, (**I**): E.06.33, (**J**): E.06.50, and (**K**): E.2025.133. (**A**–**E**); (**H**,**I**): VER 1 (Monte Cavro 4); and (**F**,**G**,**J**,**K**): VER 2. All A-form.

Nummulites hormoensis n. sp.—[84]: 53–54, Plate 3: 1–8.
Nummulites ptukhiani Z. Kacharava—[35]: 125–126, Plate 49: 33–48.
Nummulites cf. *hormoensis* Nuttall & Brighton—[25]: Plate 1: 11, 12.

Nummulites '*ptukhiani*' Z. Kacharava—[79]: 161, 164–165, Plate 1: 16–24, Plate 2: 16–21. (with synonymy)

Nummulites hormoensis Nuttall & Brighton—[53]: Plate 1: 9, 17.—[59]: 65, Figure 31h–j.—[66]: Figure 37f,l,n–u.—[45]: Figure 5f.—[62]: 80, Figure 17f–h.—[68]: 922, Figure 16d–v.

In the VER 1 sample from Monte Cavro, several reticulate *Nummulites* occur. Based on their morphometric data (Table 5), this population can be safely assigned to *N. hormoensis*, whose stratigraphic range is limited to the SBZ 18 Zone, which, as determined recently [8,62], includes the terminal Bartonian and basal Priabonian. In the last few years, this species has been described and discussed in detail in several papers from Turkey and Armenia [59,62,66,68]. Since specimens from the Monte Cavro population fit very well with this, we do not present a detailed description of this species here.

13. *Nummulites fabianii* (Prever in Fabiani, 1905)

Figure 30G–K.

Bruguieria fabianii n. sp.—Prever in [85]: 1805, 1811.

Nummulites fabianii (Prever in Fabiani)—[79]: 165, 168, Plate 1: 1–15, Plate 2: 1–15. (with synonymy)—[59]: 65, Figure 31k,l.—[66]: Figure 37z,A–M.—[45]: Figure 9c.—[60]: Figure 13A–F.—[86]: Figure 8A,B,D–G.—[68]: 922–924, Figures 16w–z,A–D and 18b,c.—[65]: 456, Plate 1: K–P.

Nummulites retiatus Roveda—[56]: 351–352, Plate 1: 13–14.

Reticulate *Nummulites* are very rare in the samples from Castel San Felice; in fact, only a few of them can be found and only in sample VER 2. Nevertheless, their quantity is just enough to assign them to *N. fabianii* based on their morphometric data (Table 5).

Formerly, *Nummulites fabianii* was believed to be an important leading fossil ("Leitfossil") of the Priabonian (interpreted as spanning the SBZ 19 and 20 Zones) [79]. However, this needs to be slightly modified due to the revision of the Bartonian/Priabonian boundary [46,47], which induced the displacement of the SBZ 18B and 18C Subzones (formerly assigned to the terminal Bartonian) to the basal Priabonian [9,62]. Thus, the stratigraphic distribution of *N. fabianii* continues to be the SBZ 19–20 interval (maybe including the early part of SBZ 21). However, this period does not encompass the entire Priabonian period. In recent years, this species has been described and discussed in detail in several papers from Italy, Romania, Greece, Turkey, and Armenia (see synonymy list). Since specimens from sample VER 2 fit very well with these, we do not repeat their descriptions here.

14. *Nummulites budensis* Hantken, 1875

Figure 31G.

Nummulites budensis n. sp.—[87]: 74, Plate 12: 4.

Nummulites budensis Hantken—[88]: 229–231, Plate 31: 16–20.—[56]: 354, Plate 2: 5, 6, 9, 10. (with synonymy)—[59]: 69, Figure 34k.—[66]: 829, Figure 39K–Q.—[45]: Figure 9d.—[64]: 18. Figure 15A–C.—[65]: 454, Figure 1J.

One specimen each of this radiate form was found in sample VER 1 (Monte Cavro) and in sample VER 2 (Castel San Felice). It can easily be identified based on its very small embryo, loose spiral, narrow and high chambers, straightness near the base, and then strong arch. *Nummulites budensis* does not yet fit into any evolutionary lineage. Its stratigraphic range was earlier thought to be SBZ 19–20 [66]. However, the finding in sample VER 1 allows us to extend the above stratigraphic range a little down into the SBZ 18C Subzone, close to the Bartonian/Priabonian boundary. The distinction from the early Rupelian *N. bouillei* and the Chattian *N. kecskemetii* is discussed in [56].

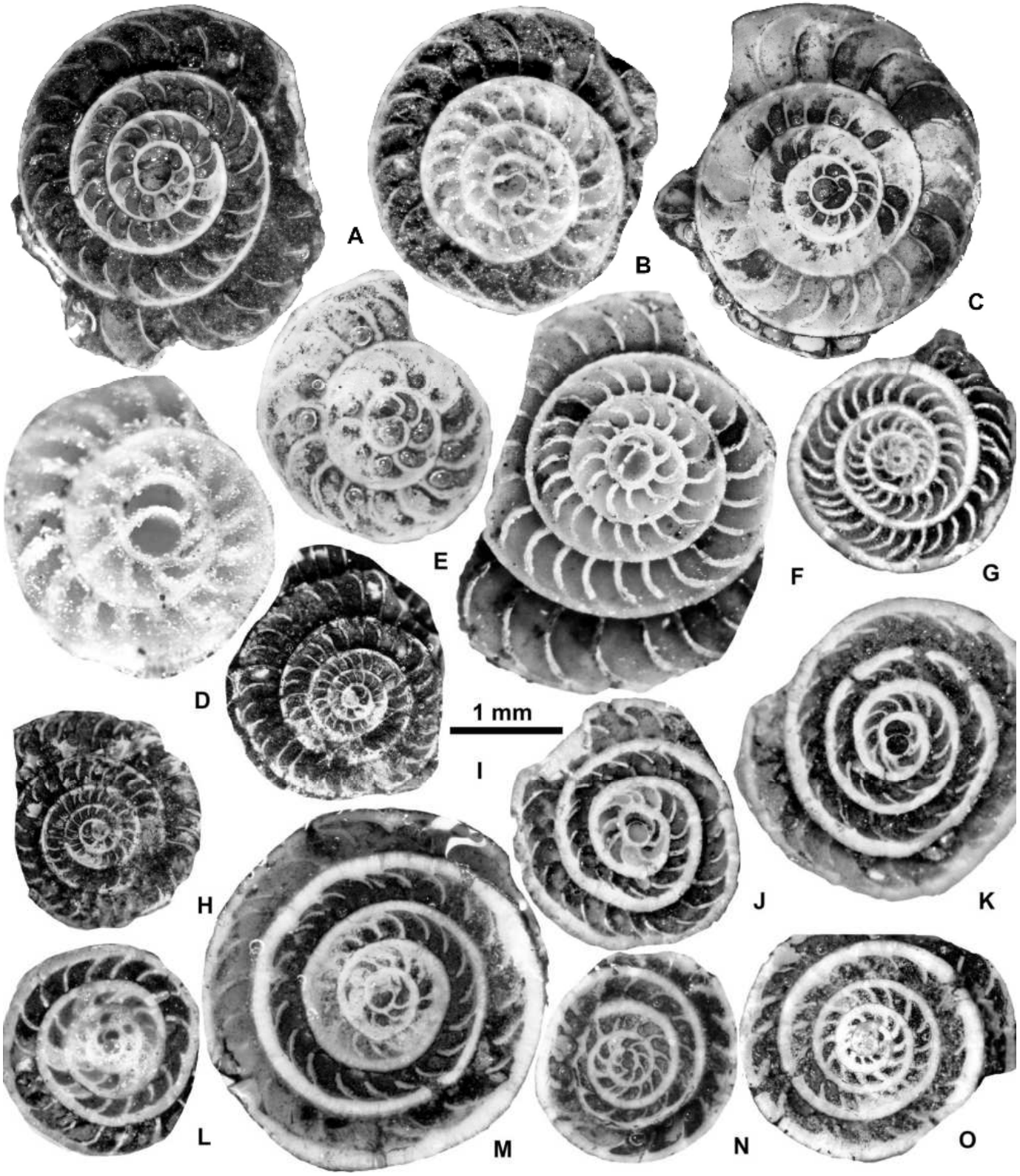

Figure 31. Equatorial sections of radiate *Nummulites*: *N. chavannesi* de la Harpe (**A**–**F**), *N. budensis* Hantken (**G**), *N. pulchellus* Hantken in de la Harpe (**H**,**I**), and *N. incrassatus* de la Harpe (**J**–**O**). (**A**): E.2025.140, (**B**): E.2025.141, (**C**): E.2025.142, (**D**): E.2025.143, (**E**): E.2025.144, (**F**): E.2025.145, (**G**): E.2025.148, (**H**): E.2025.147, (**I**): E.2025.146, (**J**): E.2025.134, (**K**): E.2025.136, (**L**): E.2025.135, (**M**): E.2025.139, (**N**): E.2025.137, and (**O**): E.2025.139. (**A**–**E**), M–O: VER 2; (**F**,**H**,**I**): VER 4, and (**G**,**J**–**L**): VER 1 (Monte Cavro 4). All A-forms.

15. *Nummulites chavannesi* de la Harpe, 1878

Figure 31A–F.

Nummulites chavannesi n. sp.—[89]: 232 (nomen nudum).

Nummulites chavannesi de la Harpe—[90]: Plate 6: 22–41.—[91]: 123–125, Plate 2: 1–3, Figures 14–21. (with synonymy)—[66]: 827, Figure 39v,x–z,A,B. (with synonymy)—[68]: 925, 927, Figure 14g–q.—[65]: 454, 456, Plate 1: G.

This radiate taxon with a distinct umbo is characterized by a moderately small- to medium-sized embryo, moderate opening spiral, and moderately arched, relatively high chambers. *Nummulites chavannesi* does not yet fit into any evolutionary lineage. It occurs in all three samples of Castel San Felice: it is quite common in sample VER 2, however, it is rare in the other two (VER 3 and 4). Compared to the specimens described under this name from other localities, the Verona individuals have the largest proloculus and differ from them in some other aspects as well. We think that *N. chavannesi* may be a collective term for closely related late Bartonian to Priabonian taxa and will need to be revised in the future. Ref. [4] indicate the latest Bartonian to Priabonian (SBZ 18–20) for the stratigraphic range of this taxon, which does not need to be modified here.

16. *Nummulites incrassatus* de la Harpe, 1883

Figure 31J–O.

Nummulites Boucheri var. *incrassata* n. var.— [90]: Plate 8: 53a.

Nummulites incrassatus de la Harpe—[66]: 823, Figure 39a–r. (with synonymy)—[68]: 917, Figure 14r–z.—[65]: 456, Plate 1: A–F.

This name is generally used for moderately small radiate *Nummulites* with a moderately small embryo, evenly coiled spiral, and slightly arched, more or less isometric chambers from the Bartonian and Priabonian. In Verona, such forms occur in Monte Cavro (sample VER 1) and also rarely in Castel San Felice (samples VER 2 and VER 3, the latter only with a single specimen). Based on the great variability of such forms, especially from the N Thrace Basin (NW Turkey), but also from other European sites [66], we did not exclude that *N. incrassatus* may be a collective term for some taxa very close to each other, needing a thorough revision. Until then, we must follow the old practice in joining these forms as *N. incrassatus*, which is believed to be the ancestor of the Rupelian *N. vascus* [35], forming an evolutionary lineage with it. Ref. [68] suggests a Bartonian to Priabonian age (SBZ 17–20) for the stratigraphic range of *N. incrassatus*, which is not contradicted in this study.

17. *Nummulites pulchellus* Hantken in de la Harpe, 1883

Figure 31H–I.

Nummulites pulchella Hantken—[90]: 160, pl. 5: 15–21.

Nummulites pulchellus Hantken in de la Harpe —[91]: 126–127, pl. 2: 4–13, Figures 26–32. (with synonymy) —[56]: 354, pl. 1: 19.—[66]: 829, Figure 39J.—[45]: Figure 6d.

Two specimens of this radiate form were found in sample VER 4 of Castel San Felice. *Nummulites pulchellus* can easily be identified based on its small embryo, moderately loose spiral, and densely spaced, narrow, high, almost straight chambers.

This taxon does not yet fit into any evolutionary lineage. Its stratigraphic range is updated as SBZ 18B–20 (the entire Priabonian in the recent interpretation) in [66], which remains valid in this paper, too.

6.2.2. Genus *Assilina* d'Orbigny, 1839

Following [77], we consider *Assilina* as nummulitids with simple short sutural canals and nonfolded septa without apertures. This genus is represented in our material with one single species, belonging to the long-lasting (Ypresian to end-Priabonian), evolute *Assilina parva–A. schwageri–A. alpina* evolutionary lineage. Although the morphometric limits between *A. schwageri* (mostly Bartonian) and *A. alpina* (mostly Priabonian) are not

yet exactly defined, the mean inner cross-diameter of the proloculus for the first species is usually below 120 µm, while for the second, it is above this value. Based on our measurements (Table 6), the few specimens from samples VER 3 and 4 can be jointly evaluated and determined as *A. alpina*.

Table 6. Statistical data of the inner cross-diameter of the proloculus of *Assilina* and *Operculina* populations from Verona (in µm).

Taxon	Sample	№	Range	Mean ± s.e.
Assilina alpina	**VER 3 + 4**	**8**	**110–160**	**129 ± 6**
	VER 3	3	120–160	145
	VER 4	5	110–130	120 ± 4
Operculina ex. gr. *gomezi*	**VER 3 + 4**	**3**	**80–105**	**92**
	VER 3	2	80–90	85
	VER 4	1		105

Assilina alpina (Douvillé, 1916)

Figure 32A–F.

Operculina alpina n. sp.—[92]: 329, Figure 1.

Operculina alpina Douvillé—[40]: 85, Plate 38: 4–6, Figure 34. (with synonymy).

Assilina alpina (Douvillé)—[56]: 356, Plate 2: 8.—[45]: Figure 9e.—[64]: 18, Figure 15I.—[68]: 925, Figures 18g–i and 19a–c.—[65]: 459, 462, Plate 3: A–D.

6.2.3. Genus *Operculina* d'Orbigny, 1826

Based on [40,77], *Operculina* is characterized by an evolute or involute flattened test with dense and high chambers and folded septa, which are intersected by stolons [66]. This latter is essential in distinguishing *Operculina* from *Assilina*. This feature can be best observed in painted split equatorial sections (see Figure 32G–I and also [66]: Figure 40o,p). This genus (as interpreted above) first appears around the Lutetian/Bartonian boundary and lasts until the end of the Priabonian with a single lineage [45], which starts with *O. bericensis*, followed by *O. roselli*, and terminates with *O. gomezi* [40], but their biometric limits have not been given.

The inner cross-diameter of the proloculus (P) does not show any clear increasing trend during the Bartonian to Priabonian interval [66] and remains in a range between 65 and 130 µm. Therefore, we rather join these forms under the name of *Operculina* ex gr. *gomezi*. They are very rare in Verona and recorded only from Castel San Felice in samples VER 3 and 4 (see Table 6 for morphometric data).

Operculina ex gr. *gomezi* Colom et Bauzá, 1950

Figure 32G–I.

Operculina canalifera gomezi n. ssp.—[93]: 219, pl. 17: a.1–3, Figures 1 and 2

Operculina gomezi Colom et Bauzá—[40]: 98, 100, Figure 38A–F. (with synonymy).—[64]: 18, Figure 13N–R.

Assilina gomezi (Colom et Bauzá)—[56]: 354, Plate 2: 7.

Operculina ex gr. *gomezi* Colom et Bauzá—[59]: 71, Figure 32x—[66]: Figure 40j–q—[68]: 925, Figure 19d–l—[65]: 458, 459, Plate 3: E–G.

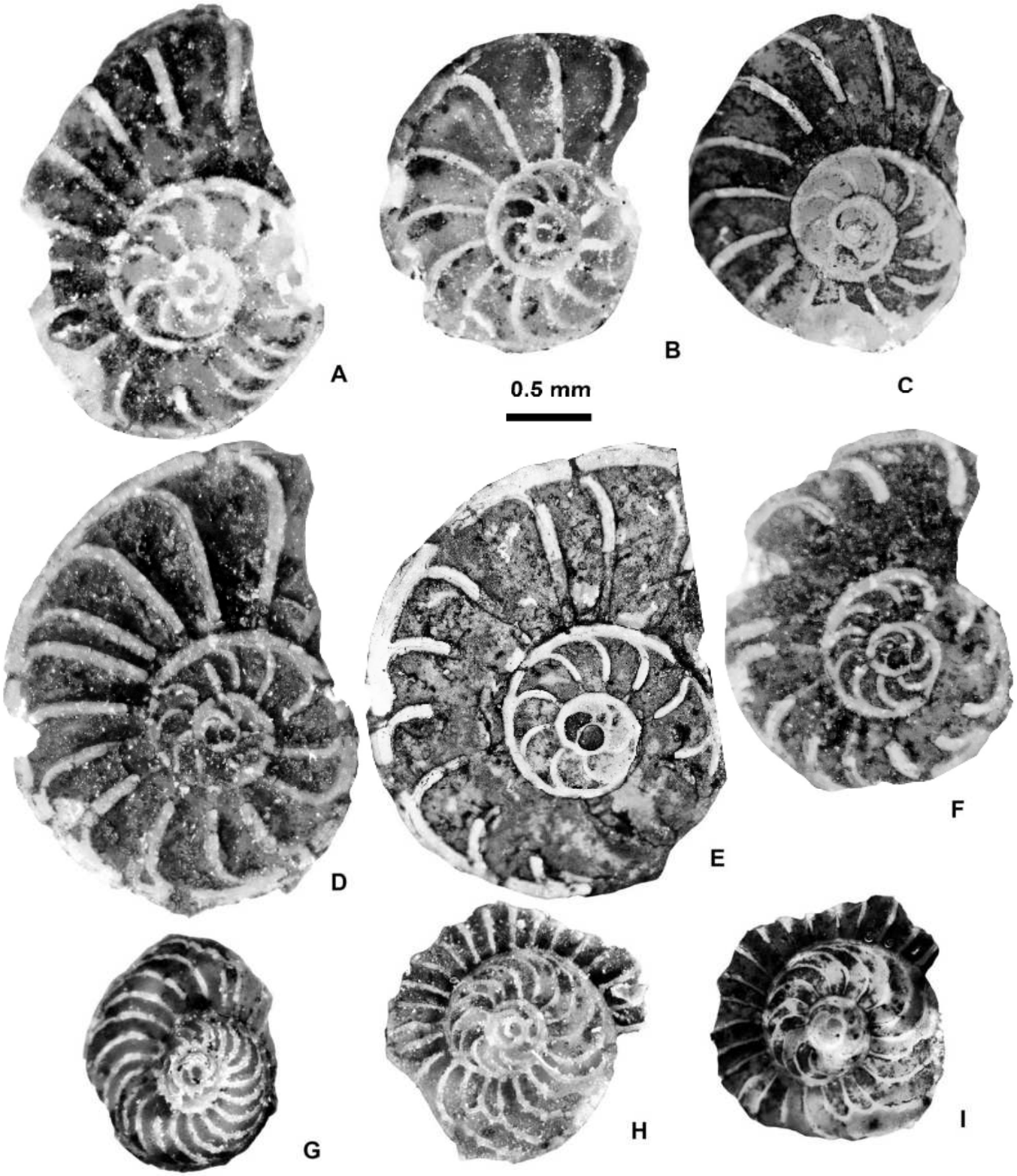

Figure 32. Equatorial sections of *Assilina alpina* Douvillé (**A**–**F**) and *Operculina* ex gr. *gomezi* Colom & Bauza (**G**–**I**). (**A**): E.2025.149, (**B**): E.2025.150, (**C**): E.2025.152, (**D**): E.2025.154, (**E**): E.2025.151, (**F**): E.2025.153, (**G**): E.2025.155, (**H**): E.2025.156, and (**I**): E.2025.157. (**A**,**B**,**E**,**G**,**H**): VER 3 and (**C**,**D**,**F**,**I**): VER 4. All A-forms.

6.2.4. Genus *Heterostegina* d'Orbigny, 1826

The genus *Heterostegina* bears all features of the genus *Operculina*, with one exception, as follows: following the first, undivided chambers, the next ones are secondarily divided

into chamberlets. Based on a widespread Western Tethyan material, Eocene representatives of this genus have recently been revised [37] and arranged into three species. These are *H. armenica*, *H. reticulata*, and *H. gracilis*; the second of them occurs in our material. Later, ref. [94] also introduced *H. indusensis* from Pakistan. The simplified numerical characterization of *Heterostegina* is based on the system introduced for *Cycloclypeus* [95] and consists of two measurements and two counts, as follows and shown in Figure 33. Morphometric data are summarized in Table 7.

P: The inner cross−diameter of the proloculus in μm.

X: The number of undivided, "operculinid" chambers before the appearance of the first subdivided, heterosteginid chamber, excluding the embryo (the first two chambers) (degree of "operculinid reduction"). Undivided chambers, sometimes reappearing after the first heterosteginid chamber, are not counted. In Figure 33, X = 1.

S: The number of chamberlets in the fourteenth chamber (including the embryo), reflecting the density of secondary chamberlets ("heterosteginid escalation"). If this chamber is not subdivided into chamberlets, S = 1. In Figure 33, S = 7.

d: The maximum diameter of the shell in the first whorl as measured along the common symmetry axis of the embryo (the first two chambers) (in μm).

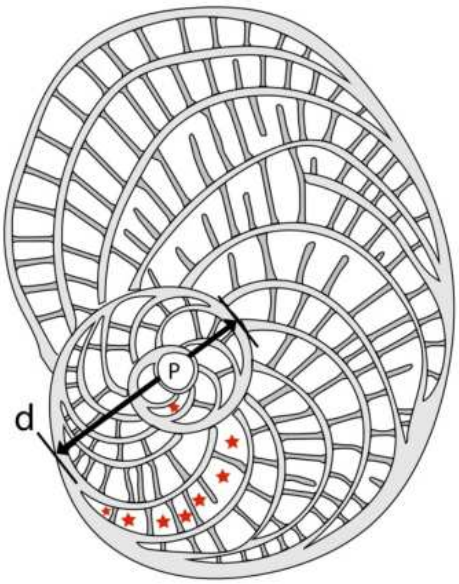

Figure 33. Measurement system for nummulitids with secondary chamberlets.

Heterostegina reticulata Rütimeyer, 1850

This species without granules has an involute, biconvex test with a central pile and slightly sigmoid septal sutures passing sooner or later into a septal network towards the edges. The size of the proloculus increases in stratigraphic order from small- to medium-sized chamberlets (with no incomplete secondary septa), which change simultaneously from rather irregularly arranged rhomboids to regularly arranged and almost rectangular shapes. Their number in chamber 14 (parameter S) also increases in stratigraphic order, but usually does not exceed 7–8. The number of operculinid (undivided) chambers (parameter X) is strongly reduced during the phylogenesis, which can be very well seen on the P–X bivariate plot of Figure 34 as well.

Based on the operculinid reduction, *Heterostegina reticulata* is subdivided into seven chrono-subspecies, as follows: *H. r. tronensis* (X_{mean} > 17; SBZ 18B), *H. r. hungarica* (X_{mean} = 11–17; SBZ 18B), *H. r. multifida* (X_{mean} = 7.2–11; SBZ 18C), *H. r. helvetica* (X_{mean} = 4.4–7.2; SBZ 18C), *H. r. reticulata* (X_{mean} = 2.8–4.4; SBZ 18C), *H. r. mossanensis* (X_{mean} = 1.7–2.8; SBZ 19A), and *H. r. italica* (X_{mean} < 1.7; SBZ 19B–20) [37].

Table 7. Statistical data of *Heterostegina* and *Spiroclypeus* populations from Verona.

Parameters		Inner Cross-Diameter of the Proloculus			Number of Post-Embryonic Pre-Heterosteginid Chambers			Number of Chamberlets in the Fourteenth Chamber			Outer Diameter of the First Whorl			Subspecific Determination
		P (μm)			X			S			d (μm)			
Taxon	**Sample**	**No**	**Range**	**Mean ± s.e.**	**No**	**Range**	**Mean ± s.e.**	**No**	**Range**	**Mean ± s.e.**	**No**	**Range**	**Mean ± s.e.**	
Heterostegina reticulata	**VER 1**	**28**	**60–135**	**91.2 ± 2.8**	**28**	**4–17**	**8.50 ± 0.57**	**28**	**1–3**	**2.00 ± 0.12**	**28**	**442–760**	**569 ± 15**	*multifida*
	VER 2	**23**	**100–160**	**133.0 ± 3.9**	**23**	**1–4**	**1.96 ± 0.15**	**22**	**3–6**	**4.41 ± 0.18**	**22**	**427–1120**	**832 ± 35**	*mossanensis*
	VER 3 + 4	**27**	**90–185**	**131.3 ± 4.8**	**27**	**1–5**	**2.26 ± 0.17**	**25**	**3–6**	**4.68 ± 0.19**	**26**	**510–1200**	**862 ± 31**	
	VER 3	11	90–185	137.4 ± 9.2	11	1–3	2.27 ± 0.24	9	3–6	5.00 ± 0.41	10	510–1200	885 ± 70	*mossanensis*
	VER 4	16	105–185	127.2 ± 5.2	16	1–5	2.25 ± 0.23	16	3–5	4.50 ± 0.18	16	710–1080	848 ± 28	
Spiroclypeus sirottii	**VER 2–4**	**52**	**55–115**	**86.6 ± 2.0**	**52**	**2–10**	**4.52 ± 0.26**	**52**	**2–5**	**2.87 ± 0.11**	**52**	**340–710**	**532 ± 11**	—
	VER 2	12	72–105	91.9 ± 3.1	12	2–6	3.92 ± 0.34	12	2–5	3.25 ± 0.27	12	461– 710	572 ± 24	
	VER 3	19	55–110	86.8 ± 3.3	19	2–10	5.11 ± 0.49	19	2–4	2.79 ± 0.12	19	340– 660	524 ± 20	
	VER 4	21	57–115	83.5 ± 3.2	21	2–8	4.33 ± 0.41	21	2–4	2.71 ± 0.17	21	410– 650	518 ± 14	

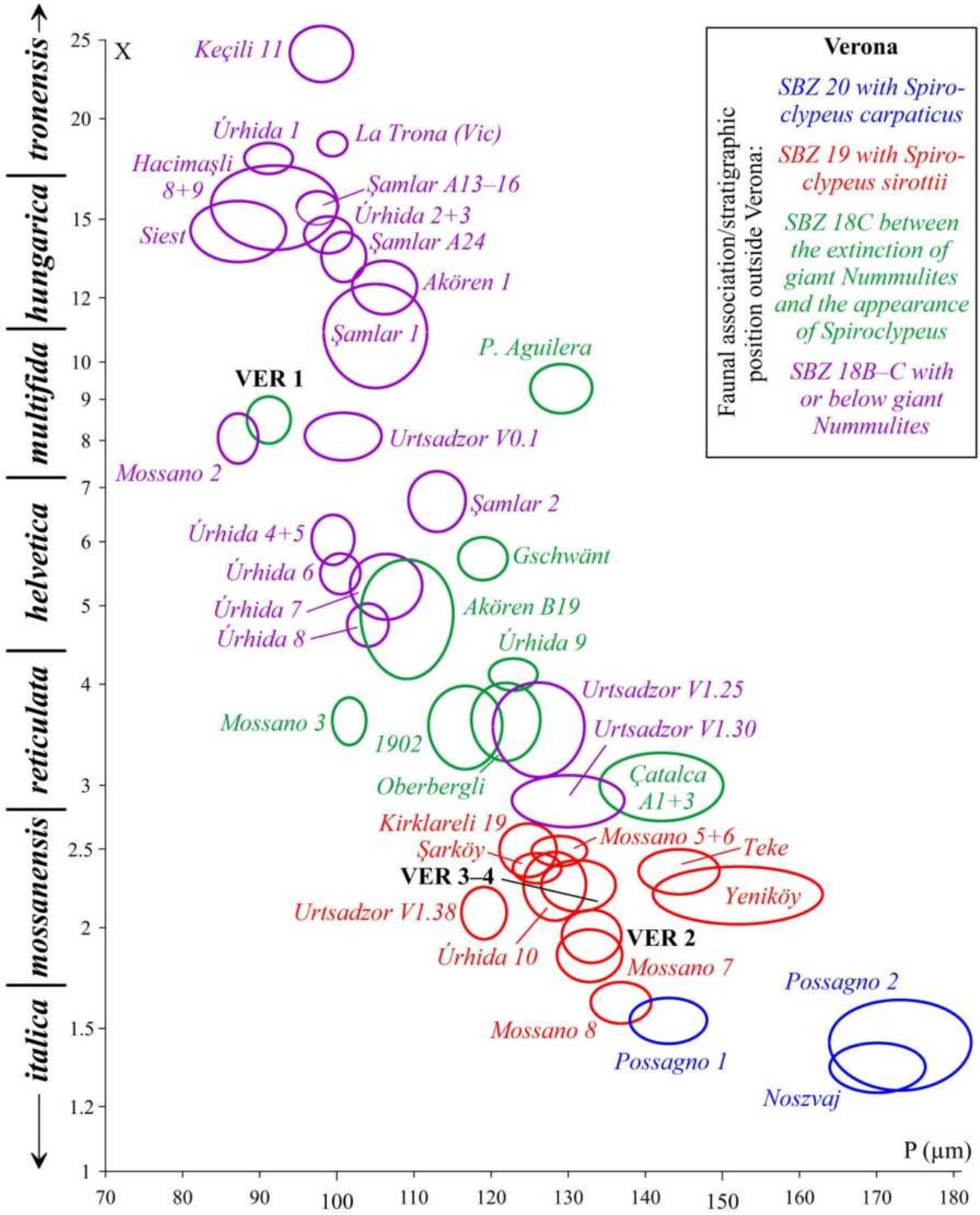

Figure 34. Distribution of *Heterostegina* populations from the vicinity of Verona (mean values at the 68% confidence level corresponding to 1 s.e.) on the P–X (proloculus diameter versus the number of undivided postembryonic chambers) bivariate plot (X is on a logarithmic scale) with the subspecific subdivision of *Heterostegina reticulata*. For the summary list of localities, see [45]. For Urtsadzor (Armenia), see [68].

Heterostegina reticulata occurs in all our samples. The population of sample VER 1 from Monte Cavro is determined as *H. r. multifida*, while those from Castel San Felice are assigned to *H. r. mossanensis*. The population of sample VER 2 appears to be slightly more advanced than the very similar populations of samples VER 3 and 4, which can, therefore, be evaluated together.

Heterostegina reticulata multifida (Bieda, 1949)

Figures 35A–D and 36.

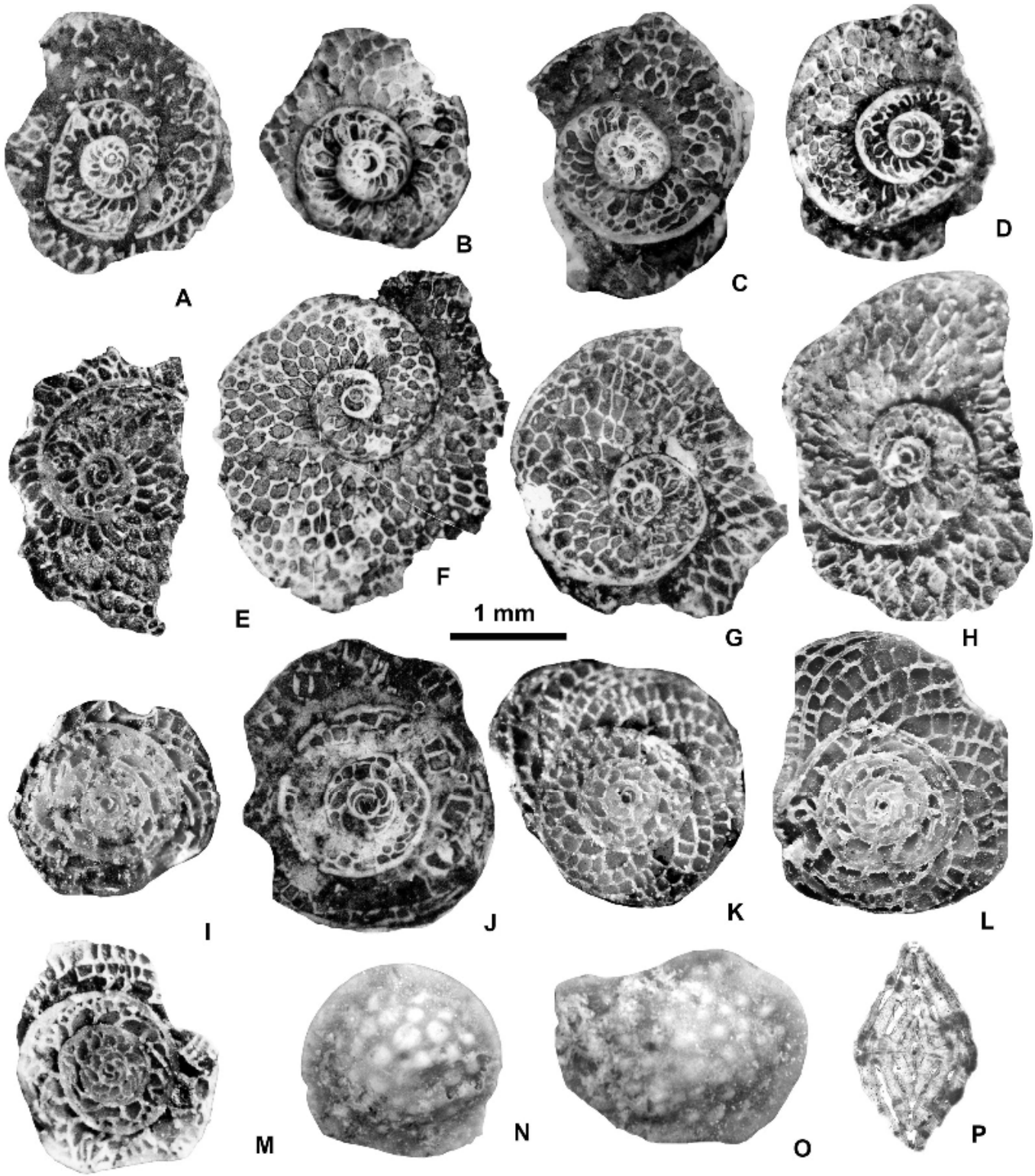

Figure 35. Equatorial and axial sections and external views of *Heterostegina reticulata multifida* Bieda (**A**–**D**), *H. reticulata mossanensis* Less et al. (**E**–**H**), and *Spiroclypeus sirottii* Less & Özcan (**I**–**P**). (**A**): E.9527, (**B**): E.9526, (**C**): E.2025.158, (**D**): E.9525, (**E**): E.9562, (**F**): E.9565, (**G**): E.2025.159, (**H**): E. 9563, (**I**): E.2025.160, (**J**): E.9588, (**K**): E.9586, (**L**): E.2025.161, (**M**): E.9587, (**N**): E.07.01, (**O**): E.07.02, and (**P**): E.08.02. (**A**–**D**): VER 1 (Monte Cavro 4); (**E**,**G**,**H**,**K**–**P**): VER 4; (**F**,**J**): VER 2; I: VER 3. All A-forms.

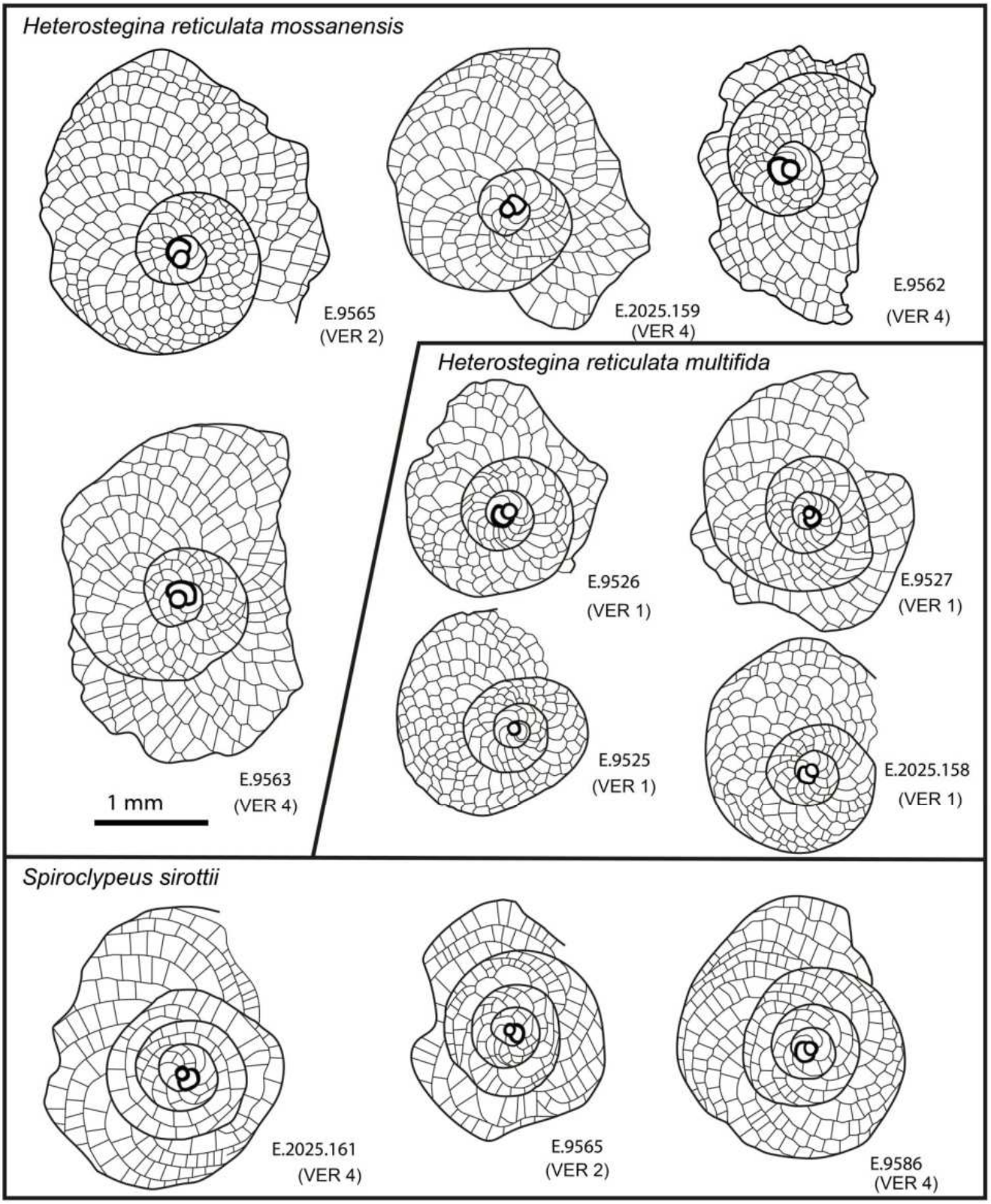

Figure 36. Line drawings of the *Heterostegina* and *Spiroclypeus* in the vicinity of Verona.

Grzybowskia multifida sp. nov.—[96] (partim): 153–158, 168–173, Plate 3: 1, 3, 7; Plate 4: 1. (non 2).

Heterostegina reticulata multifida (Bieda)—[37]: 335–336, Figure 12J–M,O–Q. (with synonymy)—[68]: Figure 20a–f.

Heterostegina reticulata mossanensis Less, Özcan, Papazzoni & Stockar, 2008

Figure 35E–H and Figure 36.

Heterostegina reticulata mossanensis n. ssp.—[37]: 336, 338, Figures 14G–R and 15A–C (with synonymy)

Heterostegina reticulata mossanensis Less, Özcan, Papazzoni & Stockar—[59]: Figure 32b–f.—[66]: Figure 42r–s.—[45]: Figure 9b.—[68]: Figure 21b.

6.2.5. Genus *Spiroclypeus* Douvillé, 1905

Spiroclypeus is a planispiral, lamellar, finely perforated, involute foraminifer [40]. Externally (Figure 35N,O), the test is biconvex with a very slightly eccentric outline. Most of the surface is covered by granules. Its chambers in the equatorial plane become secondarily subdivided into regularly arranged secondary chamberlets by well−developed, complete secondary septa at different moments of their ontogeny. The spiral chambers never develop into annular ones. The diagnostic feature of *Spiroclypeus* that distinguishes it from *Heterostegina* is the symmetrical presence of lateral chamberlets (Figure 35P) on both sides of the spiral. The network of chamberlets can be frequently seen on its very edge.

Based on a widespread material, the Eocene representatives of this genus from the Western Tethys have recently been revised, and one single evolutionary lineage was recognized [38]. Due to the similar architecture of their equatorial plane, the same measurement system is applied to *Spiroclypeus* as to *Heterostegina* (see above). Morphometric data are summarized in Table 7.

The developmental trends within the evolutionary lineage of Tethyan *Spiroclypeus* are the same as those discussed in detail for *Heterostegina reticulata*. Two different taxa can be distinguished, which we interpret as species, as no gradual transition between them is observed (unlike in the case of *Heterostegina reticulata* with subspecies). Based on the operculinid reduction (see also the P–X bivariate plot of Figure 37), the evolutionary lineage of Eocene *Spiroclypeus* in the Western Tethys is subdivided into two species [38], as follows: *S. sirottii* (X_{mean} > 2.7; SBZ 19) and *S. carpaticus* (X_{mean} < 2.7; SBZ 20).

Spiroclypeus is absent in sample VER 1 from Monte Cavro, however, it is common in all three samples (VER 2–4) of Castel San Felice. Due to their similar morphometric parameters, they can be jointly evaluated and determined as *S. sirottii.*

Spiroclypeus sirottii Less & Özcan, 2008

Figure 35I–P and Figure 36.

Spiroclypeus sirottii n. sp.— [38]: 310–311, Figure 7A–N,P,Q,T. (with synonymy)

Spiroclypeus sirottii Less & Özcan—[59]: 72, Figure 32g–m.—[66]: 838, Figure 40D,E.—[45]: Figure 9a.—[68]: 928, Figure 21c.

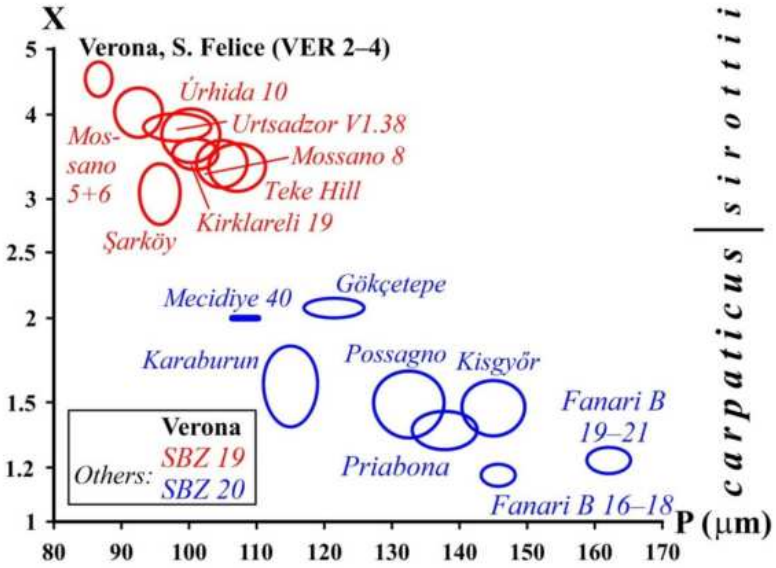

Figure 37. Distribution of the *Spiroclypeus* population from Verona (mean values at the 68% confidence level corresponding to 1 s.e.) on the P–X (proloculus diameter v. the number of undivided postembryonic chambers) bivariate plot (X is on a logarithmic scale) with the specific subdivision of Eocene *Spiroclypeus*. Information on localities in Turkey, Armenia, and Europe was given by [38,59,64–66,68].

7. Discussion

7.1. Comparison with Other LBF Key Assemblages

The LBF fauna found in sample VER 1 on Monte Cavro is rather poor. Nevertheless, it contains a sufficient number of *Heterostegina reticulata multifida*, which clearly defines the SBZ 18C Subzone. This is supported by the presence of *Nummulites hormoensis* (characteristic of SBZ 18), also in a sufficient quantity, while the genus *Spiroclypeus*, first appearing in SBZ 19, is missing. However, since radiate *Nummulites* and especially orthophragmines occur only sporadically, this assemblage cannot be considered as a key LBF fauna, just as the upper part of Monte Cavro is not really a key locality for the SBZ 18C Subzone. The most diverse LBF assemblages of this age are found in Şamlar (NW Turkey, samples 1 and 2) [66], Úrhida (Hungary, samples 4–9, mostly yet unpublished) [37], and Urtsadzor (Armenia, samples V.01, V1 25, and 30) [68].

On the other hand, the LBF fauna around Castel San Felice is both very diverse and very well preserved. From the point of view of dating, the most relevant element is the presence of *Heterostegina reticulata mossanensis*, which is limited to the SBZ 19A Subzone. This age is also supported by the mass occurrence of *Spiroclypeus sirottii*, which is characteristic of the SBZ 19 Zone, and the sporadic presence of *Nummulites fabianii* (SBZ 19–20 Zones). Orthophragmines, characteristic of the OZ 14 Zone, are abundant, and significantly predominate over the radiate *Nummulites*.

In Figure 38, the LBF fauna of Castel San Felice (samples VER 2–4) is compared with other rich assemblages of a similar age (SBZ 19A). The table shows that they are very similar to each other, with minimal differences. All these sites are considered key localities for both the SBZ 19A and OZ 14 zones. However, the preservation of the fauna is considerably better in Verona, Mossano, Úrhida, and Kırklareli than in Şarköy, Teke, and Urtsadzor. Finally, both Castel San Felice and Mossano are easily accessible, making them ideal key localities for the discussed time span.

Taxa/localities	Verona, Castel San Felice (this work)	Mossano, Priabona Marl, basal layers[1]	Úrhida 10[2]	Şarköy 2+4[3]	Teke 1–8[4]	Kirklareli C 19[5]	Urtsadzor V1. 38[6]
Discocyclina augustae olianae				×			
D. augustae augustae	×	×	×			×	cf.
D. dispansa dispansa	×	×	×				cf.
D. dispansa umbilicata				×			
D. euaensis	×		×		×	×	
D. nandori		×	×	×			
D. pratti minor	×		×				cf.
D. radians radians	cf.		×			cf.	cf.
D. samantai						×	
D. trabayensis elazigensis	×	×		×			
Nemkovella strophiolata tenella	×	×	×				
N. daguini	×			×			
Orbitoclypeus varians scalaris	×				×		
O. varians varians	×	×	×			×	×
O. zitteli		×			×		×
Asterocyclina alticostata alticostata		×				×	cf.
A. alticostata danubica	×				cf.		
A. kecskemetii			×		×		
A. stella stella		×	×	×			×
A. stellata stellaris	×	×	×	×	×	×	
A. ferrandezi ferrandezi				×	×	×	
Nummulites fabianii	×	rare			×	×	×
radiate *Nummulites* *N. incrassatus*	×	×	to be studied	not studied	not studied	×	×
radiate *Nummulites* *N. chavannesi*	×	×				×	×
radiate *Nummulites* *N. pulchellus*	×	×					
radiate *Nummulites* *N. budensis*	×						×
radiate *Nummulites* *N. cunialensis*						×	×
radiate *Nummulites* *N. stellatus*		×				×	×
Assilina alpina	×	×	×	×	×	×	×
Operculina ex gr. *gomezi*	×	×	×	×			×
Heterostegina reticulata mossanensis	×	×	×	×	×	×	×
Spiroclypeus sirottii	×	×	×	×	×	×	×
Pellatispira madaraszi							×

Figure 38. Distribution of LBF in some key localities for the SBZ 19A Zone. Thick lines indicate transitional populations. [1] [7,25], [2] [37] and GL's unpublished data, [3] [53], [4] [59], [5] [66], [6] [68].

7.2. Updating Late Lutetian–Priabonian LBF Range Charts

In recent years, several new data sets have been published on LBF assemblages from the Eocene [8,54,60–62,64,65,68,97–106].

These significantly enriched our knowledge on the stratigraphic ranges of LBF taxa living in this period, making it necessary to update previously published summaries [45,66] on this topic.

The updated stratigraphic ranges of particular orthophragmine taxa (subspecies and unsubdivided species) are shown in Figure 39, while the updated ranges of the most important Bartonian–Priabonian nummulitid taxa are summarized in Figure 40. Note that the arbitrary subdivision of the (supposedly gradual) evolutionary lineages causes overlaps

between the stratigraphical ranges of neighboring subspecies (Figure 41), since there are always spatial, ecological, and random deviations from the 'medium' evolutionary track, and, thus, the latter has a range of variation.

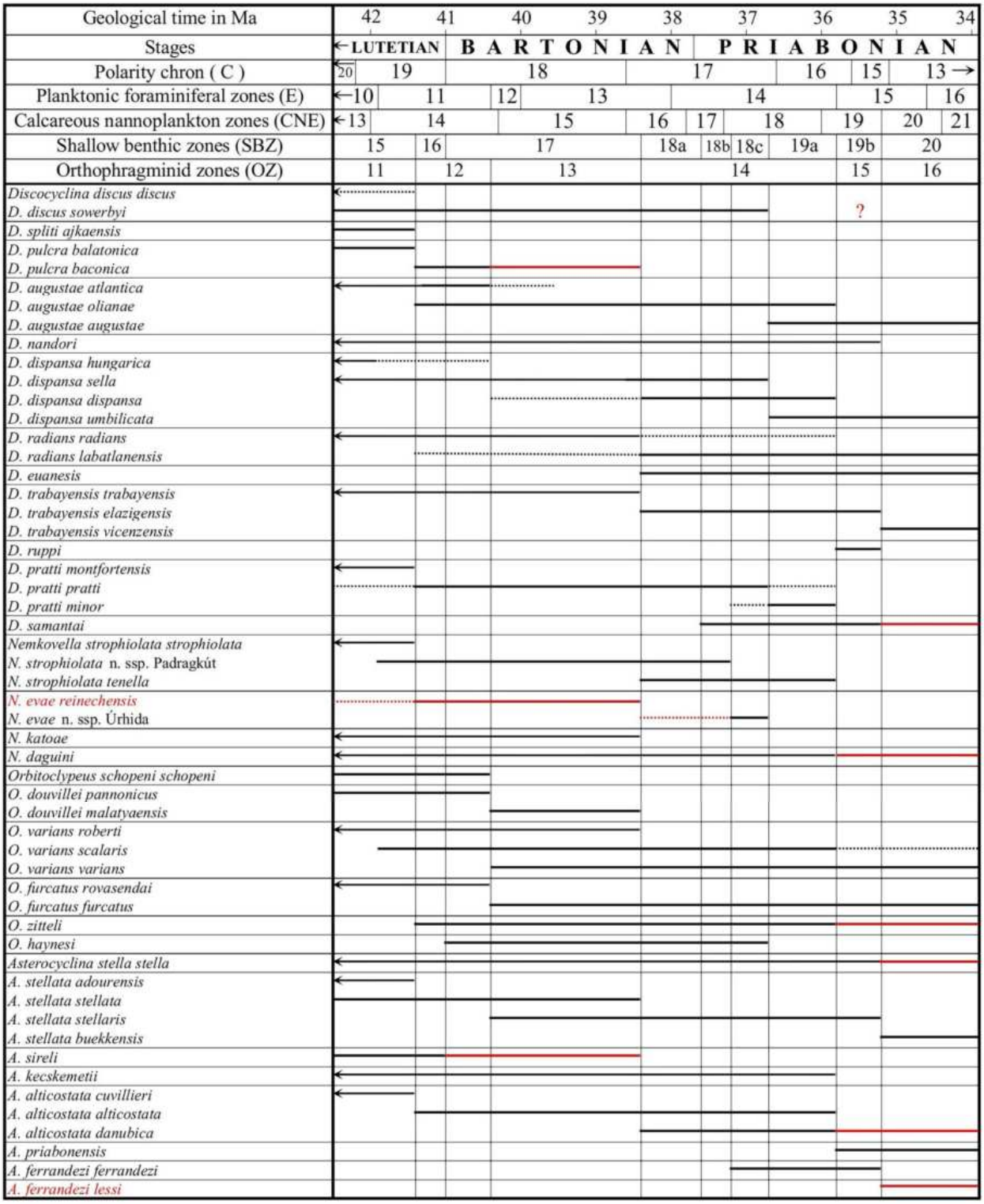

Figure 39. Updated orthophragmine range chart for the late Lutetian to terminal Priabonian interval in the Western and Central Tethys. Updates compared to the range chart in [66] are marked in red. Dashed lines indicate uncertain occurrences. Red question mark corresponds to the erratic occurrence of one single specimen of *Discocyclina discus sowerbyi* from Switzerland [54]. The time scale, position of stages, polarity chrons, and zonal subdivision by planktonic foraminifera, calcareous nannoplankton, and larger benthic foraminifera are based on [107].

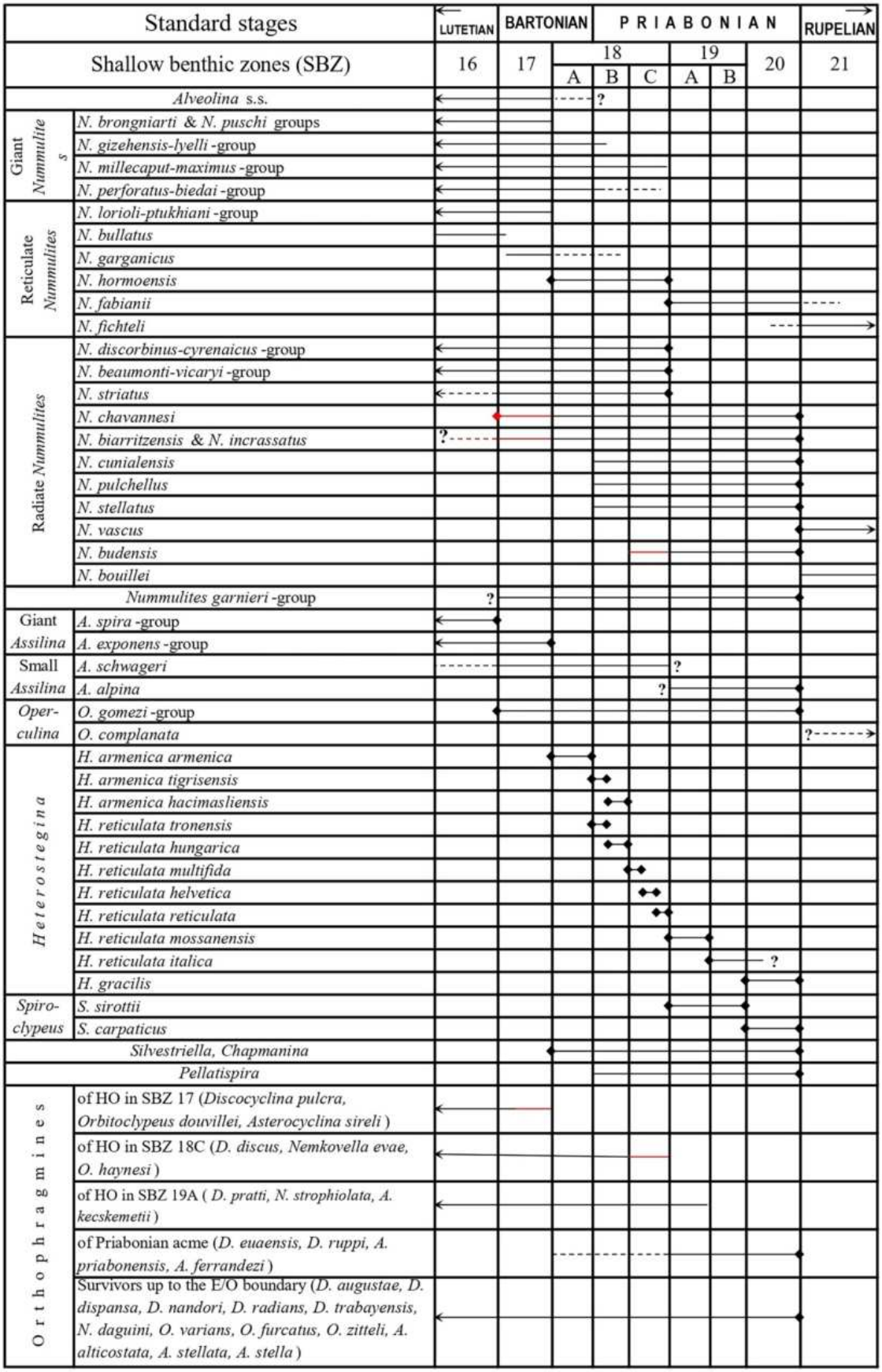

Figure 40. Updated range chart for some late Lutetian to early Rupelian larger benthic foraminiferal taxa of the peri-Mediterranean region [45] with modifications (updates are marked in red). The stratigraphic subdivision is not time-proportional.

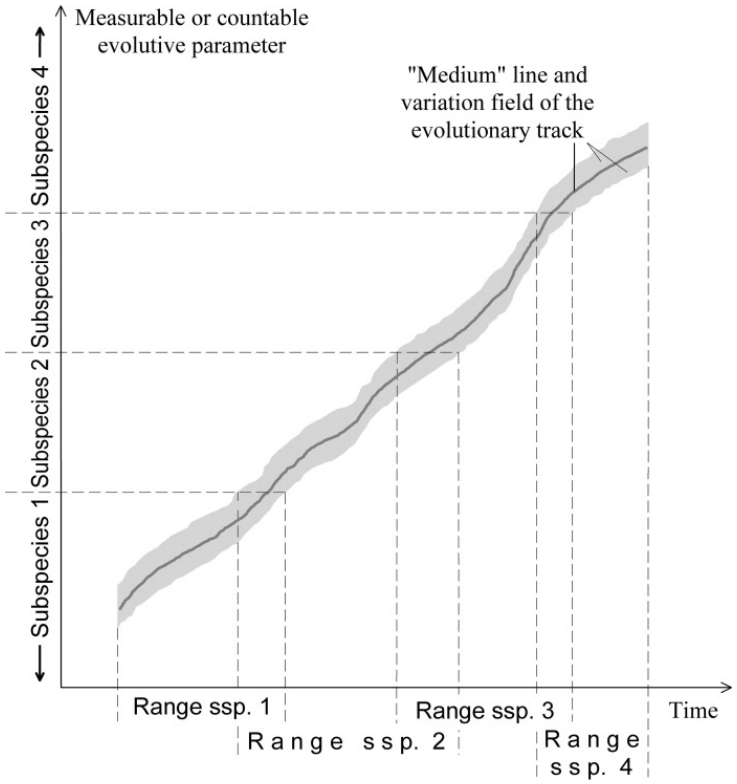

Figure 41. Relationship between the arbitrary subdivision of evolutionary lineages and the stratigraphic ranges of the obtained subspecies.

Figures 39 and 40 are spatially valid for the peri-Mediterranean region, including the territory from Spain to Armenia, and from the Alps to Tunisia, but not including the Indian subcontinent. One of the reasons for this is that the taxonomical composition of the orthophragmine fauna in this region is significantly different from that of the more western territories, although several common taxa enable observing the correlation between them [8,60,61,99,108]. The other reason is that, in our opinion, the nummulitids from the Indian subcontinent need a comprehensive revision, because the nomenclature used for them is significantly different for (mainly) the Western Tethys [35] and for India [109–111].

Author Contributions: Conceptualization, L.S.E. and G.L.; methodology, G.L. and C.A.P.; validation, L.S.E., G.L. and C.A.P.; investigation, L.S.E. and G.L.; data curation, G.L.; writing—original draft preparation, L.S.E., G.L. and C.A.P.; writing—review and editing, L.S.E.; visualization, L.S.E.; supervision, G.L. All authors have read and agreed to the published version of the manuscript.

Funding: This research received no external funding.

Data Availability Statement: The raw data will be made available by the authors on request.

Acknowledgments: The authors are grateful to the late Achille Sirotti (University of Modena) for introducing the geology of the area and presenting the localities. "L.S.E. was supported by the Stipendium Hungaricum program in the framework of his related studies. He also would like to express profound gratitude to his late advisor, Ercan Özcan, for his invaluable guidance, support, and the lasting impact he had on his academic journey. We would like to thank the whole staff of the Institute of Exploration Geosciences of the University of Miskolc for introducing the use of the equipment. The useful comments of the two reviewers greatly improved the quality of the paper.

Conflicts of Interest: The authors declare no conflicts of interest.

Abbreviations

SBZ	Shallow Benthic Zone
LBF	Larger benthic foraminifera
OZ	Orthophragmine Zone
Fm.	Formation
№	Number of specimens
s.e.	Standard error
HO	Highest occurrence

References

1. Coletti, G.; Commissario, L.; Mariani, L.; Bosio, G.; Desbiolles, F.; Soldi, M.; Bialik, O.M. Palaeocene to Miocene southern Tethyan carbonate factories: A meta-analysis of the successions of South-western and Western Central Asia. *Depos. Rec.* **2022**, *8*, 1031–1054. [CrossRef]
2. Archiac, E.J.A.d'. Description des Fossiles du Groupe Nummulitique Recueillis Par M. S. P. Pratt et M. J. Delbos Aux Environs de Bayonne et de Dax. In *Mémoires de la Société Géologique de France*, 2nd series 1850 ed; Société géologique de France: Paris, France, 1850; Volume 3, pp. 397–456. (In French)
3. Archiac, E.J.A.d'.; Haime, J. *Description des Animaux Fossils du Groupe Nummulitique de l'Inde, Précédé D'un Résumé Géologique et D'une Monographie des Nummulites*; Gide et J. Baudry Libraires-Éditeurs: Paris, France, 1853. (In French)
4. Serra-Kiel, J.; Hottinger, L.; Caus, E.; Drobne, K.; Ferrández, C.; Jauhri, A.K.; Less, G.; Pavlovec, R.; Pignatti, J.; Samsó, J.M.; et al. Larger Foraminiferal Biostratigraphy of the Tethyan Paleocene and Eocene. *Bull. Soc. Géol. Fr.* **1998**, *169*, 281–299.
5. Cahuzac, B.; Poignant, A. Essai de Biozonation de l'Oligo-Miocène Dans Les Bassins Européens à l'aide Des Grands Foraminifères Néritiques. *Bull. Soc. Géol. Fr.* **1997**, *168*, 155–169.
6. Less, G. Paleontology and stratigraphy of the European *Orthophragminae*. *Geol. Hung. Ser. Palaeontol.* **1987**, *51*, 1–373.
7. Less, G. The zonation of the Mediterranean Upper Paleocene and Eocene by *Orthophragminae*. *Opera Dela Slov. Akad. Znan. Umet.* **1998**, *34*, 21–43.
8. Özcan, E.; Yücel, A.O.; Erkızan, L.S.; Gültekin, M.N.; Kayğılı, S.; Yurtsever, S. Atlas of the Tethyan Orthophragmines. *Mediterr. Geosci. Rev.* **2022**, *4*, 3–213. [CrossRef]
9. Papazzoni, C.A.; Ćosović, V.; Briguglio, A.; Drobne, K. Towards a calibrated larger foraminifera biostratigraphic zonation: Celebrating 18 years of the application of shallow benthic zones. *Palaios* **2017**, *32*, 1–5. [CrossRef]
10. Pignatti, J.; Papazzoni, C.A. Oppelzones and their heritage in current larger foraminiferal biostratigraphy. *Lethaia* **2017**, *50*, 369–380. [CrossRef]
11. Doglioni, C.; Bosellini, A. Eoalpine and Mesoalpine tectonics in the Southern Alps. *Geol. Rundsch.* **1987**, *76*, 735–754. [CrossRef]
12. Carminati, E.; Doglioni, C. Alps vs. Apennines: The paradigm of a tectonically asymmetric Earth. *Earth-Sci. Rev.* **2012**, *112*, 67–96. [CrossRef]
13. Curzi, M.; Viola, G.; Zuccari, C.; Aldega, L.; Billi, A.; van der Lelij, R.; Kylander-Clark, A.; Vignaroli, G. Tectonic evolution of the Eastern Southern Alps (Italy): A reappraisal from new structural data and geochronological constraints. *Tectonics* **2024**, *43*, e2023TC008013. [CrossRef]
14. Bosellini, A. Dynamics of Tethyan carbonate platforms. In *Controls on Carbonate Platform and Basin Development*; Crevello, P.D., Wilson, J.L., Sarg, J.F., Read, J.F., Eds.; SEPM Special Publication; Society for Sedimentary Geology (SEPM): Claremore, OK, USA, 1989; Volume 44, pp. 3–13.
15. Zampieri, D. Tertiary extension in the Southern Trento Platform, Southern Alps, Italy. *Tectonics* **1995**, *14*, 645–657. [CrossRef]
16. Winterer, E.L.; Bosellini, A. Subsidence and sedimentation on Jurassic passive continental margin, Southern Alps, Italy. *AAPG Bull.* **1981**, *65*, 394–421. [CrossRef]
17. Luciani, V. Stratigrafia sequenziale del Terziario nella catena del Monte Baldo (provincie di Verona e Trento). *Mem. Sci. Geol.* **1989**, *41*, 263–351.
18. Rasser, M.W.; Harzhauser, M.; Anistratenko, O.Y.; Anistratenko, V.V.; Bassi, D.; Belak, M.; Berger, J.-P.; Bianchini, G.; Čičić, S.; Ćosović, V. Palaeogene and Neogene. In *The Geology of Central and Eastern Europe*; McCann, T., Ed.; Geological Society of London: London, UK, 2008; pp. 1031–1137.
19. Martire, L.; Clari, P.; Lozar, F.; Pavia, G. The *Rosso Ammonitico Veronese* (Middle-Upper Jurassic of the Trento Plateau): A Proposal of Lithostratigraphic Ordering and Formalization. *Riv. Ital. Paleontol. Stratigr.* **2006**, *112*, 227.
20. Roghi, G.; Romano, R. Le Formazioni Geologiche del Veronese nella Nuova Cartografia Geologica Nazionale. *La Lessinia—Ieri Oggi Domani. Quaderno Culturale* **2009**, *32*, 34–35.

21. Bosellini, A.; Carraro, F.; Corsi, M.; De Vecchi, G.; Gatto, G.; Malaroda, R.; Sturani, C.; Ungaro, S.; Zanettin, B. *Note Illustrative Della Carta Geologica d'Italia*; F. 49, Verona; Servizio Geologico d'Italia: Roma, Italy, 1967.
22. Zorzin, R. Geologia e paleontologia dell'area collinale di Verona. In *Storia Naturale Della Città di Verona—Mem. Mus. Civ. St. Nat. Verona, Monografie Naturalistiche 6, 2021*; Latella, L., Ed.; Cierre Edizioni: Sommacampagna, Italy, 2018; pp. 39–48.
23. De Zanche, V.; Sorbini, L.; Spagna, V. Geologia del territorio del Comune di Verona. In *Memorie Museo Civico Storia Naturale Verona, II Serie, Sez. Sci. Terra*; Museo di Storia Naturale di Verona: Verona, Italy, 1977; Volume 1, pp. 1–52.
24. Barbieri, G. I Macroforaminiferi dell'Eocene Superiore nei Lessini a Nord di Verona. Bachelor's Thesis, Università degli Studi di Modena—Istituto di Paleontologia, Modena, Italy, 1985; pp. 1–198.
25. Papazzoni, C.A.; Sirotti, A. *Nummulite* biostratigraphy at the Middle/Upper Eocene boundary in the Northern Mediterranean Area. *Riv. Ital. Paleontol. Stratigr.* **1995**, *101*, 63–80.
26. Fabiani, R. Guida geologica delle Colline di Verona. *Atti Accad. Agricolt. Sci. Lett. Verona* **1920**, *21*, 241–252.
27. Catullo, A. Memoria geognostico-paleozoica sulle Alpi Venete, con Appendice e Seconda Appendice al Catalogo degli Ammoniti delle Alpi Venete. *Mem. Soc. Ital. Sci. Res. Modena* **1848**, *24*, 187–339.
28. Bittner, A. Das Alpengebiet zwischen Vicenza und Verona. *Verh. Geol. Bundesanst.* **1877**, *8*, 226–231.
29. Oppenheim, P. Die Eocaenfauna des Monte Postale bei Bolca in Veronesischen. *Palaeontographica* **1896**, *43*, 125–222.
30. Fabiani, R. Il Paleogene del Veneto. *Mem. Istit. Geol. Univ. Padova* **1915**, *3*, 1–336. [CrossRef]
31. Brönnimann, P. Zur Morphologie von *Aktinocyclina* Gümbel 1868. *Eclogae Geol. Helv.* **1945**, *38*, 560–579.
32. Brönnimann, P. Zur Frage der verwandtschaftlichen Beziehungen zwischen *Discocyclina* s.s. und *Asterocyclina*. *Eclogae Geol. Helv.* **1945**, *38*, 579–617.
33. Hottinger, L. Recherches sur les *Alvéolines* paléocènes et éocènes. *Schweiz. Paläontol. Abh.* **1960**, *75–76*, 1–243 + Atlas.
34. Schaub, H. Contribution à la stratigraphie du *Nummulitique* du Véronais et du Vicentin. *Mem. Soc. Geol. Ital.* **1962**, *3*, 59–66.
35. Schaub, H. *Nummulites* et *Assilinae* de la Tethys Paléogène: Taxonomies, phylogenèse et biostratigraphie. *Schweiz. Paläontol. Abh.* **1981**, *104–106*, 1–236 + Atlas I–II.
36. Arni, P.; Lanterno, E. Considérations paléoécologiques et interprétation des calcaires de l'Éocène du Véronais. *Arch. Sci.* **1972**, *25*, 251–283.
37. Less, G.; Özcan, E.; Papazzoni, C.A.; Stockar, R. The Middle to Late Eocene Evolution of Nummulitid Foraminifer *Heterostegina* in the Western Tethys. *Acta Palaeontol. Pol.* **2008**, *53*, 317–350. [CrossRef]
38. Less, G.; Özcan, E. The Late Eocene Evolution of Nummulitid Foraminifer *Spiroclypeus* in the Western Tethys. *Acta Palaeontol. Pol.* **2008**, *53*, 303–316. [CrossRef]
39. Less, G. New method for the examination of equatorial sections of orbitoidal larger foraminifera. In *Magyar Állami Földtani Intézet Évi Jelentése 1979*; Magyar Állami Földtani Intézet: Budapest, Hungary, 1981; pp. 1445–1457.
40. Hottinger, L. Foraminifères operculiniformes. *Mém. Mus. Natl. Hist. Nat.* **1977**, *57*, 1–159.
41. Drobne, K. Alvéolines paléogènes de la Slovénie et de l'Istrie. *Schweiz. Paläontol. Abh.* **1977**, *99*, 1–132.
42. Drooger, C.W. Radial Foraminifera: Morphometrics and Evolution. *Verh. Kon. Ned. Akad. Wetensch., Afd. Natuurk.* **1993**, *41*, 1–242.
43. Khan, M.A.; Drooger, C.W. On variation in *Nummulites* assemblages. I and II. *Proc. Kon. Ned. Akad. Wetensch. B* **1971**, *72*, 97–121.
44. Less, G.; Kovács, L.Ó. Typological versus morphometric separation of orthophragminid species in single samples—A case study from Horsarrieu (upper Ypresian, SW Aquitaine, France). *Rev. Micropaléontol.* **2009**, *52*, 267–288. [CrossRef]
45. Less, G.; Özcan, E. Bartonian–Priabonian larger benthic foraminiferal events in the Western Tethys. *Austrian J. Earth Sci.* **2012**, *105*, 129–140. Available online: https://www.zobodat.at/pdf/MittGeolGes_105_1_0129-0140.pdf (accessed on 1 August 2025).
46. Agnini, C.; Fornaciari, E.; Giusberti, L.; Grandesso, P.; Lanci, L.; Luciani, V.; Muttoni, G.; Pälike, H.; Rio, D.; Spofforth, D.J.A.; et al. Integrated biomagnetostratigraphy of the Alano section (NE Italy): A proposal for defining the middle–late Eocene boundary. *Bull. Geol. Soc. Am.* **2011**, *123*, 841–872. [CrossRef]
47. Agnini, C.; Backman, J.; Boscolo-Galazzo, F.; Condon, D.J.; Fornaciari, E.; Galeotti, S.; Giusberti, L.; Grandesso, P.; Lanci, L.; Luciani, V.; et al. Proposal for the global boundary stratotype section and point (GSSP) for the Priabonian stage (Eocene) at the Alano section (Italy). *Episodes* **2021**, *44*, 151–173. [CrossRef]
48. Caudri, C.B. Systematics of the American *Discocyclinas*. *Eclogae Geol. Helv.* **1972**, *65*, 211–219. [CrossRef]
49. Ferràndez-Cañadell, C.; Serra-Kiel, J. Morphostructure and paleobiology of *Discocyclina* Gümbel, 1870. *J. Foraminifer. Res.* **1992**, *22*, 147–165. [CrossRef]
50. Ferràndez-Cañadell, C. A new, ribbed species of *Nemkovella* Less 1987 (Discocyclinidae), and discussion of the genus *Actinocyclina* Gümbel, 1870. *J. Foraminifer. Res.* **1997**, *27*, 175–185. [CrossRef]
51. Ferràndez-Cañadell, C. An asterigerinacean origin for *Orbitoclypeus* and *Asterocyclina* (Orbitoclypeidae, Foraminifera). *J. Foraminifer. Res.* **1998**, *28*, 135–140.
52. Özcan, E.; Mitchell, S.F.; Less, G.; Robinson, E.; Bryan, J.R.; Pignatti, J.; Yücel, A.O. A revised suprageneric classification of American orthophragminids with emphasis on late Paleocene representatives from Jamaica and Alabama. *J. Syst. Palaeontol.* **2019**, *17*, 1551–1579. [CrossRef]

53. Özcan, E.; Less, G.; Báldi-Beke, M.; Kollányi, K.; Kertész, B. Biometric analysis of middle and upper Eocene Discocyclinidae and Orbitoclypeidae (Foraminifera) from Turkey and updated orthophragmine zonation in the western Tethys. *Micropaleontology* **2006**, *52*, 485–520. [CrossRef]
54. Ferràndez-Cañadell, C.; Baumgartner-Mora, C.; Baumgartner, P.O.; Epard, J.-L. Priabonian (upper Eocene) larger foraminifera from the Helvetic Nappes of the Alps (Western Switzerland): New markers for Shallow Benthic Zones 19–20. *Micropaleontology* **2023**, *69*, 401–450. [CrossRef]
55. van der Weijden, W.J.M. *Het Genus Discocyclina in Europa: Een Monografie Naar Aanleiding Van Een Heronderzoek Van Het Tertiair-Profiel Van Biarritz*; N.V. de Leidsche Courant: Utrecht, The Netherlands, 1940.
56. Less, G. The late Paleogene larger foraminiferal assemblages of the Bükk Mts. (NE Hungary). *Rev. Esp. Micropaleontol.* **1999**, *31*, 51–60.
57. Sowerby, J.; De, C. Systematic list of organic remains, the plants determined by Mr. John Morris, and the remainder by Mr. James de Carl Sowerby. *Trans. Geol. Soc. Lond. Ser. 2* **1840**, *5*, 327–329.
58. Samanta, B.K.; Lahiri, A. The occurrence of *Discocyclina* Gümbel in the middle Eocene Fulra Limestone of Cutch, Gujarat, Western India, with notes on species reported from the Indian region. *Bull. Geol. Min. Metall. Soc. India* **1985**, *52*, 211–295.
59. Özcan, E.; Less, G.; Okay, A.I.; Báldi-Beke, M.; Kollányi, K.; Yılmaz, İ.Ö. Stratigraphy and larger foraminifera of the Eocene shallow-marine and olistostromal units of the southern part of the Thrace Basin, NW Turkey. *Turk. J. Earth Sci.* **2010**, *19*, 27–77. [CrossRef]
60. Özcan, E.; Okay, A.İ.; Bürkan, K.A.; Yücel, A.O.; Özcan, Z. Middle–Late Eocene marine record of the Biga Peninsula, NW Anatolia, Turkey. *Geol. Acta* **2018**, *16*, 133–162.
61. Ali, N.; Özcan, E.; Yücel, A.O.; Hanif, M.; Hashmi, S.I.; Ullah, F.; Pignatti, J. Bartonian orthophragminids with new endemic species from the Pirkoh and Drazinda formations in the Sulaiman Range, Indus Basin, Pakistan. *Geodin. Acta* **2018**, *30*, 31–62. [CrossRef]
62. Özcan, E.; Less, G.; Jovane, L.; Catanzariti, R.; Frontalini, F.; Coccioni, R.; Giorgioni, M.; Rodelli, D.; Rego, E.S.; Kayğılı, S.; et al. Integrated biostratigraphy of the middle to upper Eocene Kırkgeçit Formation (Baskil section, Elazığ, eastern Turkey): Larger benthic foraminiferal perspective. *Mediterr. Geosci. Rev.* **2019**, *1*, 55–90. [CrossRef]
63. Whipple, G.L. Eocene Foraminifera. In *Geology of Eua, Tonga*; Hoffmeister, I.E., Ed.; Bulletin of the Bernice P. Bishop Museum; Bishop Museum: Honolulu, HI, USA, 1932; Volume 96, pp. 79–90.
64. Yücel, A.O.; Özcan, E.; Erbil, Ü. Latest Priabonian larger benthic foraminiferal assemblages at the demise of the Soğucak Carbonate Platform (Thrace Basin and Black Sea shelf, NW Turkey): Implications for the shallow marine biostratigraphy. *Turk. J. Earth Sci.* **2019**, *29*, 85–114. [CrossRef]
65. Dimou, V.G.; Koukousioura, O.; Less, G.; Triantaphyllou, M.V.; Dimiza, M.D.; Syrides, G. Systematic paleontology and biostratigraphy of upper Eocene larger benthic foraminifera from Fanari (Thrace Basin, Greece). *Micropaleontology* **2023**, *69*, 457–486. [CrossRef]
66. Less, G.; Özcan, E.; Okay, A.I. Larger foraminiferal stratigraphy and paleoenvironments of the Middle Eocene to Lower Oligocene shallow-marine units in the northern and eastern parts of the Thrace Basin, NW Turkey. *Turk. J. Earth Sci.* **2011**, *20*, 793–845.
67. Meffert, B.F. Eocenovaja fauna iz Daralageza v Armenii. *Tr. Glav. Geol.-Razved. Upravl.* **1931**, *99*, 1–64. Leningrad–Moscow. (In Russian)
68. Zakrevskaya, E.; Less, G.; Bugrova, E.; Shcherbinina, E.; Grigoryan, T.; Sahakyan, L. Integrated biostratigraphy and benthic foraminifera of the middle-upper Eocene deposits of Urtsadzor section (Southern Armenia). *Turk. J. Earth Sci.* **2020**, *29*, 896–945. [CrossRef]
69. Gümbel, C.W. Beiträge zur Foraminiferenfauna der nordalpinen älteren Eocängebilde oder der Kressenberger Nummulitenschichten. *Abh. K. Bayer. Akad. Wiss. Math.-Phys. Kl.* **1870**, *10*, 581–730.
70. Neumann, M. Révision des *Orbitoididés* du Crétacé et de l'Éocène en Aquitaine Occidentale. *Mém. Soc. Géol. Fr.* **1958**, *37*, 1–174.
71. Özcan, E.; Erbay, S.; Abbasi, A.I.; Pereira, C.D.; Erkızan, L.S.; Kayğılı, S. The first record of *Nemkovella daguini* (Neumann, 1958) from the middle-late Eocene of Oman (Arabian Peninsula) and Meghalaya (Indian Subcontinent) and its significance in Tethys: Correlations and paleobiogeography. *Riv. Ital. Paleontol. Stratigr.* **2019**, *125*, 13–28.
72. Schlumberger, C. Troisième note sur les *Orbitoïdes*. *Bull. Soc. Géol. Fr.* **1903**, *4*, 273–289. [CrossRef]
73. Özcan, E.; Saraswati, P.K.; Yücel, A.O.; Ali, N.; Hanif, M. Bartonian orthophragminids from the Fulra Limestone (Kutch, W India) and coeval units in Sulaiman Range, Pakistan: A synthesis of shallow benthic zone (SBZ) 17 for the Indian Subcontinent. *Geodin. Acta* **2018**, *30*, 137–162. [CrossRef]
74. Kaufmann, F.J. Geologische Beschreibung des Pilatus. *Beitr. Geol. Kt. Schweiz* **1867**, *5*, 1–169.
75. Stöckar, R. I macroforaminiferi eocenici negli inclusi dei depositi Quaternari della collina di Prella (Ticino meridionale, Svizzera). *Geol. Insubrica* **1999**, *4*, 1–20.
76. Rütimeyer, L. Ueber das schweizerische Nummulitenterrain, mit besonderer Berücksichtigung des Gebirges zwischen dem Thunersee und der Emme. *Neue Denkschr. Schweiz. Naturforsch. Ges.* **1850**, *11*, 1–120.

77. Romero, J.; Hottinger, L.; Caus, E. Early appearance of larger foraminifera supposedly characteristic for the late Eocene in the Igualada Basin, NE Spain. *Rev. Esp. Paleontol.* **1999**, *14*, 79–92. [CrossRef]
78. Drooger, C.W.; Marks, P.; Papp, A. Smaller radiate *Nummulites* of northwestern Europe. *Utrecht Micropalaeontol. Bull.* **1971**, *5*, 1–137.
79. Papazzoni, C.A. Biometric analyses of *Nummulites "ptukhiani"* Z.D. Kacharava, 1969 and *Nummulites fabianii* (Prever in Fabiani, 1905). *J. Foraminifer. Res.* **1998**, *28*, 161–176.
80. Mukhopadhyay, S.K. Pseudoreticulate-Subreticulate-Reticulate *Nummulites* and their possible evolution in the middle Eocene-lower Oligocene succession of Surat-Bharuch, Gujarat India. *Micropaleontology* **2022**, *68*, 505–556. [CrossRef]
81. Hadi, M.; Forouzande, S.K.; Consorti, L.; Parandavar, M.; Vahidinia, M. Extending the stratigraphic range of *Nummulites bormidiensis* Tellini in the Neo-Tethys (Zagros basin, SW Iran) through biometry and calcareous nannofossil biostratigraphy. *Micropaleontology* **2023**, *69*, 515–532. [CrossRef]
82. Yazdi-Moghadam, M.; Sarfi, M.; Sharifi, M.; Jahani, Z. Larger benthic foraminifera and biostratigraphy of the lower Oligocene Asmari Formation: Offshore and onshore southern Iran (Zagros belt). *Micropaleontology* **2023**, *69*, 533–548. [CrossRef]
83. Cotton, L.J.; Pearson, P.N.; Renema, W. A place for *Nummulites ptukhiani*? A new lineage of reticulate *Nummulites* from Kilwa District, Tanzania. *J. Syst. Palaeontol.* **2015**, *13*, 465–486.
84. Nuttall, W.L.F.; Brighton, A.G. Larger Foraminifera from the Tertiary of Somaliland. *Geol. Mag.* **1931**, *68*, 49–65. [CrossRef]
85. Fabiani, R. Studii geo-paleontologici dei Colli Berici. *Atti R. Ist. Veneto Sci. Lett. Ed Arti* **1905**, *64*, 1805–1825.
86. Okay, A.İ.; Çolak, D.; Özcan, E. Eocene–Oligocene succession at Kıyıköy (Midye) on the Black Sea coast of Turkey: Stratigraphy, larger benthic foraminifera, and paleoenvironments. *Turk. J. Earth Sci.* **2020**, *29*, 1–22.
87. Hantken, M. von. Die Fauna der 82Clavulina-Szaboi–Schichten. I. Foraminiferen. *Mitt. Jahrb. Königl. Ungar. Geol. Anst.* **1875**, *4*, 1–93. (In German)
88. Nemkov, G.I. Nummulitides of the Soviet Union and their biostratigraphic significance. *Mater. K poznan. Geol. Stroen. SSSR* **1967**, *16*, 1–319. (In Russian)
89. Harpe, P. de la. Note sur les *Nummulites* des Alpes occidentales. *Acta Soc. Helv. Sci. Nat.* **1878**, *60*, 227–232.
90. Harpe, P. de la. Étude des *Nummulites* de Suisse et révision des espèces éocènes des genres *Nummulites* et *Assilina*. Troisième et dernière partie (Posthume). *Mém. Soc. Paléontol. Suisse Abh. Schweiz. Paläontol. Ges.* **1883**, *10*, 141–180.
91. Herb, R.; Hekel, H. *Nummuliten* aus dem Obereozän von Possagno. *Schweiz. Paläontol. Abh.* **1975**, *97*, 113–135.
92. Douvillé, H. Le Crétacé et le Tertiaire aux environs de Thônes (Haute-Savoie). *C. R. Acad. Sci. Paris* **1916**, *163*, 324–331.
93. Colom, G.; Bauzá, J. *Operculina canalifera gomezi* n. subsp. de Bartoniense de Cataluña. *Bol. Real Soc. Esp. Hist. Nat.* **1950**, *47*, 219–221.
94. Özcan, E.; Ali, N.; Hanif, M.; Hashmi, S.I.; Khan, A.; Yücel, A.I.; Abbasi, I.A. New Priabonian Heterostegina from the Eastern Tethys (Sulaiman fold belt, West Pakistan): Implications for the development of Eastern Tethyan heterostegines and their paleobiogeography. *J. Foraminifer. Res.* **2016**, *46*, 393–408. [CrossRef]
95. Drooger, C.W.; Roelofsen, J.W. *Cycloclypeus* from Ghar Hassan, Malta. *Proc. Kon. Ned. Akad. Wetensch.* **1982**, *85*, 203–218.
96. Bieda, F. Sur quelques foraminifères nouveaux ou peu connus du flysch des Carpates polonaises. *Ann. Soc. Géol. Pol.* **1949**, *18*, 151–179.
97. Ben Ismail-Lattrache, K.; Özcan, E.; Boukhalfa, K.; Saraswati, P.K.; Soussi, M.; Jovane, L. Early Bartonian orthophragminids (Foraminiferida) from Reineche Limestone, North African platform, Tunisia: Taxonomy and paleobiogeographic implications. *Geodin. Acta* **2014**, *26*, 94–121. [CrossRef]
98. Özcan, E.; Saraswati, P.K.; Hanif, M.; Ali, N. Orthophragminids with new axial thickening structures from the Bartonian of the Indian subcontinent. *Geol. Acta* **2016**, *14*, 261–282.
99. Govindan, A. Larger foraminiferal biostratigraphy of early Paleogene sections in India. *J. Geol. Soc. India* **2013**, *1*, 24–45.
100. Özcan, E.; Scheibner, C.; Boukhalfa, K. Orthophraminids (foraminifera) across the Paleocene/Eocene transition from north Africa: Taxonomy, biostratigraphy and paleobiogeographic implications. *J. Foramin. Res.* **2014**, *44*, 203–229. [CrossRef]
101. Özcan, E.; Hanif, M.; Ali, N.; Yücel, A.O. Early Eocene orthophragminids (Foraminifera) from the type-locality of *Discocyclina ranikotensis* Davies, 1927, Thal, NW Himalayas, Pakistan: Insights into the orthophragminid palaeobiogeography. *Geodin. Acta* **2015**, *27*, 267–299. [CrossRef]
102. Özcan, E.; Abbasi, I.A.; Drobne, K.; Govindan, A.; Jovane, L.; Boukhalfa, K. Early Eocene orthophragminids and alveolinids from the Jafnayn Formation, N Oman: Significance of *Nemkovella stockari* Less & Özcan, 2007 in Tethys. *Geodin. Acta* **2016**, *28*, 160–184.
103. BouDagher-Fadel, M.K.; Price, G.D. The Paleogeographic evolution of the orthophragminids of the Paleogene. *J. Foramin. Res.* **2017**, *47*, 337–357. [CrossRef]
104. Özcan, E.; Pignatti, J.; Pereira, C.; Yücel, A.O.; Drobne, K.; Barattolo, F.; Saraswati, P.K. Paleocene orthophragminids from the Lakadong Limestone, Mawmluh Quarry Section, Meghalaya (Shillong, NE India): Implications for the regional geology and paleobiogeography. *J. Micropalaeont.* **2018**, *37*, 357–381. [CrossRef]

105. Özcan, E.; Özcan, Z.; Okay, A.I.; Akbayram, K.; Hakyemez, A. The Ypresian-to Lutetian marine record in NW Turkey: A revised biostratigraphy and chronostratigraphy and implications for Eocene paleogeography. *Turk. J. Earth Sci.* **2020**, *29*, 1–27. [CrossRef]
106. Forouzande, S.K.; Hadi, M.; Vahidinia, M.; Consorti, L.; Salahi, A.; Gharaie, M.H.M.; Özcan, E. Biostratigraphy of larger foraminifera from the Middle Eocene Jahrum-Pabdeh formations (Zagros region, SW Iran) and their correlation with the planktonic foraminiferal zones. *Micropaleontology* **2023**, *69*, 487–514. [CrossRef]
107. Speijer, R.P.; Pälike, H.; Hollis, C.J.; Hooker, J.J.; Ogg, J.G. The Paleogene Period. In *Geologic Time Scale 2020*; Gradstein, F.M., Ogg, J.G., Schmitz, M.D., Ogg, G.M., Eds.; Elsevier: Amsterdam, The Netherlands, 2020; pp. 1087–1140.
108. Beavington-Penney, S.J.; Racey, A. Ecology of extant nummulitids and other larger benthic foraminifera: Applications in palaeoenvironmental analysis. *Earth-Sci. Rev.* **2004**, *67*, 219–265. [CrossRef]
109. Samanta, B.K.; Bandopadhyay, K.P.; Lahiri, A. The occurrence of *Nummulites* Lamarck (Foraminiferida) in the Middle Eocene Harudi Formation and Fulra Limestone of Cutch, Gujarat, western India. *Bull. Geol. Min. Metall. Soc. India* **1990**, *55*, 1–66.
110. Saraswati, P.K.; Patra, P.K.; Banerji, R.K. Biometric study of some Eocene *Nummulites* and *Assilina* from Kutch and Jaisalmer, India. *J. Palaeontol. Soc. India* **2000**, *45*, 91–122. [CrossRef]
111. Mukhopadhyay, S.K. A rare foraminiferal assemblage with new species of *Nummulites* and *Globigerina* from the Eocene-Oligocene transition strata of Cambay Basin, India. *Micropalaeontology* **2003**, *49*, 65–93. [CrossRef]